In Memory of

my

Father and Sister

PREFACE

This thesis is concerned with a reinvestigation of the kinetics and mechanism of the pyrolysis of acetaldehyde. In spite of a considerable amount of previous work, many details of the mechanism have remained obscure. One feature of the present work is that a special effort has been made to use purer acetaldehyde then in previous work, and to measure the rates of formation of the minor products of the reaction. A preliminary report on some of this work has been published as K. J. Laidler and M. T. H. Liu, Proc. Roy. Soc., A 297 365 (1967).

ACKNOWLEDGEMENTS

I wish to express my deepest and most sincere appreciation for the privilege of working under Professor K. J. Laidler, who has been most willing to assist in all aspects of this work. His direction and encouragement throughout the course of this investigation are most gratefully acknowledged. Thanks are also due to Drs. M. H. Back, J. L. Holmes and M. C. Lin for their valuable aid and constructive suggestions. Appreciation is also extended to my colleagues for helpful discussions. Fellowships awarded to me by the National Research Council and the Canadian Industries Limited are gratefully acknowledged.

Finally I wish to thank my wife for her assistance in preparing this thesis.

TABLE OF CONTENTS

	Page
PREFACE	i
ACKNOWLEDGEMENTS	ii
TABLE OF CONTENTS	iii
LIST OF TABLES	v
LIST OF FIGURES	vii
LIST OF PLATES	x
ABSTRACT	1
CHAPTER I INTRODUCTION	
Historical Review	4
Evidence of Free Radicals in the Reaction	7
Sensitized Decomposition	8
The Effects of Foreign Gases	11
Object of Present Investigation	12
CHAPTER II EXPERIMENTAL	
Materials	16
Apparatus	17
Procedure	20
CHAPTER III RESULTS AND ANALYSIS	
The Overall Kinetics and Mechanism	24
Ethane Production	41
Acetone Production	53
Hydrogen Production	65
Propionaldehyde Production	77

Page

Ketene Production 79

The Decomposition of the CH_2CHO Radical 80

The CO_2 and C_2H_4 Production 84

Inert Gas Effect 86

Surface Effects

(a) Packing 102

(b) Carbon Coating 105

Time-Course Studies 109

CHAPTER IV GENERAL DISCUSSION

Unimolecular Decomposition of Acetaldehyde 119

The Decomposition of the Isopropoxy Radical 133

Multiple Bond Formation 141

Possible Tunnelling in the Reaction $CH_3 + CH_3CHO \rightarrow CH_4 + CH_3CO$ 143

The Overall Chain Reaction 148

CLAIMS TO ORIGINAL RESEARCH 151

REFERENCES 153

LIST OF TABLES

Table		Page
1.	Initial rates of product formation.	26
2.	Overall rate constant as a function of pressure at 540°C.	35
3.	Overall rate constants as a function of temperature.	39
4.	Rate constants for the hydrogen atom abstraction reaction by the methyl radical.	50
5.	Apparent rate constants for the addition of the methyl radical to acetaldehyde.	62
6.	Extrapolation of k_1 from hydrogen measurements.	72
7.	The values of k_1/k_9 at 540°C, calculated from methane production.	88
8.	Effect of CO_2 on methane production.	91
9.	Effect of CO_2 on ethane formation at 540°C.	94
10.	Effect of CO_2 on rate of formation of acetone at 540°C.	97
11.	The values of k_1/k_9 at 540°C calculated from values of acetone production.	98
12.	Effect of CO_2 on rates of hydrogen production at 540°C.	101
13.	Initial rates of formation for various products at 500°C in packed and unpacked vessels.	103

Table		Page
14.	Effect of carbon coating on the overall rate of acetaldehyde pyrolysis at 480°C.	106
15.	Rate constants for the homogeneous and heterogeneous decomposition of CH_3CHO, III and the cis ⟷ trans isomerization of but-2-ene.	107
16.	The values of k_1' obtained from rates of ethane formation.	121
17.	Values of $v_{C_2H_5CHO} / [CH_3CHO]$ at 118 mm and k_1' as a function of temperature.	126
18.	Approximate enthalpies of formation and entropies of gaseous compounds and free radicals.	135
19.	Hydrogen atom abstraction reaction by methyl radical from acetaldehyde.	144
20.	Chain lengths $\bar{\phi}$ as functions of pressure and temperature.	149

LIST OF FIGURES

Figure		Page
1.	Schematic diagram of the apparatus.	19
2.	Typical yield-time plot for the formation of all products at 523°C and 117 mm Hg.	25
3.	Typical methane yield-time plots at 523°C.	30
4.	Typical v_{CH_4} vs. t plot.	31
5.	Order plot for methane production.	32
6.	Plot of v_{CH_4} vs. $\left[CH_3CHO\right]^{3/2}$.	34
7.	Order plot for methane production at 540°C, from 0.8 mm to 558 mm Hg.	36
8.	Plot of $\log_{10} k_{overall}$ vs. $\log_{10} P$ at 540°C.	37
9.	Arrhenius plot of overall rate constant.	40
10.	Typical ethane yield-time plot at 523°C.	42
11.	Typical $v_{C_2H_6}$ vs. t plot.	43
12.	Order plot for ethane formation.	45
13.	Plots of $\log_{10} k_9/k_4^2$ vs. $\log_{10} P$ (mm Hg).	46
14.	Plots of k_4 vs. 1/P (mm Hg).	51
15.	Arrhenius plot for the abstraction rate constant k_4.	52
16.	Typical acetone yield-time plot at 523°C.	54
17.	Typical $v_{acetone}$ vs. t plot at 523°C.	55
18.	Order plot for acetone formation.	59
19.	Plot of $v_{CH_3COCH_3}$ vs. $\left[CH_3CHO\right]^{3/2}$.	60

Figure		Page
20.	Arrhenius plot of k_8.	63
21.	Typical hydrogen yield-time plots at 523°C.	66
22.	Typical v_{H_2} vs. t plots at 523°C.	67
23.	Order plot for hydrogen production.	68
24.	Plot of $v_{H_2} / \left[CH_3CHO\right]$ vs. $\left[CH_3CHO\right]^{\frac{1}{2}}$.	70
25.	Arrhenius plots of k_1 and k_1".	74
26.	Plots of $\log_{10} k_{7a}$ vs. $\log_{10}$ P mm Hg.	82
27.	Arrhenius plot of k^0_{7a}.	83
28.	Order plot for C_2H_4 formation at 540°C.	85
29.	Plot of $\log_{10} k_1/k_9$ vs. $\log_{10}$ P(mm Hg).	89
30.	Typical yield-time plots for methane formation in the presence of CO_2.	90
31.	Typical yield-time plots for ethane formation in the presence of CO_2.	93
32.	Typical yield-time plots for acetone formation in the presence of CO_2.	96
33.	Typical yield-time plots for hydrogen formation in the presence of CO_2.	100
34.	Order plots for methane production at 480°C in coated and uncoated vessels.	108
35.	Comparison of calculated yield-time curves with experimental results for methane production.	111
36.	Comparison of integrated and differential rate.	112

Figure		Page
37.	Comparison of calculated yield-time curves with experimental results for acetone production.	114
38.	Comparison of calculated yield-time curves with experimental results for ethane production.	116
39.	Plot of $\left[H_2\right]/t - f(t)$ vs. $g(t)$ at 523°C.	118
40.	Plots of $\log_{10} k_1'$ vs. $\log_{10} P$ (mm Hg).	123
41.	Plots of $\left[CH_3CHO\right]/v_{C_2H_6}$ vs. $1/P^{\frac{1}{2}}$.	124
42.	Arrhenius plot of k_1' and k_1''.	125
43.	Activation energy diagram for addition and decomposition reactions at 298.2°K.	139
44.	Arrhenius plot of $k_4/k_9^{\frac{1}{2}}$.	145

LIST OF PLATES

Plate		Page
1.	A view of the apparatus.	18

ABSTRACT

Previous work on the acetaldehyde pyrolysis is shown to be vitiated by the presence, in the acetaldehyde, of impurities, mainly ethanol and crotonaldehyde. The reaction has been reinvestigated with the use of acetaldehyde, prepared from paraldehyde, which is free from these and other impurities. On the basis of a study of the kinetics of formation of the major products (methane and carbon monoxide) and of a number of minor products (hydrogen, acetone, propionaldehyde, ethane and ethylene) a reaction mechanism is proposed. This includes all of the reactions in the original Rice-Herzfeld scheme, together with a number of other elementary processes, in particular

$$CH_3 + CH_3CHO \longrightarrow CH_4 + CH_2CHO$$

The decomposition of the radical CH_2CHO into CH_2CO and H provides an additional source of hydrogen, the rate of production of which is therefore not a measure of the rate of the initiation process. Acetone is believed to arise mainly by the reactions

$$CH_3 + CH_3CHO \rightleftharpoons i\text{-}PrO$$

$$i\text{-}PrO \longrightarrow CH_3COCH_3 + H$$

and only to a negligible extent by the combination of CH_3 and CH_3CO.

The apparent rate constant for the addition of the methyl radical to acetaldehyde was found to be expressed by the equation

$$\log k \ (\text{cc mole}^{-1}\text{sec}^{-1}) = 10.22 - \frac{12,350}{2.303\ RT}$$

The equilibrium constant

$$K = \frac{[\text{i-PrO}]}{[CH_3]\ [CH_3CHO]}$$

has been calculated from thermodynamic data, and the rate constant for i-PrO $\longrightarrow CH_3COCH_3 + H$ has been evaluated as

$$\log k \ (\text{sec}^{-1}) = 12.83 - \frac{19,100}{2.303\ RT}$$

The main chain-ending step is concluded to be

$$CH_3 + CH_3 \longrightarrow C_2H_6$$

with a small contribution from

$$CH_3 + CH_2CHO \longrightarrow CH_3CH_2CHO$$

The work provides further evidence for the falling-off, at low pressures, of the second-order coefficient for the combination of methyl radicals. The overall order for the decomposition of acetaldehyde was confirmed to be 3/2 from 480° to 540°C at pressures from 50 to 559 mm Hg. The rate constant can be expressed as

$$\log k_{\text{overall}} \ (\text{cc}^{\frac{1}{2}}\text{mole}^{-\frac{1}{2}}\text{sec}^{-1}) = 13.45 - \frac{49,100}{2.303\ RT}$$

At lower pressures from 1 to 40 mm there is a fall-off in $k_{overall}$, the order of the reaction having increased to 1.7.

From the rates of ethane and hydrogen production the activation energy for the initiation process is found to be 78.2 $\pm$ 2 kcal.

At low pressures the addition of CO_2 increased the rates of production of hydrogen and ethane to a greater extent than those of methane and acetone. The rate constants for both initiation and termination are well in their pressure-dependent regions under the conditions of the inert-gas experiments. The production of methane and acetone, however, is only a function of the ratio of these two rate constants, so that the effect due to inert gas is expected to be much smaller. The inert-gas effect is completely consistent with the mechanism proposed. The rates of production of various products are slightly affected by increasing the surface:volume ratio of the reaction vessel, but the rate constants for different elementary processes are concluded to be essentially homogeneous.

CHAPTER I

INTRODUCTION

Historical Review

Early work on the acetaldehyde pyrolysis showed that only two major products were formed, methane and carbon monoxide, according to the stoichiometric equation

$$CH_3CHO \longrightarrow CH_4 + CO$$

The thermal decompositions of gaseous hydrocarbons, aldehydes and ketones were first thought to be elementary unimolecular reactions. The pyrolysis of acetaldehyde, in particular, was believed to proceed by a direct unimolecular split into CH_4 + CO with an activation energy of 46 kcal (1). Rice and Herzfeld (2) suggested that the pyrolysis of acetaldehyde is a free-radical chain mechanism so that the activation energy of 46 kcal does not refer to any particular elementary process. Letort (3-5) made an extensive study of this reaction and showed that the initial rate of reaction varied with the initial pressure of acetaldehyde according to the equation

$$\log R_0 = 1.50 \log P_0 + \text{constant}$$

The order of the reaction is therefore 3/2. Letort found the rate constant to be given by

CHAPTER I

INTRODUCTION

Historical Review

Early work on the acetaldehyde pyrolysis showed that only two major products were formed, methane and carbon monoxide, according to the stoichiometric equation

$$CH_3CHO \longrightarrow CH_4 + CO$$

The thermal decompositions of gaseous hydrocarbons, aldehydes and ketones were first thought to be elementary unimolecular reactions. The pyrolysis of acetaldehyde, in particular, was believed to proceed by a direct unimolecular split into CH_4 + CO with an activation energy of 46 kcal (1). Rice and Herzfeld (2) suggested that the pyrolysis of acetaldehyde is a free-radical chain mechanism so that the activation energy of 46 kcal does not refer to any particular elementary process. Letort (3-5) made an extensive study of this reaction and showed that the initial rate of reaction varied with the initial pressure of acetaldehyde according to the equation

$$\log R_0 = 1.50 \log P_0 + \text{constant}$$

The order of the reaction is therefore 3/2. Letort found the rate constant to be given by

$$k = 2.3 \times 10^{12} \, e^{\frac{-46,000}{RT}} \; cc^{\frac{1}{2}} \, mole^{-\frac{1}{2}} \, sec^{-1}$$

Boyer, Niclause and Letort (6) later reported that the reaction was homogeneous and that the 3/2-order rate constant was

$$k = 2.2 \times 10^{12} \, e^{\frac{-48,000}{RT}} \; cc^{\frac{1}{2}} \, mole^{-\frac{1}{2}} \, sec^{-1}$$

Travers and Seddon (7-10) also investigated this reaction and found that their results differed widely from those of other laboratories. They concluded that the process is much more complicated than found by previous workers. Their experimental technique required the use of a fresh surface each time, and it therefore appears that the surfaces of the vessel play an important role in their work.

Hinshelwood and co-workers (11-13) measured the rate of decomposition with initial pressures ranging from 0.2 to 1100 mm. The curve they obtained by plotting the reciprocal of the time of half decomposition against the initial pressure shows an abrupt change of slope, and the results were interpreted by the theory that the acetaldehyde molecule can be activated in a number of distinct ways. On the basis of packed-vessel studies they concluded that the influence of surface is negligible and that the reaction is essentially homogeneous. In 1958, Freeman, Danby and Hinshelwood (14) reinvestigated this decomposition over a temperature range of 504 to 525°C and found small amounts of H_2, C_2H_6 and C_2H_4. They concluded

that both chain and molecular processes were operating in the system and that on the addition of nitric oxide the rate of free-radical initiation is increased to a larger extent than that of the molecular rearrangement. There has been much controversy regarding the importance of a molecular mechanism, but there is much evidence to suggest that the molecular mechanism is insignificant; some of this evidence is referred to later.

Imai, Yoshida and Toyama (15) investigated this decomposition at a lower temperature range of 380 - 460°C and found that the 3/2-order rate constant could be expressed as

$$k = 10^{12.1} e^{\frac{-43,300}{RT}} \text{ mole}^{-\frac{1}{2}} \text{ cc}^{\frac{1}{2}} \text{ sec}^{-1}$$

In 1963, Trenwith (16) measured the rate of formation of hydrogen and found that it is second-order in acetaldehyde. The production of hydrogen, however, showed a short induction period which is independent of initial acetaldehyde pressure but is inversely proportional to temperature. Furthermore, the induction period is removed by increasing the surface area of the reaction vessel. In a later paper, Dexter and Trenwith (17), on the basis of the fact that the rate of acetone formation is much greater than the rate of formation of ethane, concluded that the principal chain-ending step is $CH_3 + CH_3CO \longrightarrow CH_3COCH_3$

and to a lesser extent $CH_3 + CH_3 \longrightarrow C_2H_6$. Eusuf and Laidler (18) found that the rate of ethane formation is second-order in acetaldehyde and concluded, on the basis of the mechanism, that the initiation process must be second-order. Very recently, Côme, Dzierzynski, Martin and Niclause (19,20) have shown that the order of hydrogen production is about 1.35 and the order of ethane production is around 1.2; they conclude that in the radical-chain mechanism the initiation is first-order and that termination, by the combination of two methyl radicals, is second-order.

Evidence of Free Radicals in the Reaction

In 1932, Rice, Johnston, and Evering (21) detected methyl radicals in this decomposition, by the Paneth method. Methyl radicals have also been detected by Letort (22) using the same method. Burton, Ricci and Davis (23) were able to prove the presence of radicals at 500°C by the use of radioactive lead mirrors which made the Paneth test sufficiently sensitive that the experiments could be carried out over the temperature range in which the pyrolysis is carried out. Patat and Sachsse (24-27) showed that the rate of the para-ortho hydrogen conversion was enhanced in the presence of decomposing acetaldehyde, thus proving the presence of atoms or radicals.

Mixtures of CH_3CHO and CD_3CDO have been decomposed by several workers (28-31) with a view to establishing the nature of the decomposition. They all observed extensive isotopic mixing and concluded that the reaction occurs via free radicals. If the reaction did not involve free radicals, only CH_4 and CD_4 would be observed. Rice and Varnerin (32) decomposed CH_3CHO in the presence of C_2D_6 and investigated the rate of production of CH_3D and CH_4. They found that the ratio of CH_3D/CH_4 was proportional to the percentage of aldehyde that had decomposed, so that the contribution due to the molecular process was negligible.

Sensitized Decomposition

Acetaldehyde has been found to decompose by a chain mechanism with a sizeable chain length. For this reason, the decomposition is very sensitive to the presence of small amounts of material which can form free radicals faster than acetaldehyde does. Thus, Allen and Sickman (33,34) have shown that azomethane induced the decomposition of acetaldehyde at 300°C, chain lengths as great as 500 being obtained. The azomethane acts as the source of methyl radicals.

Calvert and Gruver (35) photolyzed azomethane in the presence of acetaldehyde. The probable reactions in

Mixtures of CH_3CHO and CD_3CDO have been decomposed by several workers (28-31) with a view to establishing the nature of the decomposition. They all observed extensive isotopic mixing and concluded that the reaction occurs via free radicals. If the reaction did not involve free radicals, only CH_4 and CD_4 would be observed. Rice and Varnerin (32) decomposed CH_3CHO in the presence of C_2D_6 and investigated the rate of production of CH_3D and CH_4. They found that the ratio of CH_3D/CH_4 was proportional to the percentage of aldehyde that had decomposed, so that the contribution due to the molecular process was negligible.

Sensitized Decomposition

Acetaldehyde has been found to decompose by a chain mechanism with a sizeable chain length. For this reason, the decomposition is very sensitive to the presence of small amounts of material which can form free radicals faster than acetaldehyde does. Thus, Allen and Sickman (33,34) have shown that azomethane induced the decomposition of acetaldehyde at 300°C, chain lengths as great as 500 being obtained. The azomethane acts as the source of methyl radicals.

Calvert and Gruver (35) photolyzed azomethane in the presence of acetaldehyde. The probable reactions in

this system, leading to the products ethane, carbon monoxide and acetone, are

$$(CH_3)_2 N_2 + h\nu \longrightarrow 2CH_3 + N_2$$

$$CH_3 + CH_3CHO \longrightarrow CH_4 + CH_3CO$$

$$CH_3CO \longrightarrow CH_3 + CO$$

$$CH_3CO + CH_3 \longrightarrow CH_3COCH_3$$

$$2CH_3 \longrightarrow C_2H_6$$

It is interesting to note that the rate of formation of ethane is always much greater than the rate of acetone formation in the temperature range of 22 to 127°C, indicating that the recombination of methyl radicals always dominates. The decomposition was found to be sensitized by biacetyl (36,37), possibly owing to the occurrence of the reactions

$$(CH_3CO)_2 \longrightarrow 2\,CH_3CO$$

and

$$CH_3CO \longrightarrow CH_3 + CO$$

The decomposition was also induced by free radicals from the decomposition of ethylene oxide (38,39), diethyl ether (40,41) and ethyl iodide (42,43).

Letort (5) showed that oxygen has an accelerating effect on the rate of acetaldehyde decomposition. Even as

little as 10^{-3} percent of O_2 will double the rate of decomposition, or up to a few thousand molecules of aldehyde can be decomposed by one molecule of oxygen. Niclause and Letort (44,45) showed that the decomposition can be induced at temperatures as low as 150°C. The mechanism proposed for the reaction is

$$O_2 + CH_3CHO \longrightarrow CH_3CO + HO_2$$

followed by

$$HO_2 + CH_3CHO \longrightarrow H_2O_2 + CH_3CO$$

Early studies (46,47) have shown that small amounts of iodine will catalyze the decomposition of this reaction above 300°C. Recent work of O'Neal and Benson (48) has made the general pattern of iodine catalysis apparent, and the mechanism is as follows:

$$I_2 + M \rightleftharpoons 2I + M$$

$$I + CH_3CHO \rightleftharpoons CH_3CO + HI$$

$$CH_3CO + I_2 \rightleftharpoons CH_3COI + I$$

$$CH_3COI \rightleftharpoons CH_2CO + HI$$

$$CH_3CO + M \longrightarrow CH_3 + CO + M$$

$$CH_3 + HI \longrightarrow CH_4 + I$$

$$CH_3 + I_2 \rightleftharpoons CH_3I + I$$

The reaction is initiated by an iodine atom attack on acetaldehyde to produce hydrogen iodide and an acetyl radical. The acetyl radical may be trapped by iodine to form organic iodide intermediates, which may back react with iodine or decompose into products. Properties predicted from the mechanism agreed satisfactorily with observed reaction orders and rates.

The Effects of Foreign Gases

There have been numerous investigations of the effects of foreign gases on the rate of acetaldehyde decomposition, and the results obtained under different conditions or in different laboratories show quite important discrepancies. Fletcher and Hinshelwood found that both hydrogen (49,50) and helium (51) increase the rate of reaction. On the other hand, Bril, Goldfinger, Letort, Matthys and Niclause (52,53), using H_2, N_2 and CO_2, found that foreign gases inhibit the reaction slightly. They concluded that the termination step, the combination of methyl radicals, is in its third-order region and that the initiation is probably second-order. The fact that second-order initiation was favoured received strong support from the work of Trenwith (16) who found that the hydrogen production (which was thought to be a measure of the rate of initiation) is second-order

in acetaldehyde. Dexter and Trenwith (17) observed that the rates of both initiation and termination steps increase on the addition of CO_2 and that the initial overall rate of decomposition of acetaldehyde remains unchanged. Eusuf and Laidler (18) found that the rate of ethane formation is increased by the addition of nitrogen and that the overall rate of reaction is decreased.

Object of Present Investigation

In spite of a considerable amount of work on the thermal decomposition of acetaldehyde, many details of the mechanism have remained obscure and confusing. Some of the results are consistent with the original mechanism of Rice and Herzfeld (2):

$$CH_3CHO \longrightarrow CH_3 + CHO$$

$$CHO \longrightarrow CO + H$$

$$H + CH_3CHO \longrightarrow CH_3CO + H_2$$

$$CH_3 + CH_3CHO \longrightarrow CH_4 + CH_3CO$$

$$CH_3CO \longrightarrow CH_3 + CO$$

$$CH_3 + CH_3 \longrightarrow C_2H_6$$

This scheme successfully accounts for the following features of the reaction:

(1) The main reaction products are methane and carbon monoxide; these are produced in the chain-propagating steps.
(2) The order of the reaction is three-halves; this is explained if the order of the termination reaction is one greater than the order of the initiation reaction (e.g. if initiation is first-order and termination is second-order).

There are, however, a number of experimental results that cannot be reconciled with this mechanism, such as the following:

(1) According to the mechanism the only minor products should be hydrogen and ethane. In addition, however, significant amounts of acetone, propionaldehyde and ethylene are formed (16,17). Indeed Dexter and Trenwith (17) found that the initial rate of acetone production is much greater than that of ethane production, from which they concluded that the methyl radical combination cannot be the main termination step.

(2) Eusuf and Laidler (18), in agreement with the results of Bril, Goldfinger, Letort, Matthys and Niclause (52), found that the overall rate of reaction is reduced by the addition of inert gases, and from this they concluded that the methyl radical combination must be in its pressure-dependent region. The recent work of Quinn (54) and of Lin and Back (55) has, however, indicated that the methyl radical combination should be in its second-order region under most of the conditions used in the acetaldehyde

pyrolysis. There is also some confusion on the experimental side about inert-gas effects; Niclause (56) later reported that there was no effect on the overall rate, and Dexter and Trenwith (17) found an effect on the rates of both the initiation and the termination reactions, but no effect on the initial overall rate.

(3) Trenwith (16) found that the hydrogen production was second-order in acetaldehyde. If the Rice-Herzfeld scheme is accepted this can only mean that initiation is second-order in acetaldehyde; this, however, leads to the incorrect overall order if the termination process is taken to be second-order. In addition, an induction period found for hydrogen production (16) cannot be accounted for satisfactorily by any current theory.

(4) Eusuf and Laidler (18) found the rate of ethane production, which on the basis of the mechanism must be equal to the rate of the initiation process, to be second-order in acetaldehyde and to be increased by the addition of inert gas. Again, this result is inconsistent with the overall order if the termination reaction is second-order.

It is evident that several of the reported experimental results are inconsistent with the Rice-Herzfeld mechanism, and that some of these (particularly those relating to inert-gas effects) are mutually inconsistent. The present work was undertaken with the object of resolving these difficulties. It was suspected that some of the experimental anomalies, especially those relating to the

rates of production of minor products, were due to traces of impurities in the acetaldehyde employed, and great care was therefore taken to test, by vapour-phase chromatography, nuclear magnetic resonance spectroscopy and mass spectrometry, for such impurities and to work with samples of acetaldehyde that were substantially purer than had previously been employed. When this was done the kinetic results were somewhat different from those previously obtained. They could be reconciled with a scheme of reactions based on the original Rice-Herzfeld mechanism but including a number of important reactions.

CHAPTER II

EXPERIMENTAL

Materials

Acetaldehyde obtained from Eastman Organic Chemicals and from the Matheson Company, and purified by a number of bulb-to-bulb distillations, showed identical kinetic behaviour, even as far as the minor products were concerned. However the fact that there was a high initial rate of ethylene production, as found by Trenwith (17), led to the suspicion that ethylene was being formed from an impurity. This was confirmed by pyrolyzing partially-decomposed acetaldehyde, which produced ethylene at a considerably lower rate. Vapour-phase chromatography and nuclear magnetic resonance studies indicated that the main impurities were ethanol and crotonaldehyde. These impurities are not removed from the acetaldehyde by distillation.

It was found that no detectable impurities were present in acetaldehyde prepared from paraldehyde, and this was the material used in the remainder of the investigations. Eastman Research Grade paraldehyde was distilled, and the fraction of b.p. 124^{0}C was collected. This was distilled under nitrogen with addition of a small quantity of concentrated sulphuric acid, and acetaldehyde boiling at 21^{0}C was collected and purified by trap-to-trap distillation and degassed at -160^{0}C to remove traces of oxygen. It was

stored at -78°C and redistilled each time before use. No trace of any impurity in this material was revealed by vapour-phase chromatography, nuclear magnetic resonance spectroscopy or mass spectrometry.

Apparatus

The decomposition was carried out in a conventional static system, as shown in Plate 1. The essential features of the apparatus are shown schematically in Fig. 1.

The reaction vessel was a quartz sphere 515 cc. in volume, with a S/V ratio of 0.6 cm^{-1}. In the packed-vessel studies, a different sphere with a S/V ratio of 9.38 cm^{-1} was employed. The reaction vessel was enclosed in a furnace consisting of a steel cylinder of 1.5 cm thickness, which was heated by two windings of resistance wire. The heating of the outer winding was controlled by the adjustment of a Variac. The heating of the inner winding was also controlled through a Variac in conjunction with a Thermoelectric thermoregulator which was activated by means of a thermocouple placed in the middle of the cylinder. The temperature was controlled to within 0.2°C using the above arrangement. The temperature of the reaction vessel and of the steel cylinder was measured using chromel-alumel thermocouples (reference junction at 0°C) connected to a Croydon type P-3 potentiometer. The temperatures of the reaction vessel and the cylinder were found to be the same. The thermocouples were calibrated at three different

Plate 1

A view of the apparatus

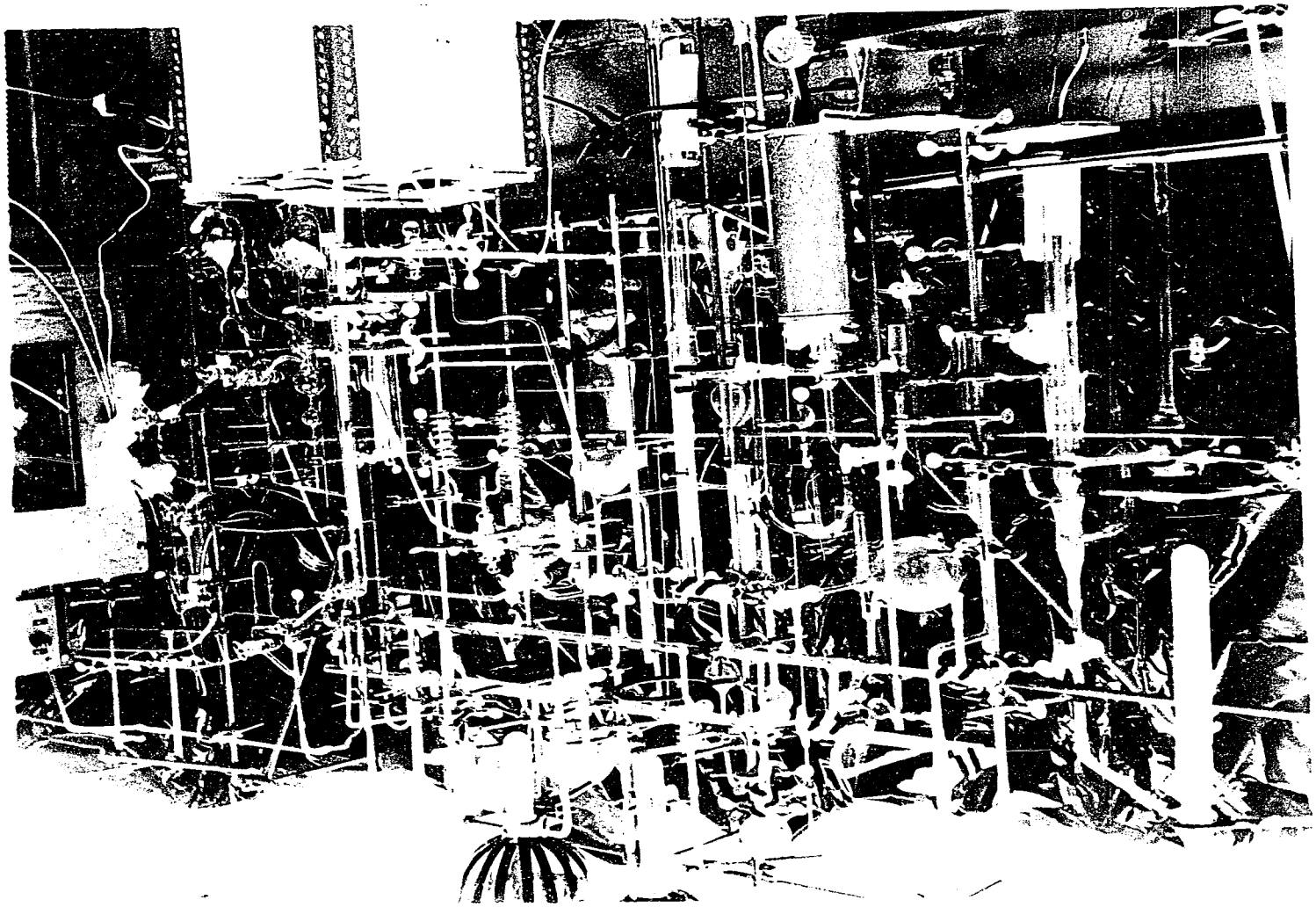

Figure 1

Schematic diagram of the apparatus

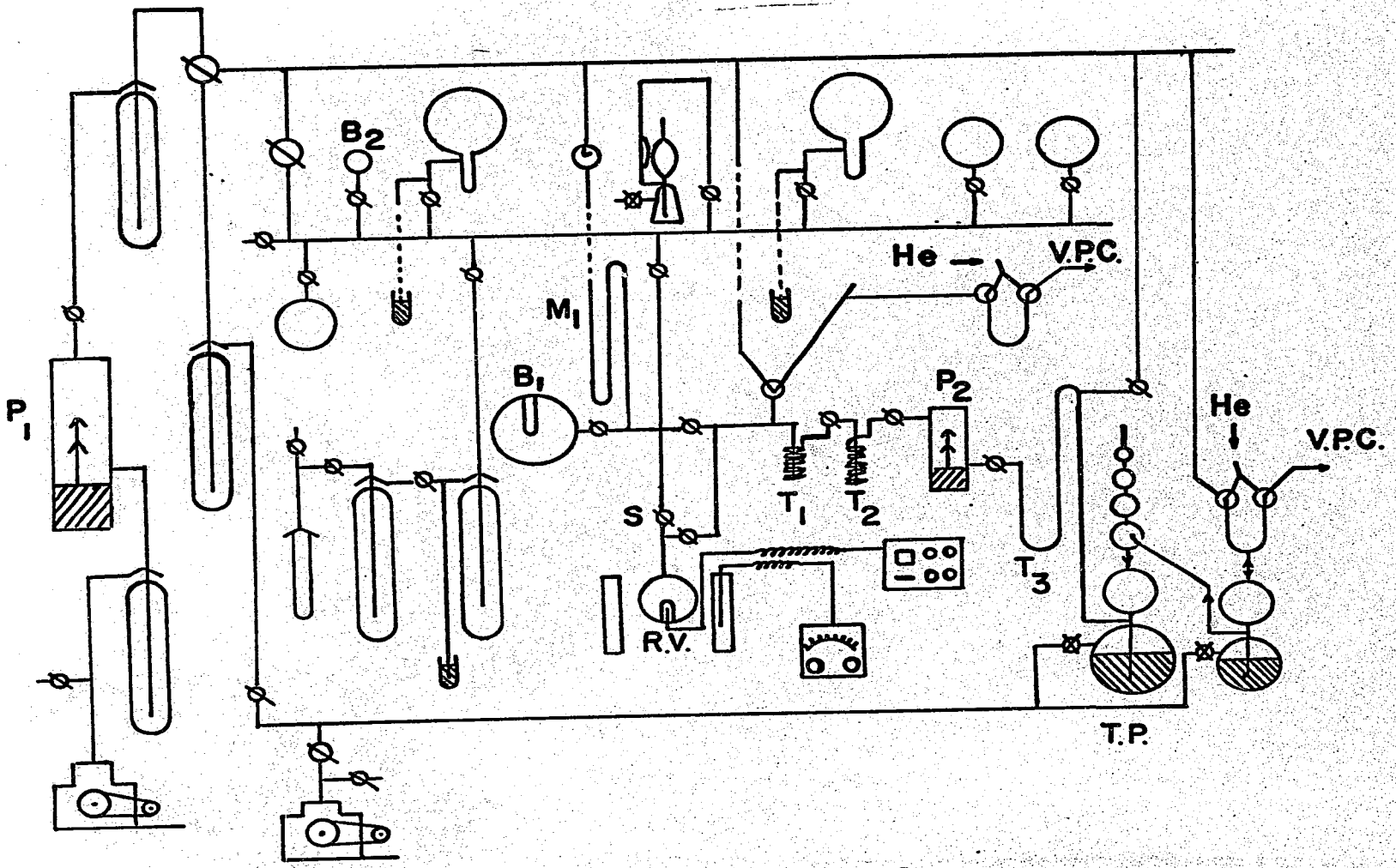
B2
M1
B1
P1
P2
He
V.P.C.
S
T1
T2
T3
R.V.
T.P.
He
V.P.C.

temperatures, namely the freezing point of tin (231.9°C), lead (327.3°C) and zinc (419.5°C). In determining the emf of a thermocouple at a freezing point, the time in which observations may be taken is limited to the period of freezing, after which the material must be melted again before further observations are made. In the case of boiling points, there is no such limit in time since the material can be boiled continuously. On the other hand, it is not necessary to apply a pressure correction to the freezing point.

Procedure

Before each experiment the system was evacuated to a pressure of 10^{-5} mm. A sample of acetaldehyde was admitted to a 2-litre bulb (B_1) and was allowed to expand into the reaction vessel by opening stop-cock S. When inert gas was added to acetaldehyde, a cold finger was provided in bulb S to ensure complete mixing. For the experiments in which the pressure of acetaldehyde was low (20-50 mm.) a small bulb B_2, of volume 152.2 cc, was used for the expansion. Since low pressures of acetaldehyde could not be read accurately on the manometer (M_1), it was necessary to have a calibration curve for this purpose. This was achieved by expanding a certain amount of inert gas into the reaction vessel using a 3 cc. tube on the manifold so that the initial pressure was always greater than 20 mm Hg. The concentration of the inert gas after

expansion was measured by means of a gas burette, and the pressure in the vessel could then be calculated.

At the end of each run the products and reactant were fractionated through traps at -130°C (n-propanol slush), -150°C (2-methylbutane slush) and -210°C (solid nitrogen). A mercury diffusion pump (P_2) in conjunction with a Toepler pump (T.P.) was used to pump the products and reactant from the reaction vessel.

The non-condensables, hydrogen, carbon monoxide and methane, were measured in a gas burette and analyzed on a 4-metre 100-mesh silica-gel column maintained at 0°C. Analysis on a 1-metre silica-gel column at 30°C showed that the -210°C fraction contained ethane, carbon dioxide, ethylene and the residual methane. The volumes of these gases were also measured by gas burette. The total volume less the volumes of the minor products would be the volume of methane and carbon monoxide formed. Since the chain length of acetaldehyde pyrolysis is over 1000 under the present experimental conditions, the rates of formation of methane and carbon monoxide are equal. Acetone was measured by transferring all the condensable products to a sampling U-tube, followed by gas-chromatographic analysis on a 5-metre column of 20% tetraethylene glycol dimethyl ether on chromosorb P (hexamethyldisilazane treated) at 30°C with a flow rate of 100 cc. per min. The area of the acetone peak was measured since the peak height measurement could not yield a good calibration curve. The column was calibrated using a measured amount of acetone mixed with an

appropriate quantity of the reactant used in pyrolyses. All columns were 1/4 inch in diameter. A good base line was obtained by installing Edwards pressure controllers in both reference flow and sensing flow of the chromatograph. Since a thermal conductivity detector measures a differential conductivity between a carrier gas and a mixture of solute in the carrier gas, it is obvious that the greatest sensitivity will be obtained when the carrier and the solute have widely differing conductivities. Since most products have low conductivities, a carrier gas of high conductivity should be used. Helium was chosen as a carrier gas in all cases. However, the determination of hydrogen in helium poses a problem because the thermal conductivity of hydrogen is higher than that of helium and a negative peak should result. In actual fact, at low concentrations the thermal conductivity of hydrogen appears to be lower than that of helium. Therefore, it gives a positive response peak like those obtained with other components; these peaks are reliable for quantitative determination of hydrogen in helium (57-59). Large amounts of hydrogen give rise to peaks responding in both directions - so called W-peaks - and these double peaks are not reliable for quantitative measurements. Fortunately, the amounts of hydrogen formed in the present investigation were small and the response was sufficiently linear and reproducible.

Attempts have been made to detect ketene in the system, but it was not found. This, however, does not prove

the presence or absence of ketene, because ketene polymerizes with acetaldehyde to a small extent at low temperatures. A transparent polymer was noted in the -130°C and -150°C traps after each run. When acetaldehyde was pyrolyzed together with small amounts of ketene at 450°C, 80% of the ketene was found to be consumed.

CHAPTER III

RESULTS AND ANALYSIS

The major products in this pyrolysis were carbon monoxide and methane. The minor products were hydrogen, ethane, acetone, ethylene, propionaldehyde and carbon dioxide. Fig. 2 shows the relative rates of the minor product formation. It is to be seen in this figure that for hydrogen production there is no sign of the induction period found by Trenwith (16). There is also no initial rapid formation of ethylene, which was found by Dexter and Trenwith (17) and by us when we used impure acetaldehyde. The initial rates of some of the products are given in Table 1. These rates are averages from 3 to 8 experiments, and were obtained not from initial slopes but by extrapolating rates to zero time.

The Overall Kinetics and Mechanism

It has been established by many workers that the main products of the thermal decomposition of acetaldehyde are equal quantities of methane and carbon monoxide (11,60, 61). This was confirmed by carrying out low-conversion runs and measuring the amounts of carbon monoxide and methane by gas chromatography. In all our runs the amounts of methane and carbon monoxide were too large to be measured by gas chromatography. Therefore, the amount of total gas was

Figure 2

Typical yield-time plot for the formation of all products at 523°C at 117 mm Hg.

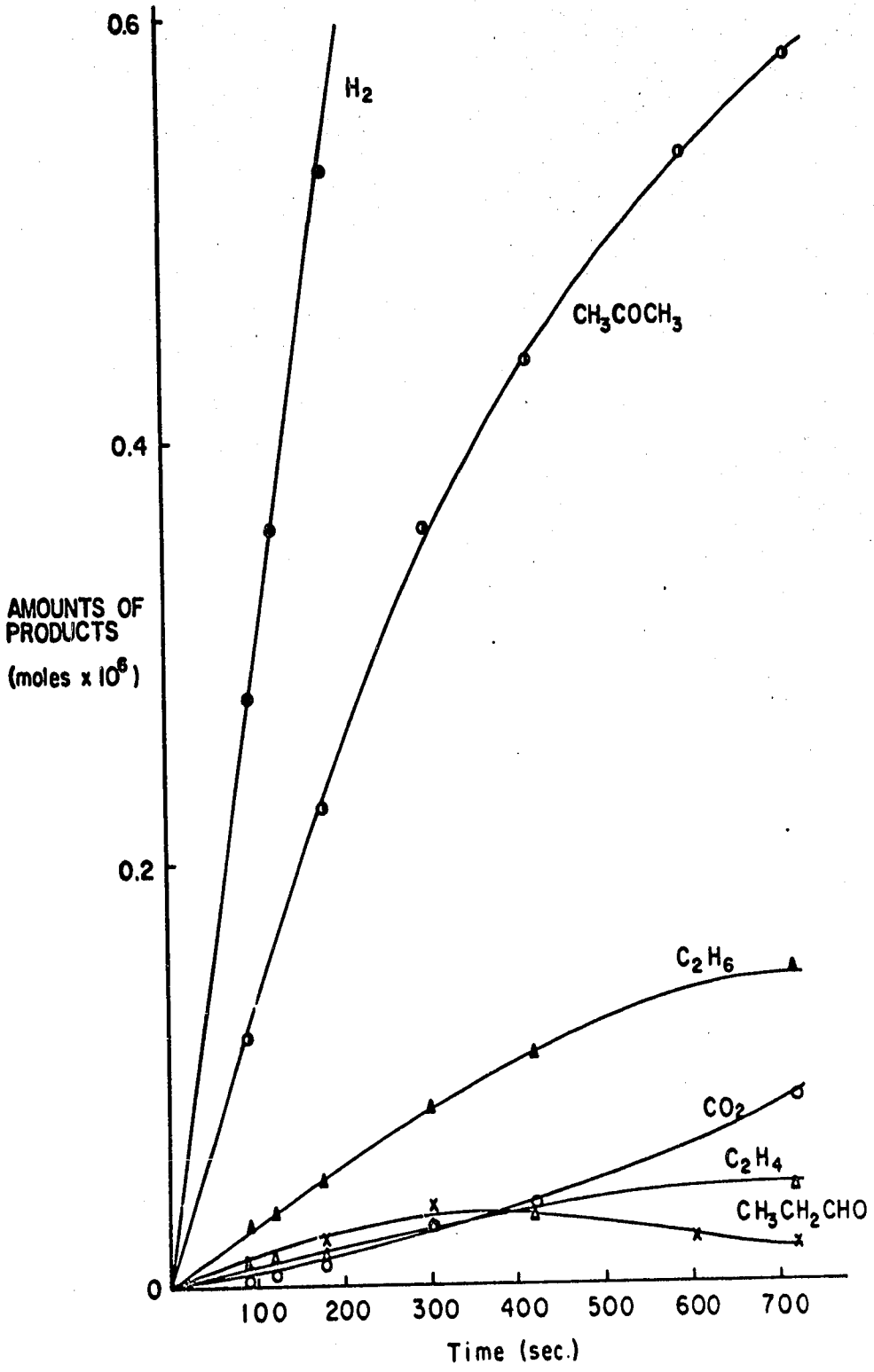
0.6
0.4
0.2
0
AMOUNTS OF PRODUCTS
(moles x 10^6)
H2
CH3COCH3
C2H6
CO2
C2H4
CH3CH2CHO
100
200
300
400
500
600
700
Time (sec.)

Table 1 – Initial rates of product formation.
All rates are in mole cc^{-1} sec^{-1}.

Pressure of Acetaldehyde (mm Hg)	$v_{CH_4} \times 10^{10}$	$v_{H_2} \times 10^{13}$	$v_{acetone} \times 10^{13}$	$v_{C_2H_6} \times 10^{13}$	$v_{C_2H_5CHO} \times 10^{13}$
T = 480°C					
77	3.30	4.1	2.4	0.219	–
118	6.24	8.08	4.34	0.332	ca. 0.1–0.2
150	9.13	10.97	6.39	0.437	–
195	13.2	15.97	9.25	0.576	–
295	25.2	29.83	17.5	0.890	–
559	65.3	79.16	–	1.75	–
T = 500°C					
20	1.00	–	–	0.1265	–
30	1.85	–	–	0.263	–
50	4.07	–	–	0.546	–
77	7.79	11.6	5.8	0.95	–
118	14.80	21.83	11.0	1.49	ca. 0.5
150	20.82	30.7	16.0	1.80	–
195	32.40	44.98	23.7	2.62	–
295	60.2	79.5	44.7	4.0	–
559	160.4	207.8	–	7.95	–

Table 1 (continued)

Pressure of Acetaldehyde (mm Hg)	$v_{CH_4} \times 10^{10}$	$v_{H_2} \times 10^{13}$	$v_{acetone} \times 10^{13}$	$v_{C_2H_6} \times 10^{13}$	$v_{C_2H_5CHO} \times 10^{13}$
T = 523°C					
11	1.10	-	-	0.220	-
20	2.28	5.60	-	0.540	-
30.5	3.50	-	-	0.952	-
40	6.20	13.6	6.51	1.65	-
55	10.0	22.4	10.00	2.31	-
77	17.5	32.5	15.6	3.83	ca. 1.5
117	32.6	61.2	27.2	5.88	ca. 1.5
150	48.0	82.5	37.5	7.27	ca. 2
195	71.0	128.7	57.5	9.46	ca. 3
292	129.0	230.0	-	15.73	-
558	360.0	555.0	-	30.67	-
T = 540°C					
22	4.8	14.0	4.3	1.6	-
42	12.4	32.0	11.5	4.0	-
79	36.4	80.0	31.8	10.0	-
118	62.0	140.0	52.0	14.2	ca. 5
152	93.0	198.0	78.0	20.4	-
198	143.0	295.0	121.5	28.6	-
296	250.0	500.0	-	41.7	-
563	650.0	1230.0	-	80.0	-

determined by means of a gas burette. This method of determination was found to be highly accurate and reproducible. Fig. 3 shows the yield-time plot for methane, and the initial rates of methane formation at each pressure were obtained in the manner shown in Fig. 4. The order of methane production was 1.5 at pressures above 100 mm Hg. and some falling-off of the rate constant was noted at lower pressures. The double logarithmic plot of methane production against initial acetaldehyde pressure is given in Fig. 5. Besides the major products, other minor products such as hydrogen, acetone, ethane and propionaldehyde were formed. To explain these results, especially the products obtained, we suggest the following mechanism, which is the Rice-Herzfeld scheme to which a number of reactions have been added:

[1] $CH_3CHO \longrightarrow CH_3 + CHO$

[2] $CHO \longrightarrow CO + H$

[3] $H + CH_3CHO \longrightarrow H_2 + CH_3CO$

[4] $CH_3 + CH_3CHO \longrightarrow CH_4 + CH_3CO$

[5] $CH_3CO \longrightarrow CH_3 + CO$

[6] $CH_3 + CH_3CHO \longrightarrow CH_4 + CH_2CHO$

[7a] $CH_2CHO \longrightarrow CH_2CO + H$

[7b] $CH_2CHO + CH_3CHO \longrightarrow CH_3CHO + CH_3CO$

[8] $CH_3 + CH_3CHO \longrightarrow CH_3COCH_3 + H$

[9] $CH_3 + CH_3 \longrightarrow C_2H_6$

[10] $CH_3 + CH_2CHO \longrightarrow CH_3CH_2CHO$

By applying the steady-state treatment, we find for the steady-state concentration of the radicals:

$$[CH_3CO] = \frac{k_4}{k_5} [CH_3CHO] [CH_3]$$

$$[CH_3] = \left(\frac{k_1}{k_9}\right)^{\frac{1}{2}} [CH_3CHO]^{\frac{1}{2}} \text{ (neglecting reaction [10])}$$

$$[H] = \frac{k_1}{k_3} + \frac{k_{7a}}{k_3} \frac{[CH_2CHO]}{[CH_3CHO]} + \frac{k_8}{k_3} [CH_3]$$

$$[CH_2CHO] = \frac{k_6 [CH_3] [CH_3CHO]}{k_{7a} + k_{7b} [CH_3CHO] + k_{10} [CH_3]}$$

Reaction [1], the initiation reaction, is concluded to be essentially in its first-order region. The rate of ethane formation is significantly greater than that of propionaldehyde formation, so that the main termination step is [9]; a variety of evidence (54,55) has shown that this reaction is second-order under the usual pyrolysis conditions.

First-order initiation and $\beta\beta$ termination (62) lead to 3/2-order kinetics, in agreement with the results of many workers for this reaction (14,15,36,63); in the

Figure 3

Typical methane yield-time plots at 523°C.

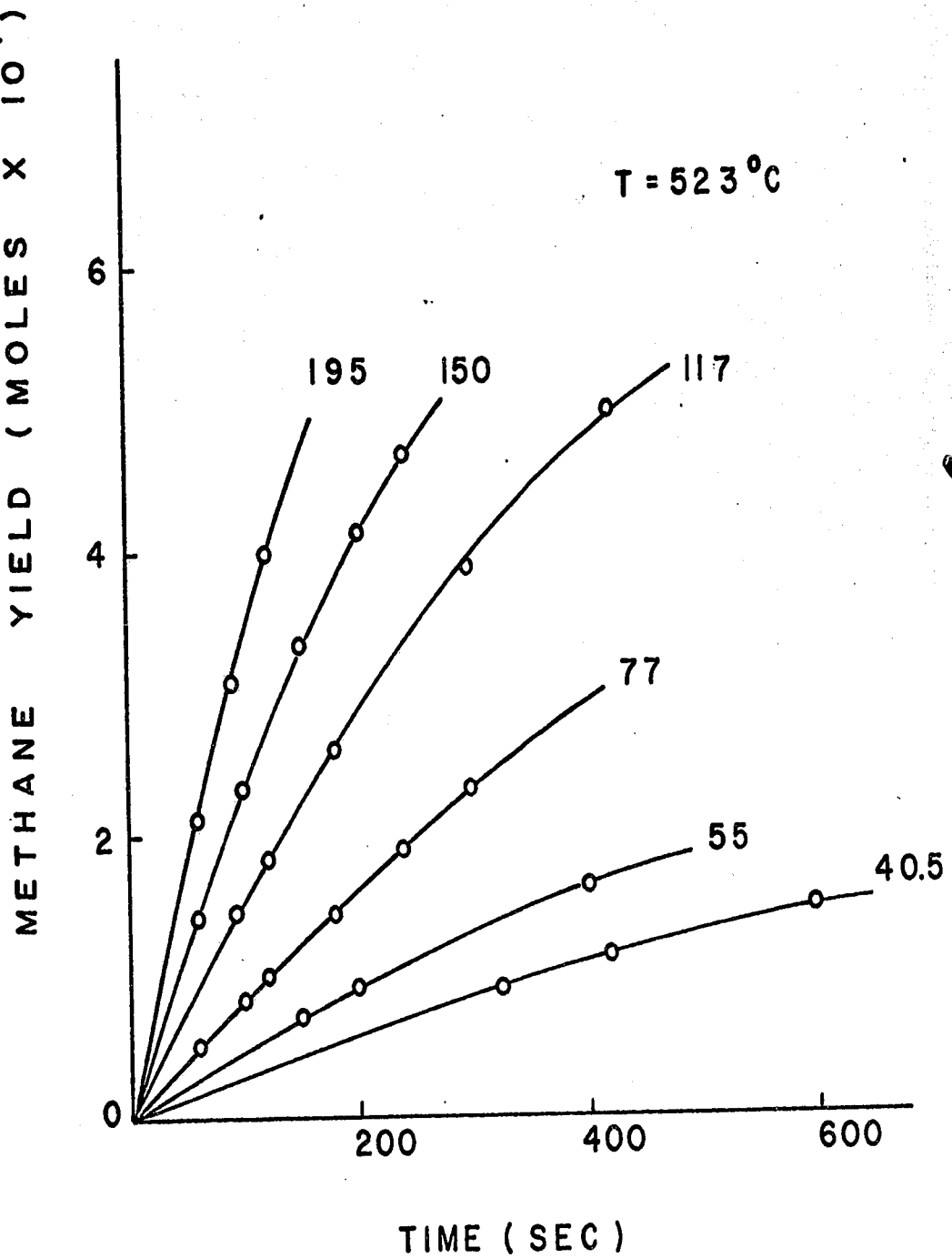
METHANE YIELD (MOLES X 10^4)
T = 523 °C
195
150
117
77
55
40.5
0
2
4
6
200
400
600
TIME (SEC)

Figure 4

Typical v_{CH_4} vs. t plot.

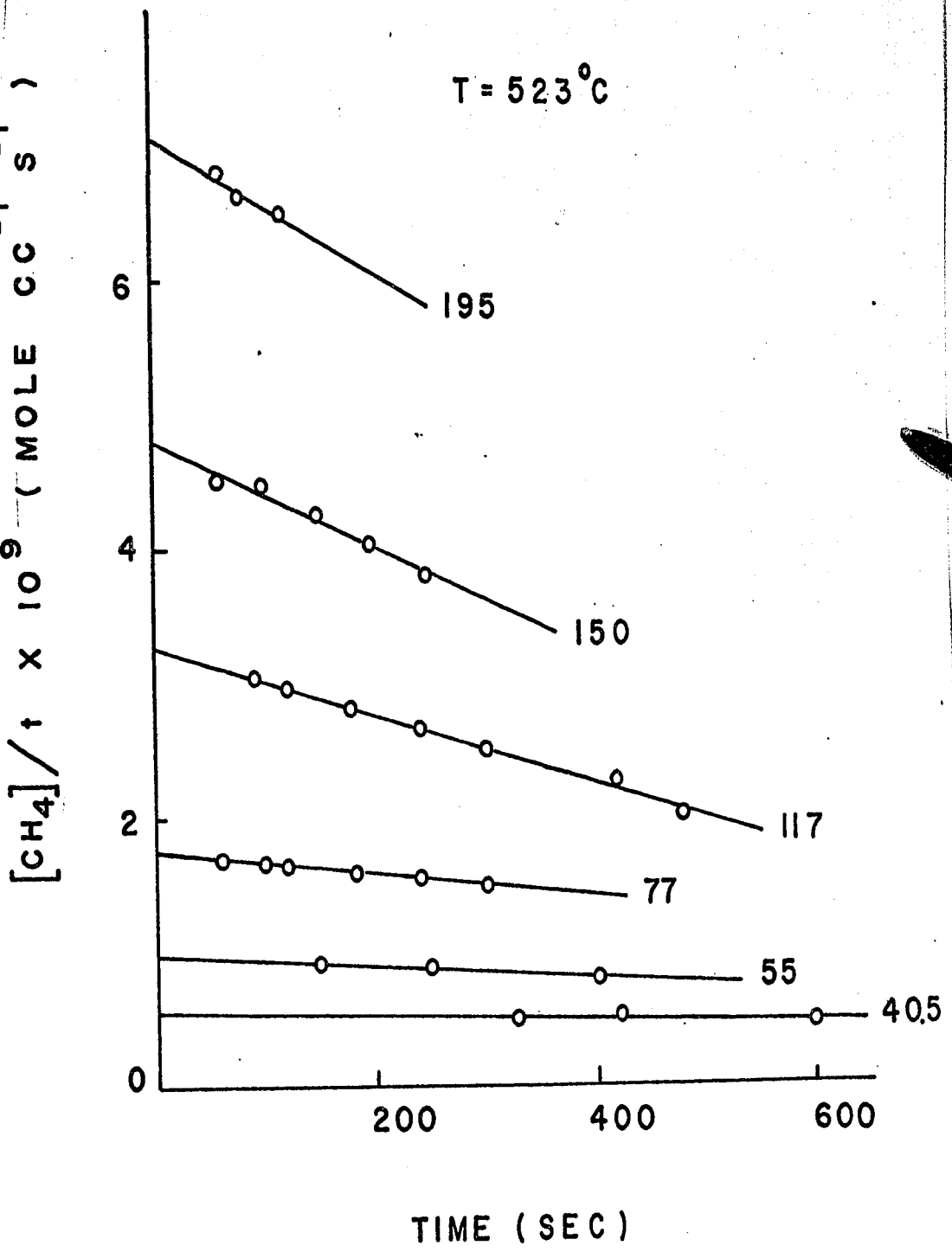
T = 523°C
195
150
117
77
55
40.5
6
4
2
0
200
400
600
TIME (SEC)
[CH4]/t X 10^9 (MOLE CC^-1 S^-1)

Figure 5

Order plot for methane production.

Data obtained from packed vessel (S/V = 9.4) are given by x and those from unpacked (S/V = 0.60) by o.

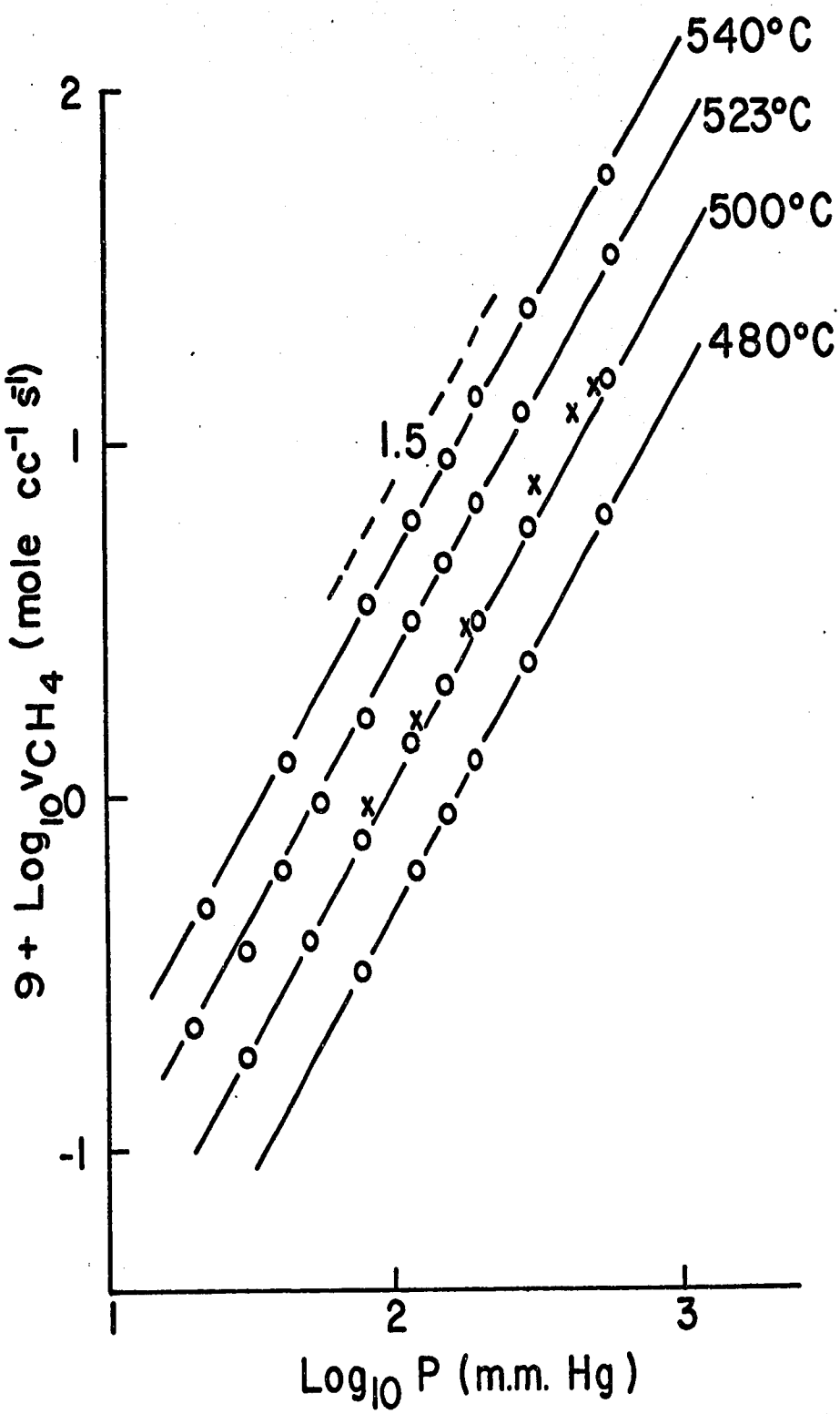
540°C
523°C
500°C
480°C
1.5
2
1
0
-1
9 + Log10 VCH4 (mole cc-1 s-1)
1
2
3
Log10 P (m.m. Hg)

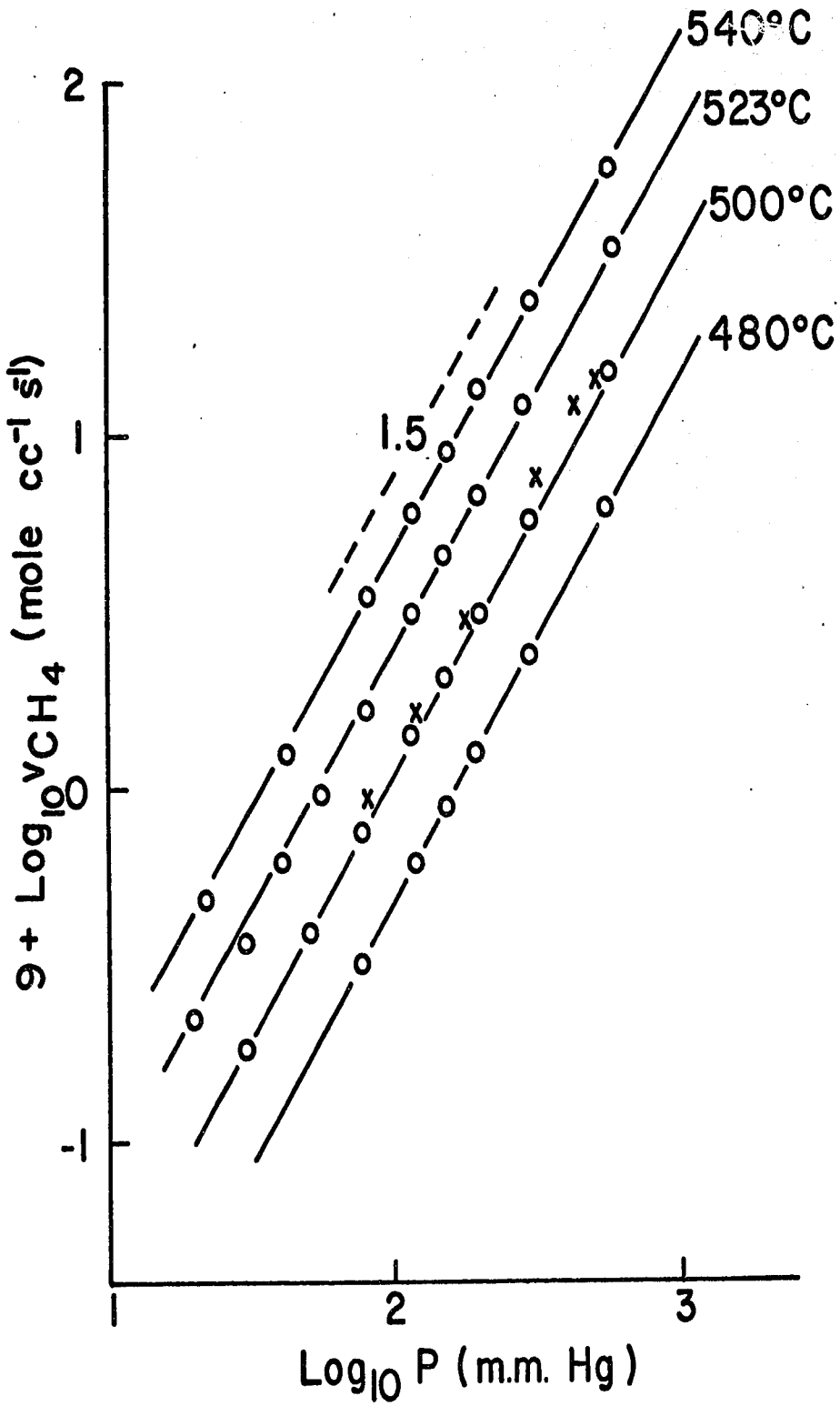
540°C
523°C
500°C
480°C
1.5
2
1
0
-1
9 + Log10 VCH4 (mole cc-1 s-1)
1
2
3
Log10 P (m.m. Hg)

present investigation it was confirmed that the methane and carbon monoxide production is strictly 3/2-order in acetaldehyde. If one plots the initial rates of formation for methane against $\left[CH_3CHO\right]^{3/2}$, a linear relationship is observed as seen in Fig. 6. If the minor termination step [10] is ignored the rate of disappearance of acetaldehyde, approximately equal to the rates of formation of carbon monoxide and methane, is found to be

$$-\frac{d\left[CH_3CHO\right]}{dt} = \frac{d\left[CH_4\right]}{dt} = \frac{d\left[CO\right]}{dt}$$

$$= k_4 \left(\frac{k_1}{k_9}\right)^{1/2} \left[CH_3CHO\right]^{3/2} \qquad (1)$$

Since earlier work (64) indicated that there was a slight falling-off of the overall rate constant at low pressures, it was decided that further work should be done to confirm this effect. Rates of production of methane were measured at 540°C at pressures from 0.8 mm to 558 mm Hg. The results are shown in Table 2 and in Fig. 7, in which the rate of methane formation is plotted against initial pressures of acetaldehyde in logarithmic units. The order of methane formation is exactly 1.5 at high pressures (>100 mm Hg) and is about 1.7 when the initial pressures have gone below 20 mm Hg. It is seen from Fig. 8 that significant falling-off of the overall rate constant is observed. As $k_{overall}$ is also a measure of the square root of the ratio k_1/k_9, it is concluded that k_1 is falling off faster than k_9. The fact that k_1

Figure 6

Plot of v_{CH_4} vs. $\left[CH_3CHO\right]^{3/2}$.

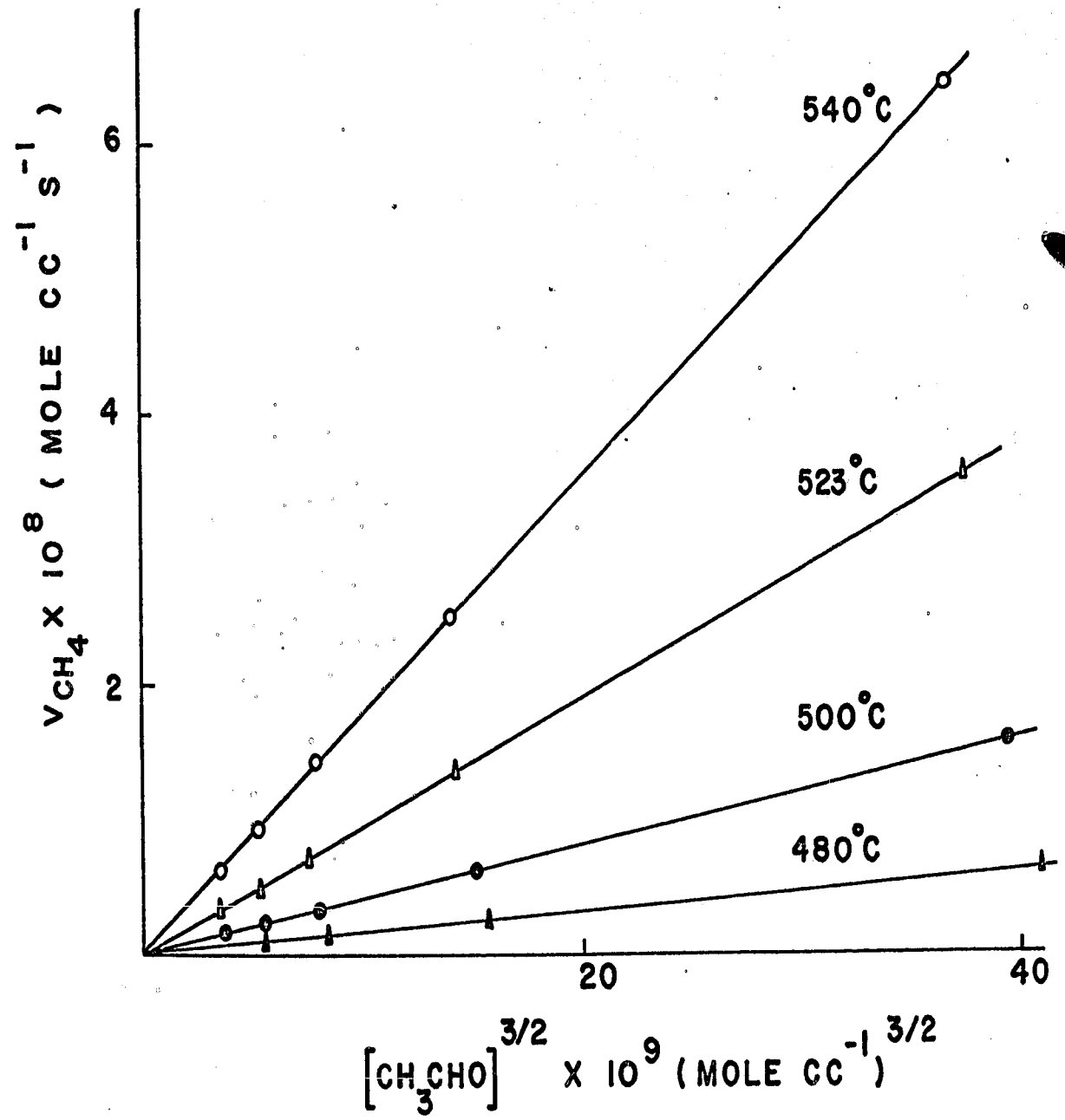
540°C
523°C
500°C
480°C
6
4
2
20
40
$v_{CH_4} \times 10^8$ (MOLE CC^{-1} S^{-1})
$[CH_3CHO]^{3/2} \times 10^9$ (MOLE CC^{-1})$^{3/2}$

Table 2 - Overall rate constant as a function of pressure at 540°C

Pressure of CH_3CHO mm Hg	$v_{CH_4} \times 10^{12}$ (mole cc^{-1} sec^{-1})	$k_{overall}$ ($cc^{\frac{1}{2}}$ $mole^{-\frac{1}{2}}$ sec^{-1})
563	65000	1.76
292	25000	1.77
198	14300	1.85
152	9300	1.79
118	6200	1.75
79	3640	1.87
42	1240	1.64
22	480	1.67
11.2	172	1.65
4.23	34.3	1.42
1.84	9.3	1.35
1.28	5.2	1.28
0.787	2.3	1.19

Figure 7

Order plot for methane production at 540°C, from 0.8 mm to 558 mm Hg.

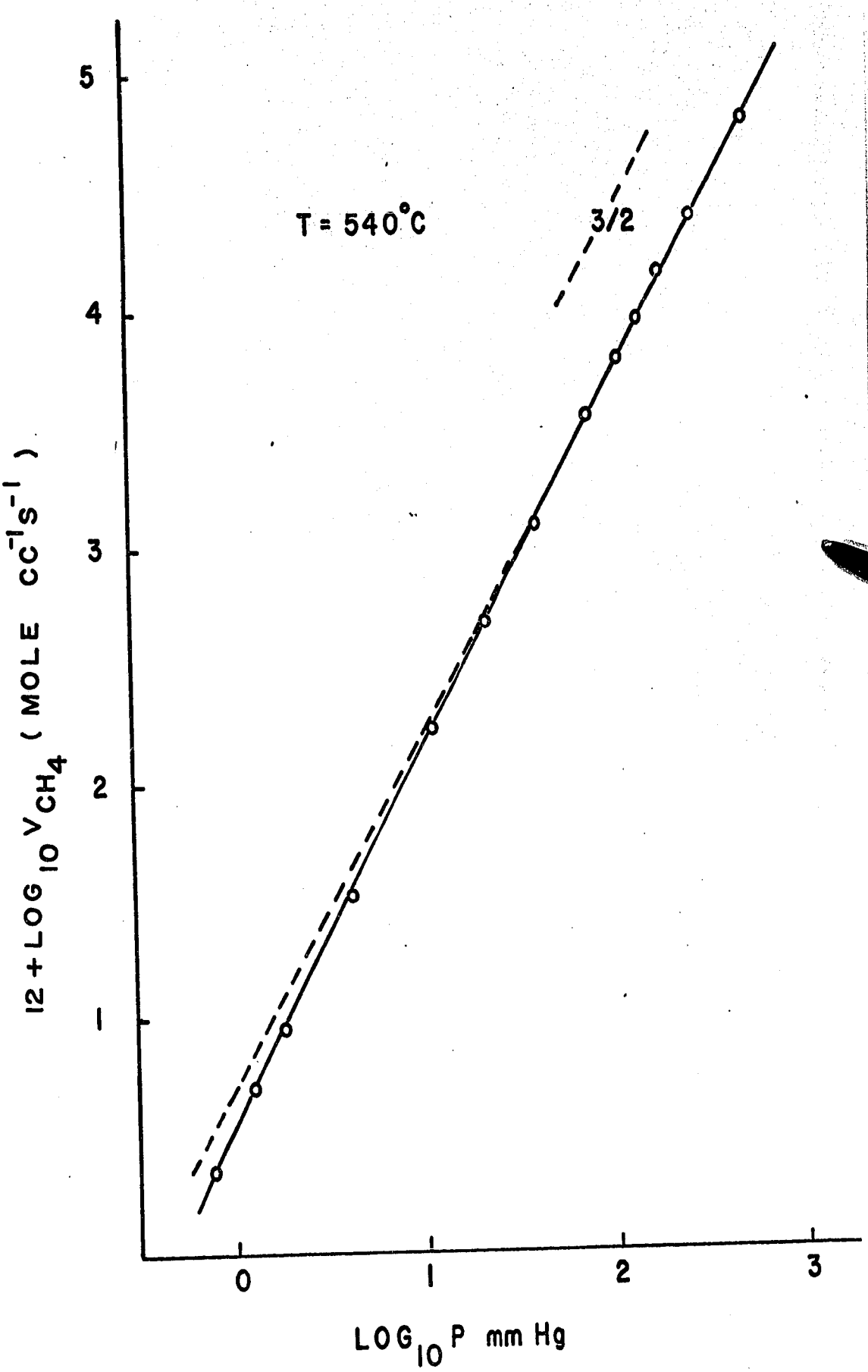
T = 540°C
3/2
5
4
3
2
1
0
1
2
3
12 + LOG10 VCH4 (MOLE CC-1S-1)
LOG10 P mm Hg

Figure 8

Plot of $\log_{10} k_{overall}$ vs. $\log_{10} P$ at 540°C.

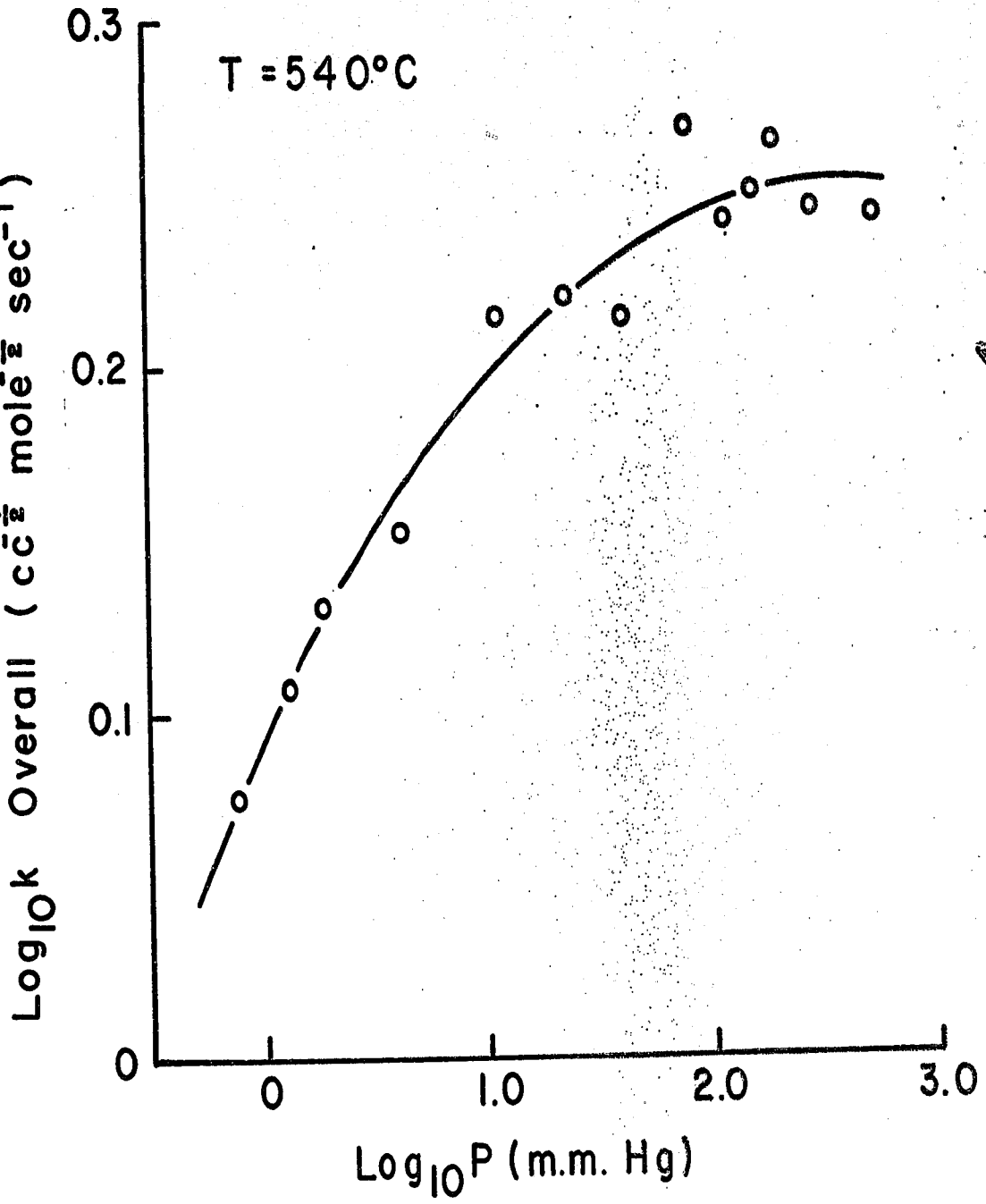
T = 540°C
0.3
0.2
0.1
0
0
1.0
2.0
3.0
Log10k Overall (cc^-1/2 mole^-1/2 sec^-1)
Log10P (m.m. Hg)

falls off earlier than k_9 is understandable since acetaldehyde has one atom less than ethane, so that acetaldehyde has three vibrational degrees of freedom less than ethane. The knowledge of the ratio k_1/k_9 is important, not only because it can explain the proposed mechanism, but because it can clarify the inert-gas effects that we have observed and that have been found by Dexter and Trenwith (17). A discussion of this is given in a later section.

The overall rate constant at each temperature is obtained by averaging all the values at high pressures. These results are given in Table 3 and the Arrhenius plot is shown in Fig. 9. The rate constant thus obtained was given by

$$\log k_{overall} \ (cc^{\frac{1}{2}} \ mole^{-\frac{1}{2}} \ sec^{-1})$$

$$= (13.45 \pm 0.2) - \frac{49,082 \pm 1025}{2.303 \ RT}$$

The activation energy agrees satisfactorily with the value of 48.0 kcal per mole obtained by Boyer, Niclause and Letort (63) and of 47.6 kcal per mole obtained by Eusuf and Laidler (18). It is interesting to compare these results with those obtained from the thermal decomposition of trifluoroacetaldehyde (65). The overall activation energies in both processes are the same. The frequency factor in trifluoroacetaldehyde is about double that of acetaldehyde. It is expected that the kinetics in both systems should be very similar.

Table 3 - Overall rate constants as a function of temperature

Pressure mm Hg	$k_{overall}$ ($cc^{\frac{1}{2}}$ $mole^{-\frac{1}{2}}$ sec^{-1})	average $k_{overall}$ ($cc^{\frac{1}{2}}$ $mole^{-\frac{1}{2}}$ sec^{-1})
T = 480°C		
118	0.157	
150	0.160	
195	0.156	0.157
295	0.160	
559	0.150	
T = 500°C		
118	0.388	
150	0.379	
195	0.399	0.394
295	0.398	
559	0.406	
T = 523°C		
118	0.906	
150	0.911	
195	0.915	0.911
292	0.905	
558	0.918	
T = 540°C		
118	1.748	
152	1.793	
198	1.853	1.784
296	1.773	
563	1.756	

Figure 9

Arrhenius plot of overall rate constant.

Data obtained from present work are given by o and those of Eusuf and Laidler by x. The data of Arthur and Bell (65) for the CF_3CHO pyrolysis are given by δ .

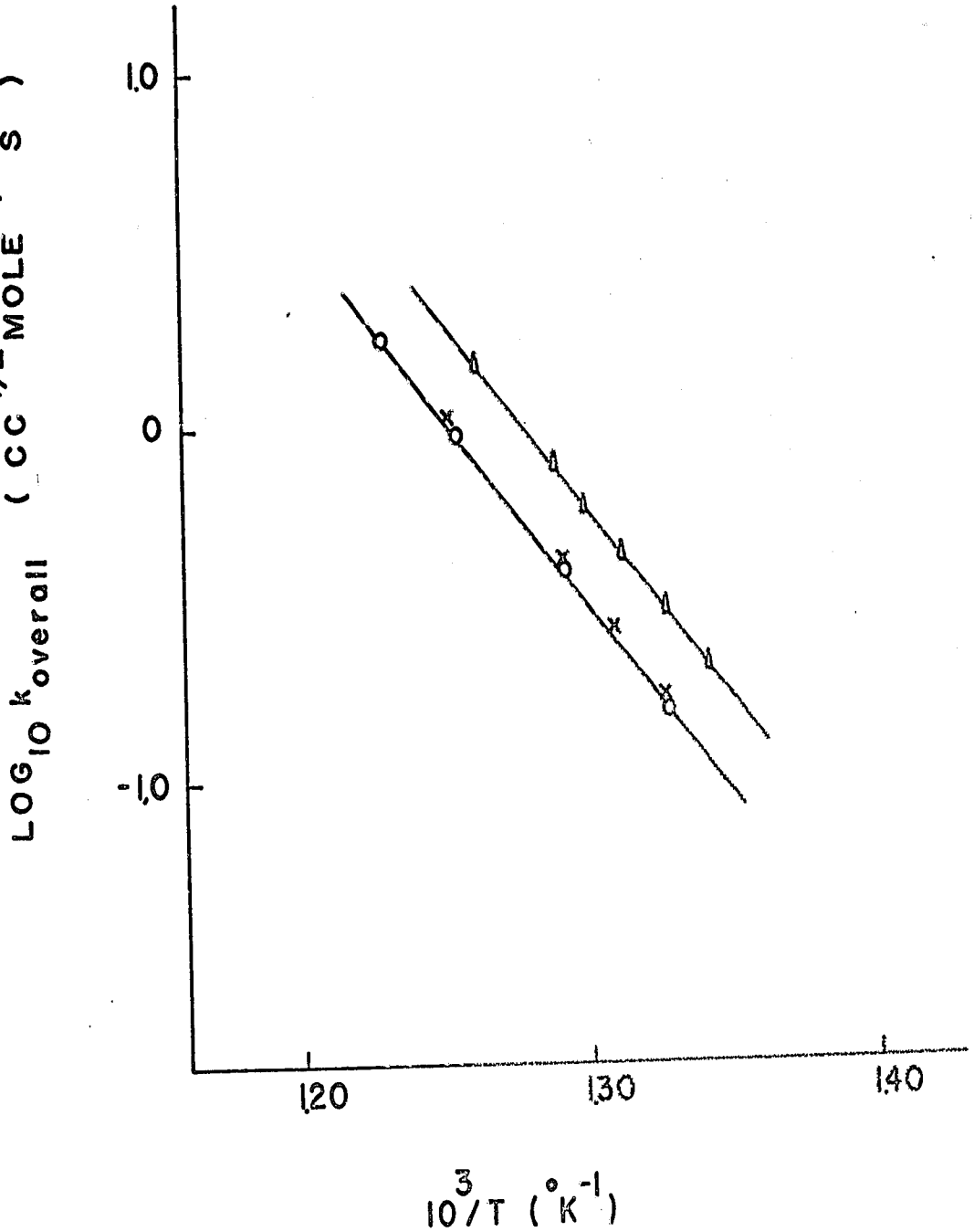
1.0
0
-1.0
1.20
1.30
1.40
$LOG_{10} k_{overall}$ ($cc^{1/2} MOLE^{-1/2} s^{-1}$)
$10^3/T$ ($^\circ K^{-1}$)

From equation (1) it is noted that $k_{overall}$ is identified with $k_4(k_1/k_9)^{\frac{1}{2}}$ and therefore $E_{overall} = E_4 + \frac{1}{2} E_1 - \frac{1}{2} E_9$. The value of E_4 has been measured at 8.4 kcal per mole (cf. later section). It is assumed that $E_9 \simeq 0$ for the recombination of methyl radicals. The average value for the activation energy of 80.3kcal per mole for reaction [1] (cf. later section) gives 48.6 kcal per mole for the experimental activation energy, in excellent agreement with the directly observed value. In the same manner, the frequency factor can be calculated to be 4.6×10^{13} sec^{-1}, also in agreement with the value obtained. It appears, therefore, that the scheme of reactions proposed for the thermal decomposition gives a satisfactory explanation of the results. From the overall rate constant it is possible to calculate k_1 using the value of k_4 (see later section) and the k_9 value of Shepp (66). It can also be estimated directly from the rate of formation of ethane on the assumption that reaction [9] is the only termination step.

Ethane Production

The yield-time plot of ethane formation is given in Fig. 10. The sharp increase in ethane formation, observed by Eusuf and Laidler (18) was not found in the present work. That effect may be caused by impurities in the acetaldehyde they employed. The initial rates of ethane formation are obtained by extrapolation, as shown in Fig. 11. The

Figure 10

Typical ethane yield-time plot at 523°C.

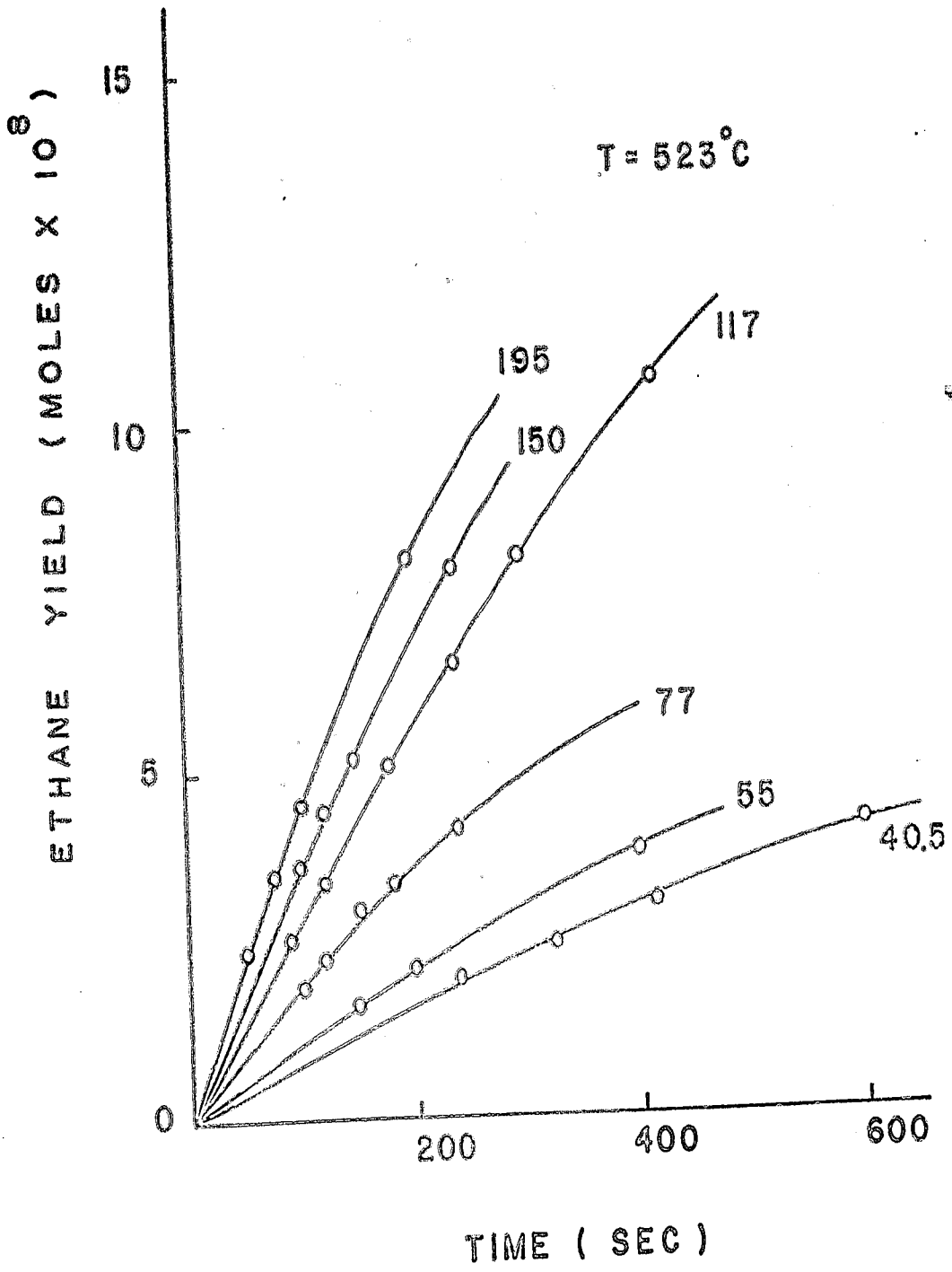
ETHANE YIELD (MOLES X 10^8)
15
10
5
0
T = 523°C
195
150
117
77
55
40.5
200
400
600
TIME (SEC)

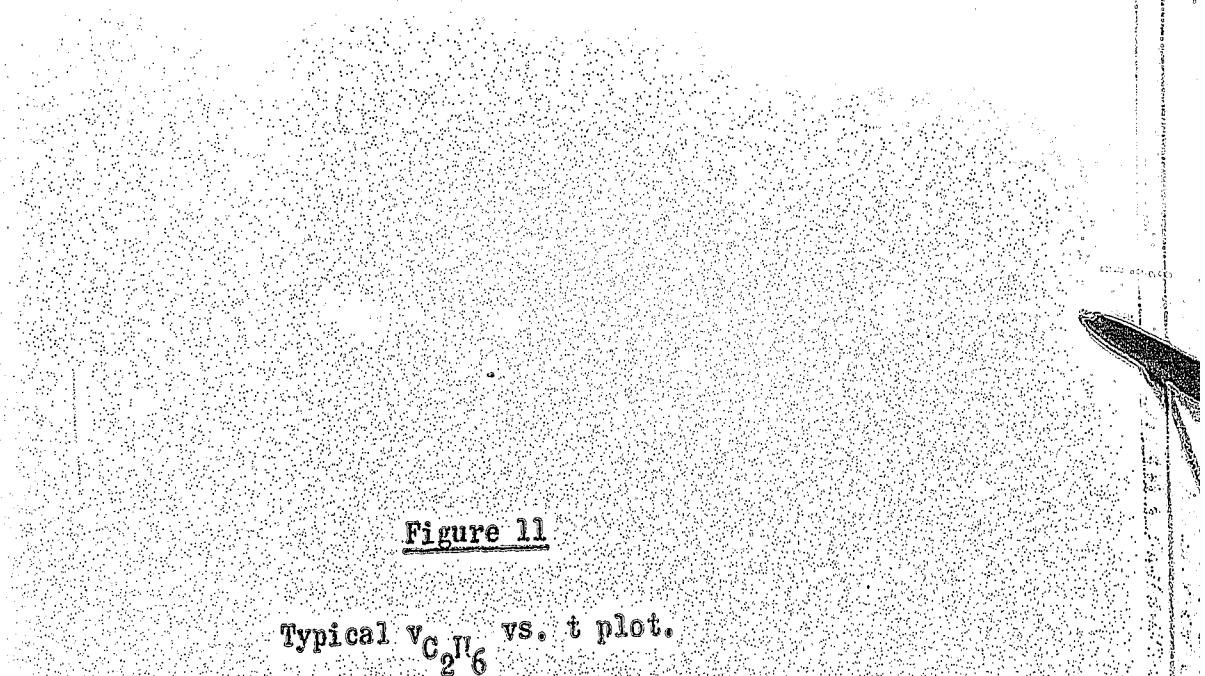

Figure 11

Typical $v_{C_2H_6}$ vs. t plot.

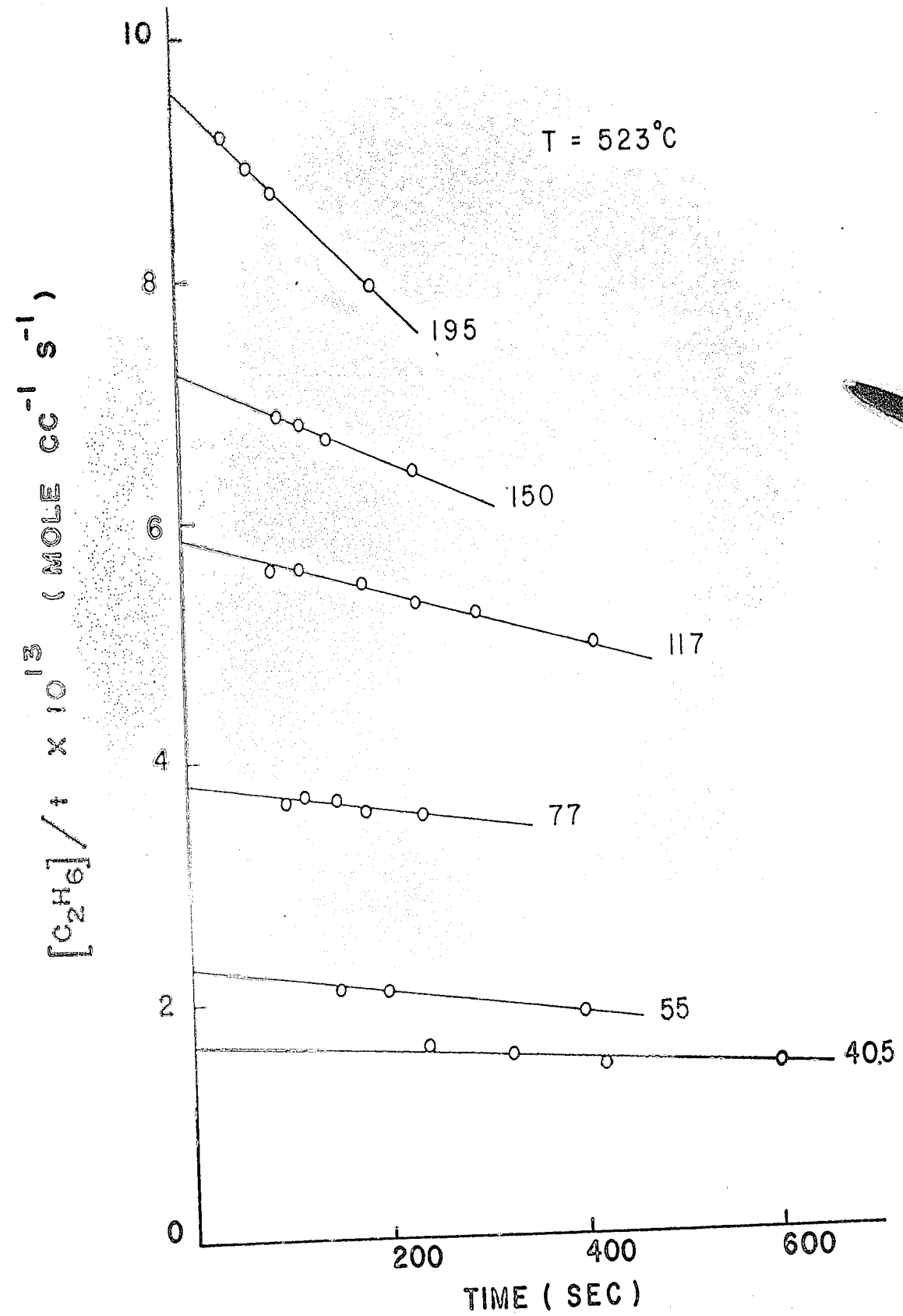
T = 523°C
195
150
117
77
55
40.5
10
8
6
4
2
0
200
400
600
TIME (SEC)
$[C_2H_6]/t \times 10^{13}$ (MOLE CC^{-1} S^{-1})

logarithm of the rate of ethane formation is plotted against the logarithm of the acetaldehyde pressure in Fig. 12. The order is approximately unity (1.1 to be exact) at higher pressures, but there is a significant falling-off at pressures below 80 mm Hg. The formation of methane can result from reactions [4] and [6]. The ratio v_6/v_4 or k_6/k_4 is of the order 10^{-2} under the experimental conditions, and hence the methane production due to reaction [6] is extremely small compared with reaction [4]; it can therefore be neglected. If reaction [4] is the only source of methane, and reaction [9] the only source of ethane,

$$\frac{k_9}{k_4^2} = \frac{v_{C_2H_6}}{v_{CH_4}^2} \left[CH_3CHO\right]^2 \qquad (2)$$

Fig. 13 shows a plot of the logarithm of the right-hand-side of this equation against the logarithm of the acetaldehyde pressure; again the falling-off of k_9 at low pressures is observed. In our earlier work (64) we plotted only the square root of this ratio, which did not reveal this falling-off of k_9. If this ratio is magnified, as in Fig. 13, it is seen that k_9 is slightly pressure dependent even at the higher pressures. It is not possible to derive the value of k_9 from the above experimental quantities, because k_4 is also derived from k_9. The fall-off of k_9 has been observed at various pressure regions in different systems. Dodd and Steacie (67) found a significant decrease of k_9 at about 10 mm

Figure 12

Order plot for ethane formation.

Data obtained from packed vessel (S/V = 9.4) are given by x and those from unpacked are (S/V = 0.60) by o.

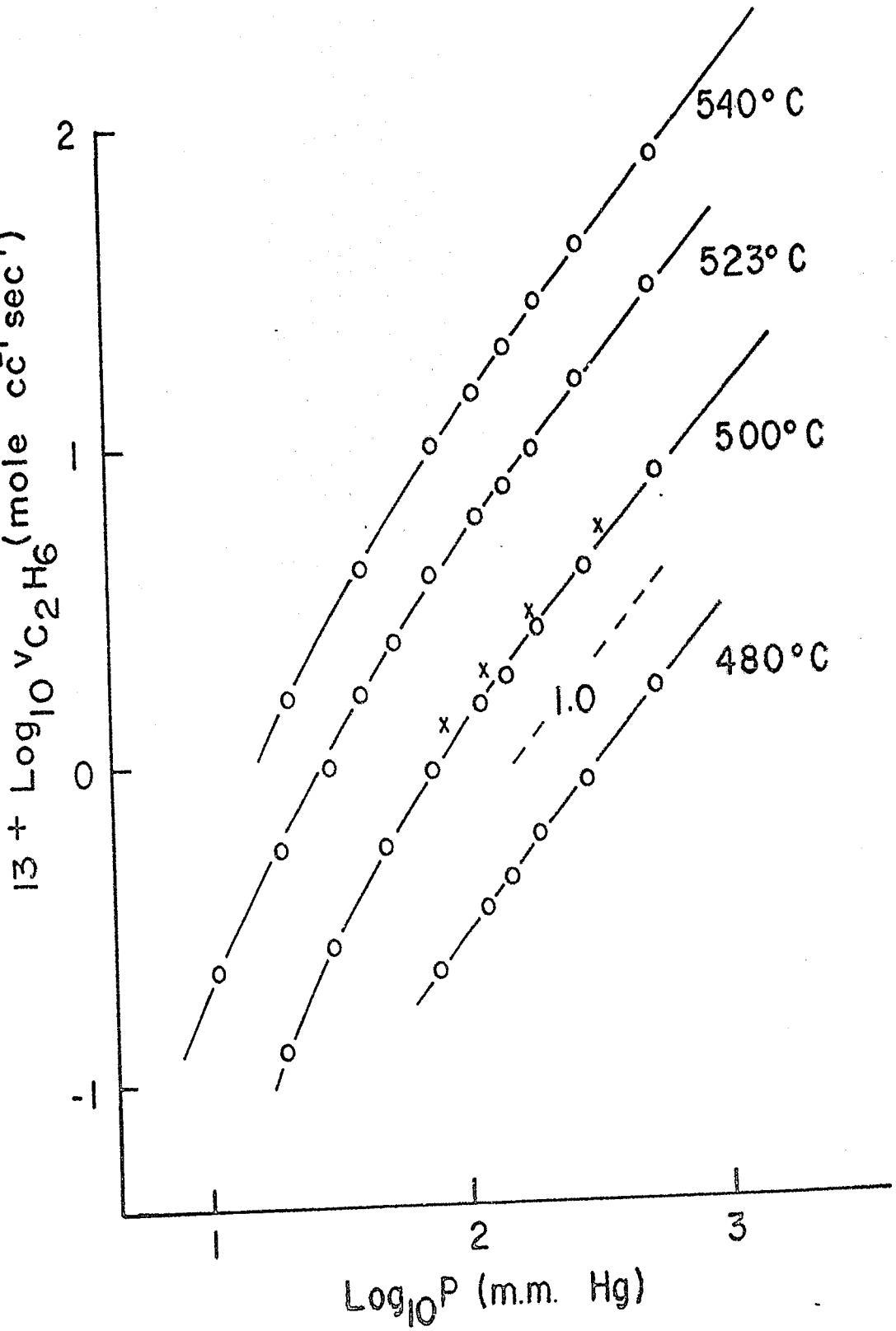
540° C
523° C
500° C
480° C
1.0
2
1
0
-1
1
2
3
$13 + \mathrm{Log}_{10} v_{C_2H_6}$ (mole cc^{-1} sec^{-1})
$\mathrm{Log}_{10} P$ (m.m. Hg)

Figure 13

Plots of $\log_{10} k_9/k_4^2$ vs. $\log_{10} P$ (mm Hg).

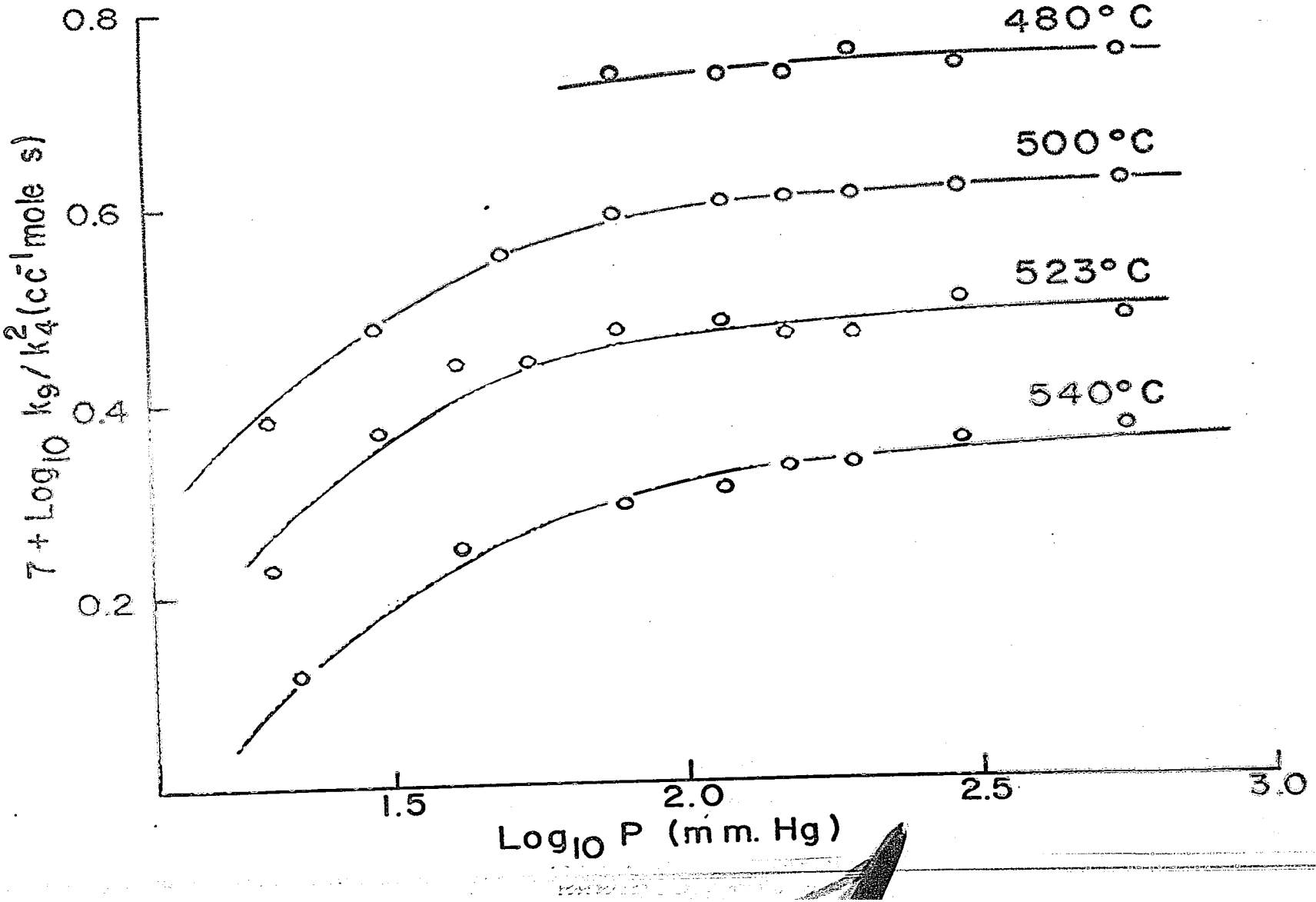
480° C
500° C
523° C
540° C
0.8
0.6
0.4
0.2
7 + Log10 k9 / k4^2 (cc^-1 mole s)
1.5
2.0
2.5
3.0
Log10 P (mm. Hg)

of acetone at 247°C. In the ethane pyrolysis at 550°C Lin and Back (55) have observed a fall-off of the rate coefficient for methyl radical combination below about 200 mm Hg pressure, while in the mercury-photosensitized decomposition of dimethyl ether at 200 to 300°C Loucks and Laidler (68) have observed a fall-off at 100 mm Hg pressure. From the photolysis of azomethane at temperatures of 25 to 180°C, Toby and Weiss (69) have shown an appreciable decrease of the coefficient at about 15 mm of azomethane. The comparison of the pressure dependence of k_9 among these systems is not well understood but is generally believed that the more complex molecules will have higher efficiency in energy transfer. Lin and Back (70) have shown that for two different third bodies of efficiencies λ and λ'

$$\lambda W = \lambda' W'$$

Here W is the collision frequency, defined as $Z\,[X]$, where Z is the collision number, and $[X]$ is the concentration of the third body. Recombination of very simple radicals in the gas phase usually requires a third body in order to prevent the molecule formed on collision from immediately redissociating. Complex radicals do not need this third body, for they possess many internal degrees of freedom which can accommodate the excess energy sufficiently long for it to be removed in a single subsequent collision. The Lindemann theory for the recombination of methyl radicals is

$$CH_3 + CH_3 \underset{b}{\overset{a}{\rightleftharpoons}} C_2H_6^*$$

$$C_2H_6^* + X \xrightarrow{d} C_2H_6 + X^*$$

Steady-state treatment leads to

$$k_9 = \frac{k_a k_d [X]}{k_b + k_d [X]}$$

$$= \frac{k_a [X] \lambda Z}{k_b + [X] \lambda Z}$$

$$= \frac{k_a \lambda W}{k_b + \lambda W}$$

When k_9 and k_9' in two different systems are equal,

$$\frac{k_9}{k_9'} = \frac{\lambda W (k_b + \lambda' W')}{\lambda' W' (k_b + \lambda W)} = 1$$

and hence

$$\lambda W = \lambda' W'$$

It is evident that if $\lambda' > \lambda$, k_9 will fall off at a higher pressure than k_9'.

The value of k_4 can be calculated from equation (3) from the rates of formation of methane and ethane at a particular pressure and using Shepp's value of k_9 (66):

$$\frac{k_9^{\frac{1}{2}}}{k_4} = \frac{v_{C_2H_6}^{\frac{1}{2}}}{v_{CH_4}} \left[CH_3CHO\right] \qquad (3)$$

The values of k_4 at different pressures and temperatures are listed in Table 4. The values of k_4 thus obtained are not constant because k_9 is pressure-dependent. It is therefore necessary to extrapolate the values of k_4 to high pressure where k_9 is not pressure dependent (i.e. $k_9 \longrightarrow k_9^{\infty}$). The extrapolations are shown in Fig. 14. The Arrhenius plot of the rate constant k_4 obtained from extrapolation is given in Fig. 15 and its parameters are

$$\log k_4 = (12.24 \pm 0.06) - \frac{8440 \pm 210}{2.303\ RT}$$

Côme et al. (19,20) have recently studied the decomposition of acetaldehyde at 500°C with initial pressures from 50 to 400 mm Hg, and reported that the order of ethane formation was 1.2, in agreement with our finding. They have concluded that this long-chain radical mechanism is essentially initiated by a first-order process and terminated by recombination of two methyl radicals in the second-order region. They suggested that the order of ethane formation was slightly higher than one because of the occurrence of bimolecular processes such as

$$2CH_3CHO \longrightarrow CH_3CHOH + CH_3CO$$

Table 4 - Rate constants for the hydrogen atom abstraction reaction by the methyl radical

Pressure mm Hg	$k_4 \times 10^{-9}$ (cc mole^{-1} sec^{-1})	extrapolated $k_4 \times 10^{-9}$ (cc mole^{-1} sec^{-1})
T = 480°C		
77	6.38	
118	6.40	
150	6.42	6.25
195	6.22	
295	6.32	
559	6.15	
T = 500°C		
77	7.50	
118	7.40	
150	7.40	
195	7.35	7.26
295	7.30	
559	7.28	
T = 523°C		
40	8.78	
55	8.80	
77	8.68	
117	8.44	8.50
150	8.72	
195	8.69	
292	8.2	
558	8.57	
T = 540°C		
79	10.95	
118	10.48	
152	10.23	9.48
198	10.15	
296	9.83	
563	9.70	

Figure 14

Plots of k_4 vs. 1/P (mm Hg).

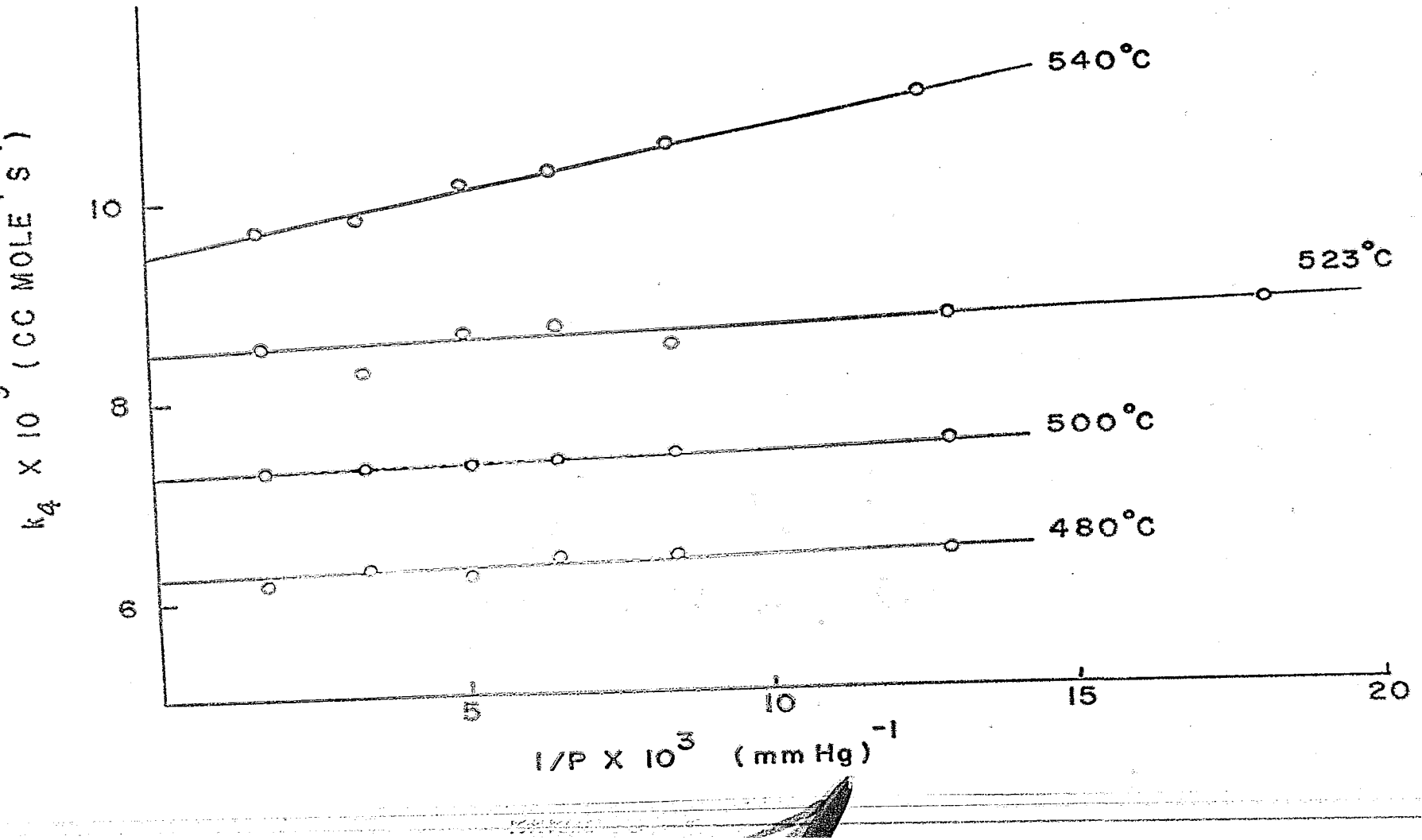
540°C
523°C
500°C
480°C
10
8
6
5
10
15
20
$k_4 \times 10^{-9}$ (CC MOLE^{-1} S^{-1})
1/P X 10^3 (mm Hg)$^{-1}$

Figure 15

Arrhenius plot for the abstraction rate constant k_4.

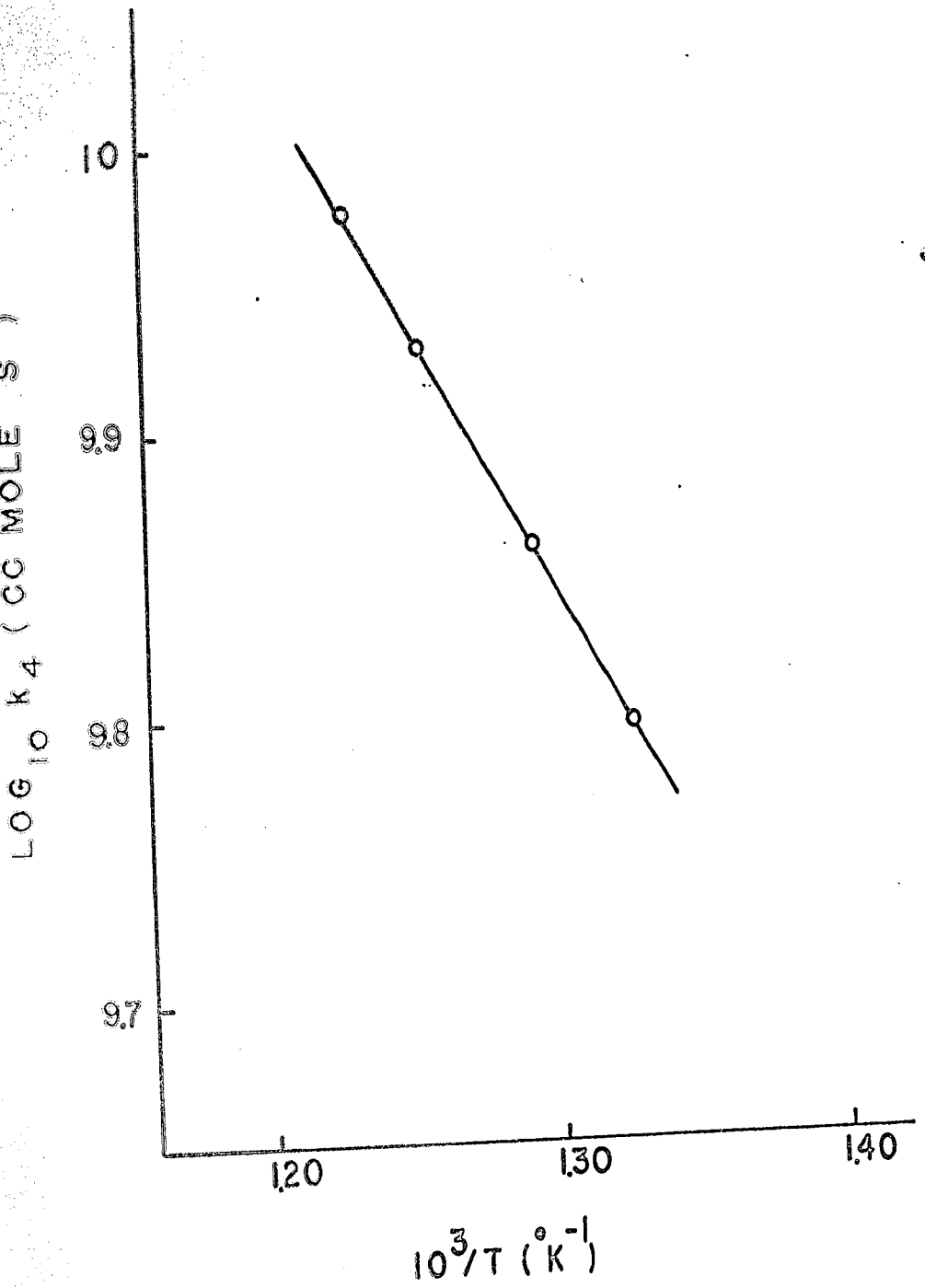
10
9.9
9.8
9.7
LOG10 k4 (CC MOLE-1 S-1)
1.20
1.30
1.40
10^3/T (°K^-1)

followed by

$$CH_3CHOH \longrightarrow CH_3CHO + H$$

or

$$CH_3CHOH + CH_3CHO \longrightarrow CH_3CH_2OH + CH_3CO$$

They also proposed that the higher order of ethane formation could be due to a supplementary formation of C_2H_6 by the process

$$CH_3 + CH_3CHO \longrightarrow C_2H_6 + CHO$$

This reaction is rather unlikely to occur and also inconsistent with the observed inert-gas effect observed by Dexter and Trenwith (17). It is believed, however, that this effect is probably due to a very slight pressure dependence of the initiation at high pressures.

Acetone Production

The typical yield-time plot for acetone formation at 523°C is given in Fig. 16, and the rate vs. time plot is shown in Fig. 17. Trenwith (17) found that the rate of acetone production was greater than the rate of ethane production, and the present work confirms this. Trenwith assumed that acetone is formed by the reaction

[13] $$CH_3CO + CH_3 \longrightarrow CH_3COCH_3,$$

which he therefore concluded to be the main termination step. Eusuf and Laidler (18) pointed out that the overall

Figure 16

Typical acetone yield-time plot at 523°C.

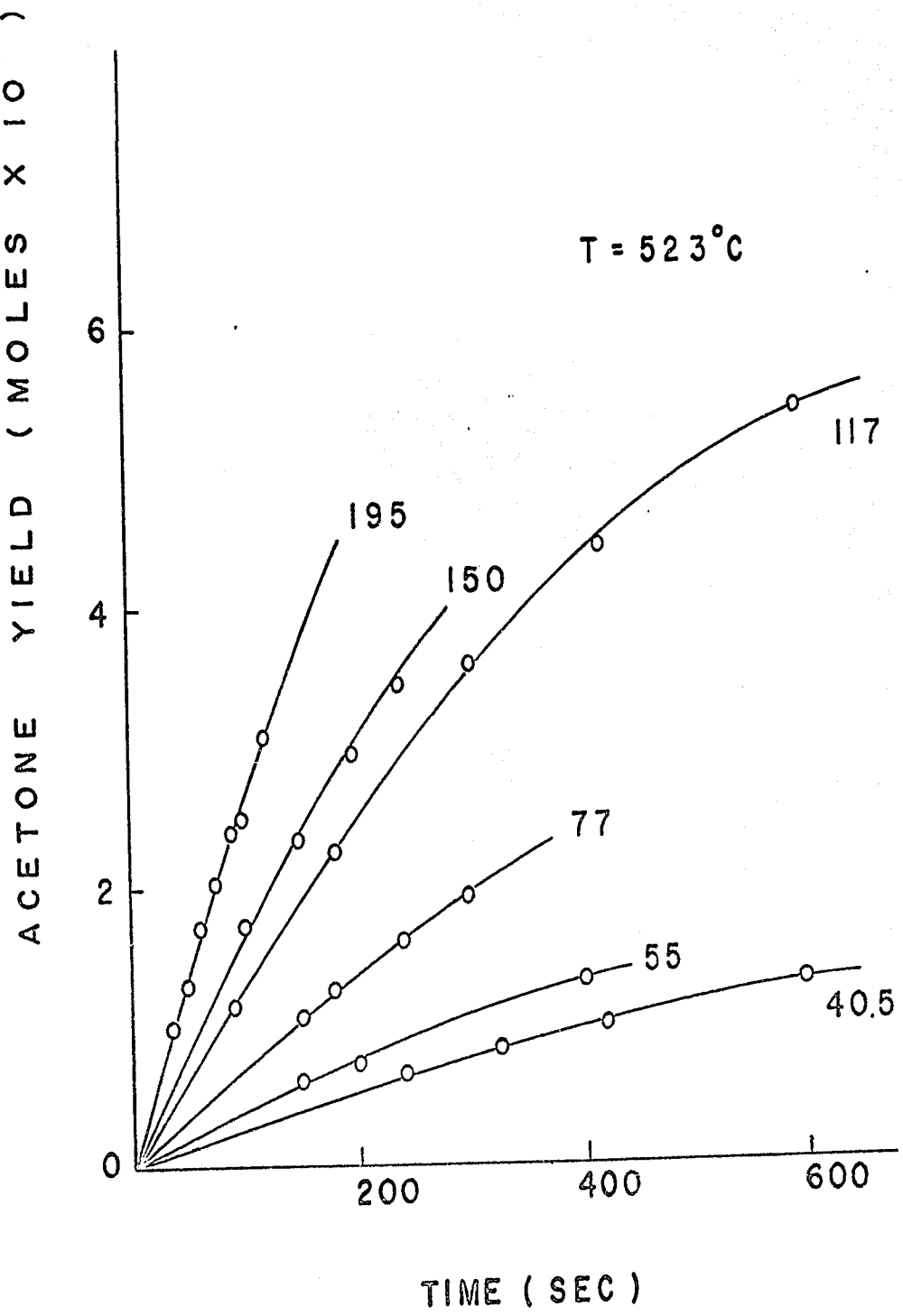
ACETONE YIELD (MOLES X 10^{7})
T = 523°C
195
150
117
77
55
40.5
0
2
4
6
200
400
600
TIME (SEC)

Figure 17

Typical $v_{acetone}$ vs. t plot at 523°C.

The figures represent the pressures in mm.

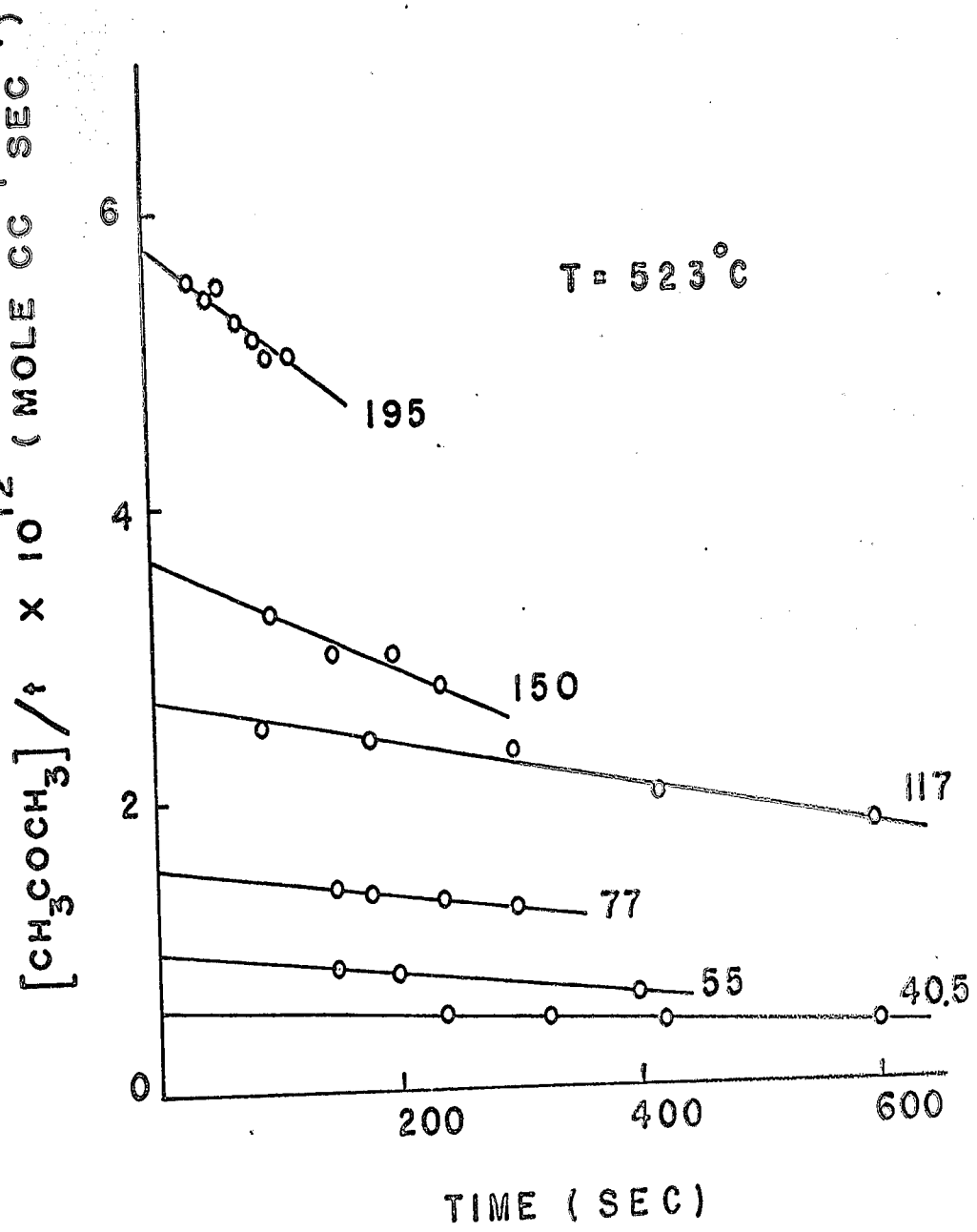
$[CH_3COCH_3]/t \times 10^{12}$ (MOLE CC^{-1} SEC^{-1})
T = 523°C
195
150
117
77
55
40.5
0
2
4
6
200
400
600
TIME (SEC)

order of three-halves cannot be explained if this is the main termination step, and suggested that acetone is formed by reaction [8], a reaction which involves an intermediate of structure

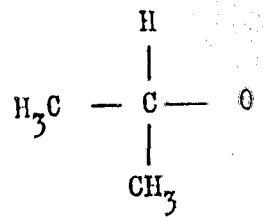

There are other objections to reaction [13] as an important termination step. If this reaction occurred, acetyl radicals would dimerize with the formation of biacetyl, and a rough estimate shows that the rate of formation of biacetyl should be comparable to that of acetone. Such amounts of biacetyl would be easily detectable using the techniques of the present investigation, but none was found. It is also possible to estimate the relative concentrations of CH_3CO and CH_3 in the reaction system. The steady-state condition leads to

$$\frac{[CH_3CO]}{[CH_3]} = \frac{k_4 [CH_3CHO]}{k_5} , \qquad (4)$$

where k_5 is a constant (k_5^∞) at high pressures and becomes proportional to pressure ($k_5^o [CH_3CHO]$) at low pressures. O'Neal and Benson (71) have obtained values of k_5^∞ and k_5^o, and the use of these values, together with our value of k_4 or those of Kerr and Calvert (72) and Brinton & Volman (73,74), leads to the conclusion that $[CH_3CO] / [CH_3]$

is 10^{-2} to 10^{-3} under the conditions of the present experiments. The methyl-methyl combination will therefore be by far the most important termination process.

This conclusion is supported by a consideration of the rates of formation of methane found in the present experiments. If acetone were formed mainly by reaction [13] it can be shown that

$$v_{CH_3COCH_3} = \frac{k_{13}}{k_5 k_9^{\frac{1}{2}}} \; v_{CH_4} \; v_{C_2H_6}^{\frac{1}{2}} \qquad (5)$$

The use of O'Neal and Benson's value for k_5 and of that of Shepp (66) for k_9, with k_{13} assumed equal to k_9, leads to a rate of acetone production which is two to three orders of magnitude lower than that observed.

Furthermore, if acetone were formed by reaction [13], the rate of its formation would be proportional to the square of the acetaldehyde concentration. This may be deduced from the steady-state concentrations of the radicals, viz

$$[CH_3CO] \simeq \frac{k_4}{k_5} \; [CH_3] \; [CH_3CHO]$$

$$[CH_3] \simeq \left(\frac{k_1}{k_9}\right)^{\frac{1}{2}} \; [CH_3CHO]^{\frac{1}{2}}$$

from which it follows that

$$v_{acetone} = k_{13} \; [CH_3] \; [CH_3CO]$$

$$= k_{13} \; \frac{k_4 k_1}{k_5 k_9} \; [CH_3CHO]^2$$

If acetone is formed by reaction [8], on the other hand, the order will be 3/2:

$$v_{acetone} = k_8 \left(\frac{k_1}{k_9}\right)^{1/2} \left[CH_3CHO\right]^{3/2} \qquad (6)$$

This is actually observed in the double logarithmic plot of $v_{CH_3COCH_3}$ against the initial pressure, P (CH_3CHO) which is given in Fig. 18. The order of reaction varies from 1.45 to 1.50 for the temperature range studied. Fig. 19 shows a plot of $v_{CH_3COCH_3}$ against $\left[CH_3CHO\right]^{3/2}$. Straight lines passing through the origin can be drawn.

The alternative proposal that acetone is formed by reaction [8], as suggested by Eusuf and Laidler (18), seems to be consistent with all of the facts. Thus the value of k_8 can be calculated from the data in two completely different ways, with excellent agreement:

(1) From the rates of formation of acetone and ethane at 523°C, and using k_9 from Shepp (66),

$$\frac{v_{CH_3COCH_3}}{v_{C_2H_6}^{\frac{1}{2}}} = \frac{k_8}{k_9^{\frac{1}{2}}} \left[CH_3CHO\right], \qquad (7)$$

whence $k_8 = 7.1 \times 10^6$ ml mole^{-1}s^{-1}.

(2) From the rates of formation of acetone and methane, and using our value of k_4, at 523°C

$$\frac{v_{CH_3COCH_3}}{v_{CH_4}} = \frac{k_8}{k_4}, \qquad (8)$$

Figure 18

Order plot for acetone formation.

Data obtained from packed vessel (S/V = 9.4) are given by x and those from unpacked (S/V = 0.60) by o.

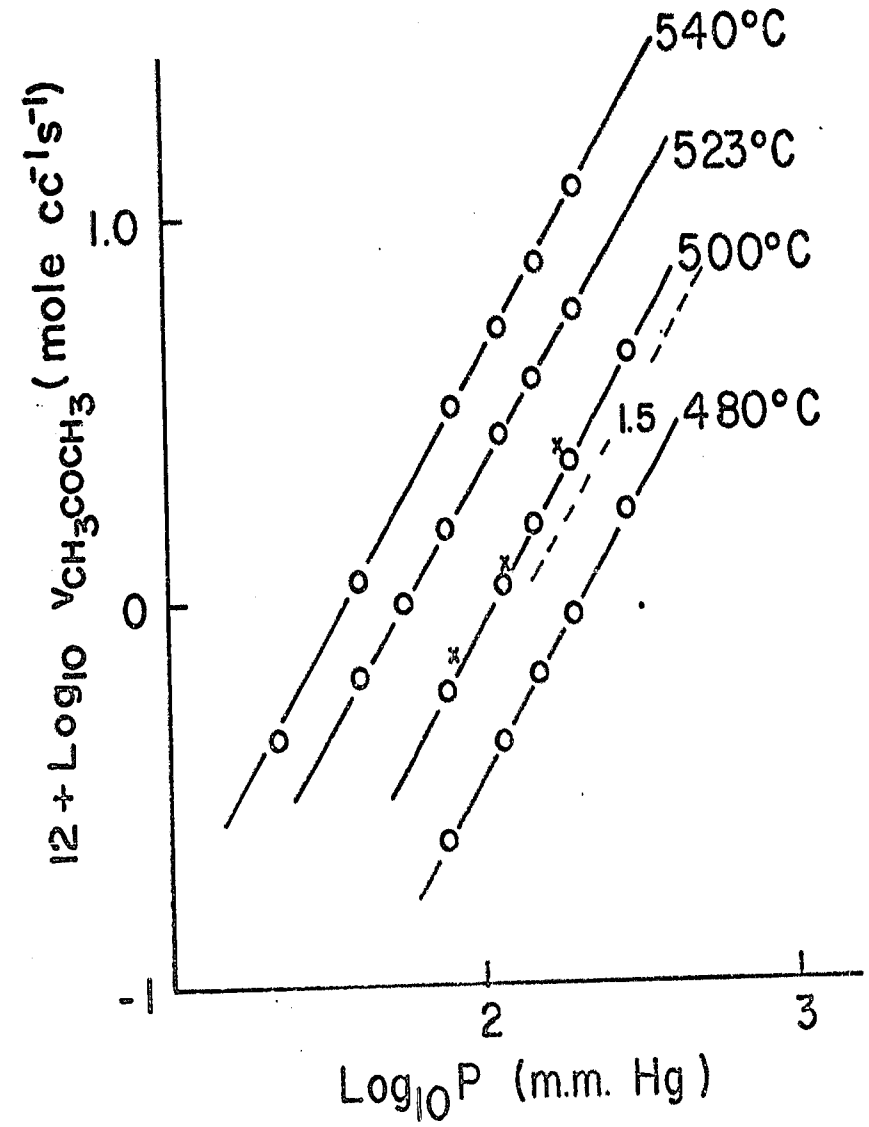
540°C
523°C
500°C
480°C
1.5
1.0
0
-1
2
3
12 + Log10 vCH3COCH3 (mole cc-1s-1)
Log10P (m.m. Hg)

Figure 19

Plot of $v_{CH_3COCH_3}$ vs. $\left[CH_3CHO\right]^{3/2}$.

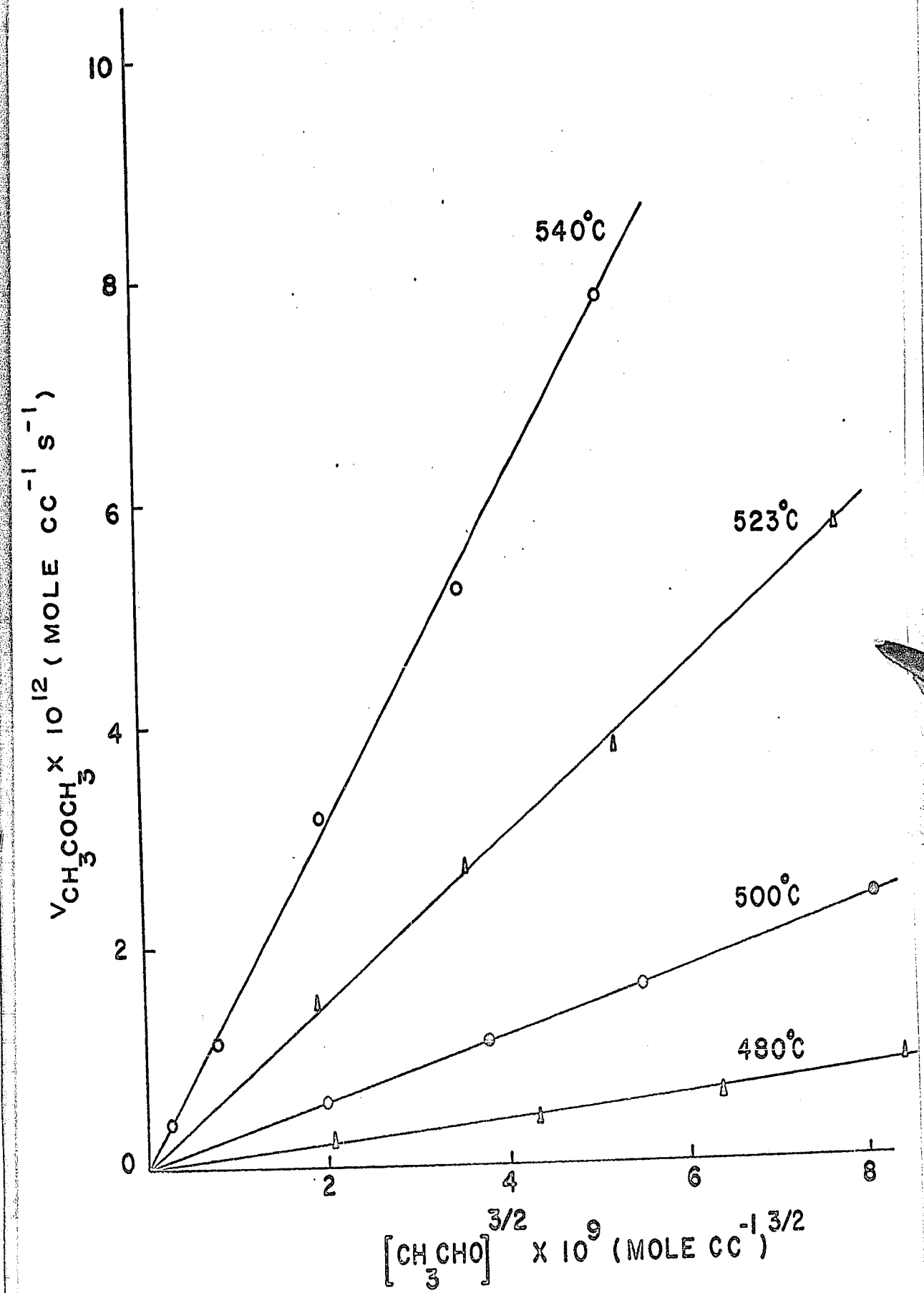
10
8
6
4
2
0
2
4
6
8
540°C
523°C
500°C
480°C
$v_{CH_3COCH_3} \times 10^{12}$ (MOLE CC^{-1} S^{-1})
$[CH_3CHO]^{3/2} \times 10^9$ (MOLE $CC^{-1})^{3/2}$

whence $k_8 = 6.9 \times 10^6$ ml. $mole^{-1}s^{-1}$.

It has been shown that it is possible to derive k_8 from either equation (7) or (8); since k_9 is pressure-dependent under the present experimental conditions, equation (8) is chosen to derive k_8. The values of k_8 at different temperatures are listed in Table 5.

Fig. 20 shows an Arrhenius plot; from it the following expression is derived:

$$\log k_8 \text{ (cc mole}^{-1}\text{sec}^{-1}) = 10.22 \pm 0.07 - \frac{12350 \pm 260}{2.303\ RT}$$

Reaction [8] is a two-stage reaction and should be written as

[11] $CH_3 + CH_3CHO \rightleftharpoons (CH_3)_2\ \dot{C}H$

[12] $(CH_3)_2\ \dot{C}H \longrightarrow (CH_3)_2\ CO + H$

the details of which will be discussed in Chapter IV.

Since the isopropoxy radical is an intermediate of reaction [8] the possibility of other reaction products such as isopropyl alcohol and isopropyl methyl ether was not overlooked. These were not detected in our system. The steady-state concentration of isopropoxy radicals can be estimated; the ratio of $[\text{i-PrO}] / [CH_3]$ is about 10^{-7}-10^{-8} and that of $[CH_3CO] / [CH_3]$ is 10^{-2}-10^{-3} as pointed out in an earlier section. Since the recombination of methyl and acetyl radicals to produce acetone is negligible, it is

Table 5 - Apparent rate constants for the addition of the methyl radical to acetaldehyde.

Pressure mm Hg	$k_8 \times 10^{-6}$ cc mole^{-1}sec^{-1}	k_8 ave $\times 10^{-6}$ cc mole^{-1} sec^{-1}
T = 540°C		
118	7.95	
152	7.95	7.98
198	8.05	
T = 523°C		
117	7.11	
150	6.66	6.89
195	6.90	
T = 500°C		
118	5.38	
150	5.57	5.41
195	5.31	
295	5.38	
T = 480°C		
118	4.34	
150	4.37	4.36
195	4.38	
295	4.34	

Figure 20

Arrhenius plot of k_8.

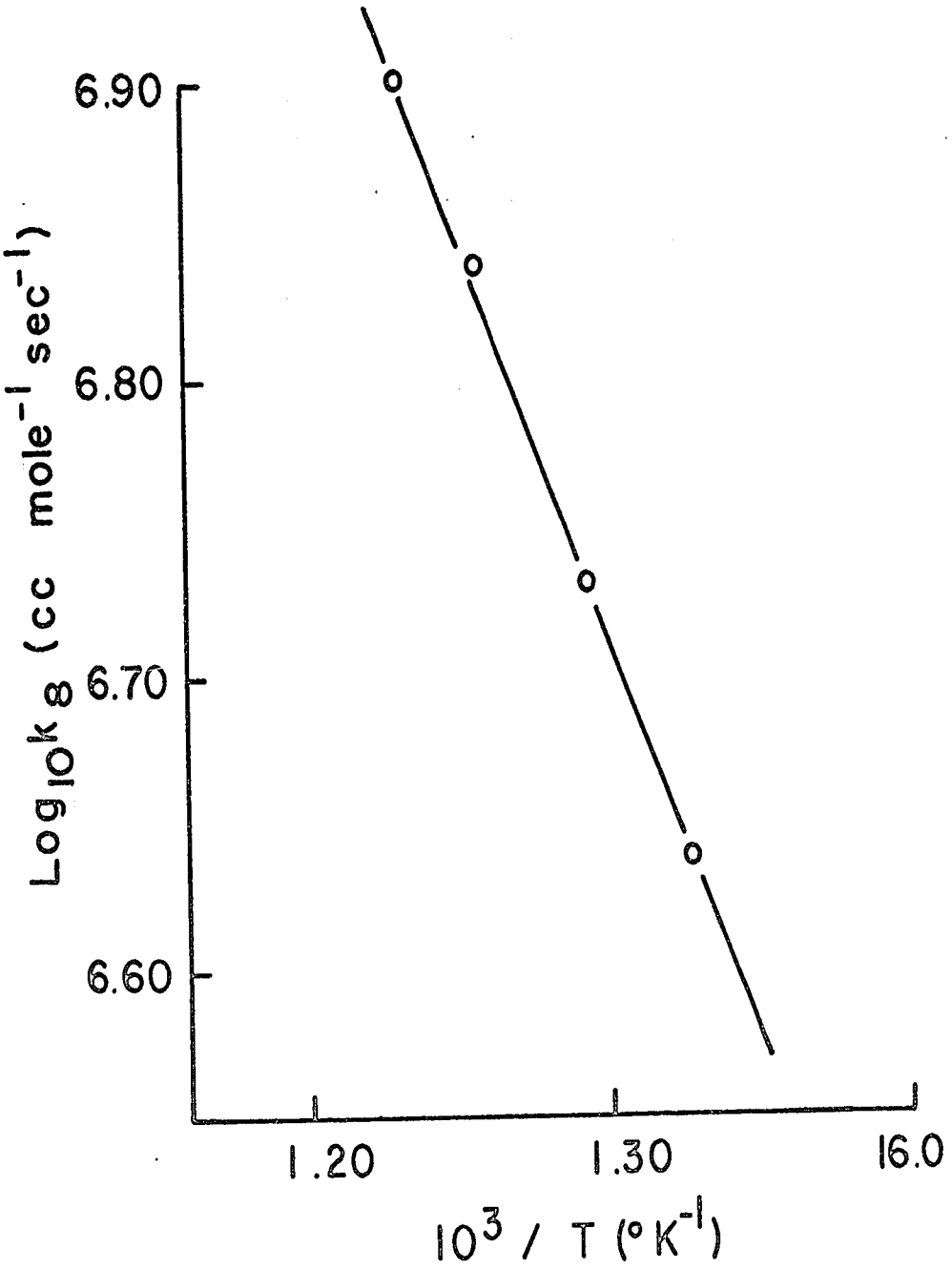
6.90
6.80
6.70
6.60
$Log_{10} k_8$ (cc $mole^{-1}$ sec^{-1})
1.20
1.30
16.0
10^3 / T (°K^{-1})

likely that CH_3 + i-PrO $\longrightarrow$ i-PrO CH_3 or i-PrO + $CH_3CHO \longrightarrow$ i-PrOH + CH_3CO is not important. The concentration of the isopropoxy radical is of the order 10^{-20} mole per cc.

Reaction products such as vinyl methyl ether have been proposed (19,20) as being formed in the acetaldehyde pyrolysis by the following reactions:

$$[14] \quad CH_3 + CH_3CHO \rightleftharpoons CH_3 - CH - OCH_3$$

$$[15] \quad CH_3 - CH - O - CH_3 \longrightarrow CH_2 = CH - O - CH_3 + H$$

An analogue of reaction [14] would be

$$[16] \quad CH_3 + CH_2O \longrightarrow CH_3OCH_2$$

The activation energy of the back reaction has been measured to be 25.5 kcal per mole in the photosensitized decomposition of dimethyl ether (68). From the heat of formation of the methoxymethyl radical, the enthalpy change of reaction [16] was found to be 9.9 kcal per mole, and the activation energy for the forward reaction was estimated to be 15.6 kcal per mole.

Similarly, the activation energy for the addition of the methyl radical to formaldehyde to give the ethoxy radical can be estimated (75) to be 4-8 kcal per mole. One can establish that the activation energy for the methyl radical addition to the oxygen end of formaldehyde is about 10 kcal per mole higher than the addition to the carbon end. If this parallel holds true for the methyl

addition to acetaldehyde, the apparent activation energy for reactions [14] and [15] would be about 20 kcal per mole, which is 7.5 kcal per mole higher than the one in reaction [8].

Hydrogen Production

Trenwith (16) reported that hydrogen production showed an induction period and that the process was second-order in acetaldehyde. In the present study, no induction period was found as is indicated by the typical yield-time plot for hydrogen formation in Fig. 21. This has also been recently confirmed by Côme, Dzierzynski, Martin and Niclause (19,20). The initial rates are obtained by extrapolating rates to zero time as shown in Fig. 22. It is noted that the slopes increase rapidly as the pressure of acetaldehyde increases, and it is obvious that rates at short heating times cannot be taken as initial rates as has been done by several other authors. The order of hydrogen production was 1.4 as shown by the double logarithmic plot in Fig. 23. This is again in agreement with Côme et al. (19,20); they found that the order of hydrogen production was 1.35 under similar experimental conditions. If the simple Rice-Herzfeld mechanism were valid the hydrogen production would be a measure of the rate of the initiation process, and this was Trenwith's conclusion. In terms of the mechanism proposed, however, hydrogen can result from

Figure 21

Typical hydrogen yield-time plots at 523°C.

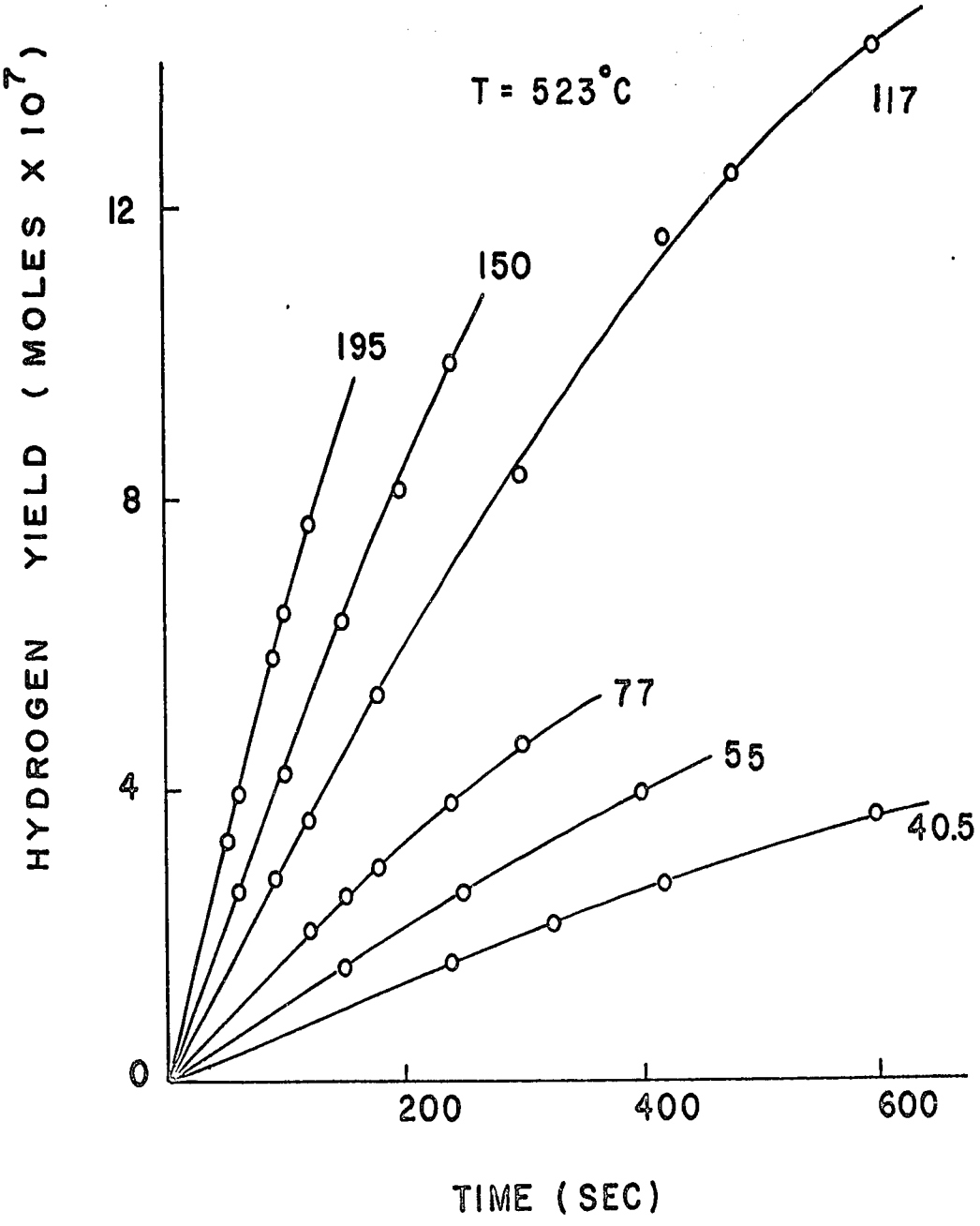
T = 523°C
HYDROGEN YIELD (MOLES X 10^7)
TIME (SEC)
0
4
8
12
200
400
600
195
150
117
77
55
40.5

Figure 22

Typical v_{H_2} vs. t plots at 523°C.

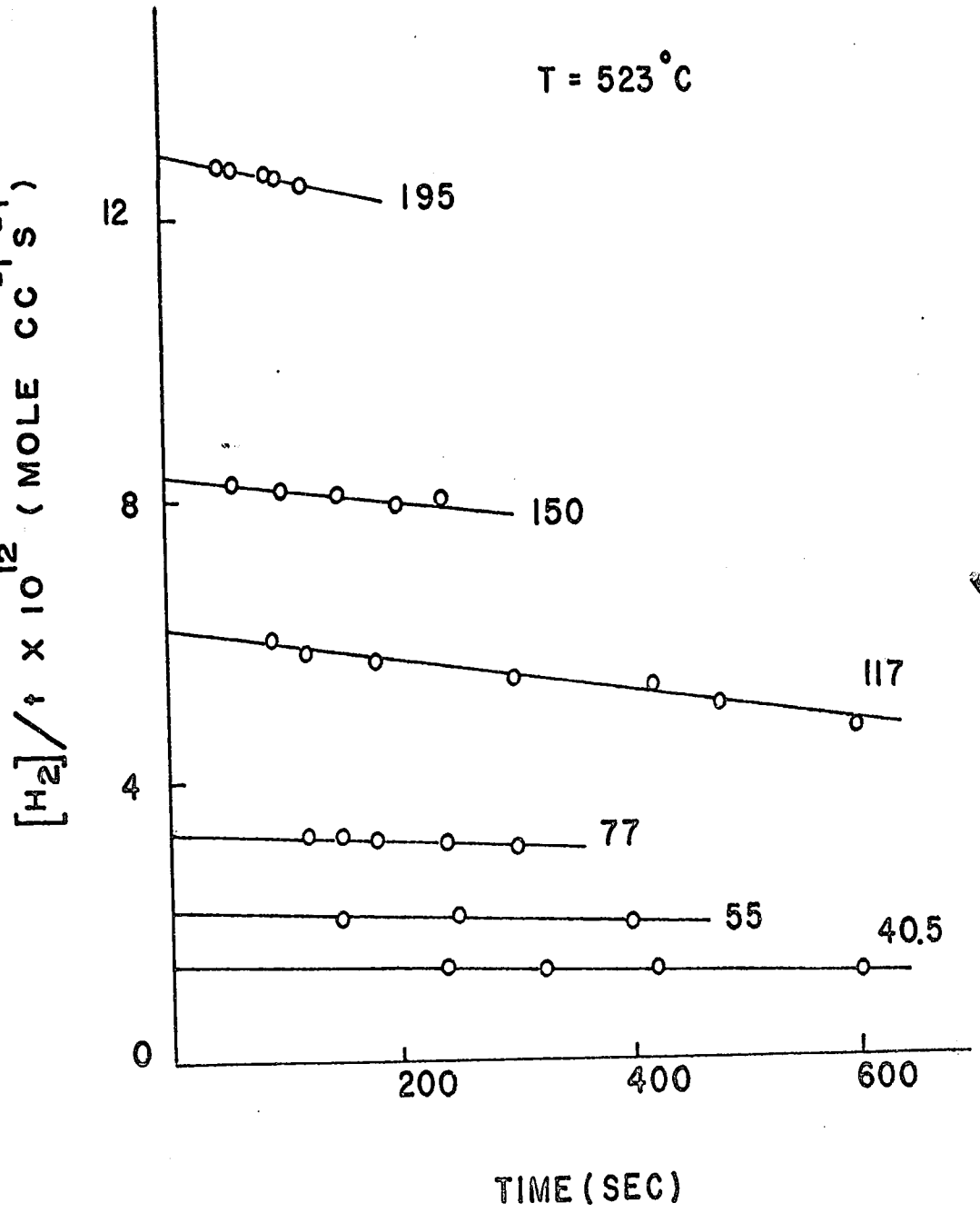
T = 523°C
195
150
117
77
55
40.5
12
8
4
0
200
400
600
$[H_2]/\tau \times 10^{12}$ (MOLE $CC^{-1}S^{-1}$)
TIME (SEC)

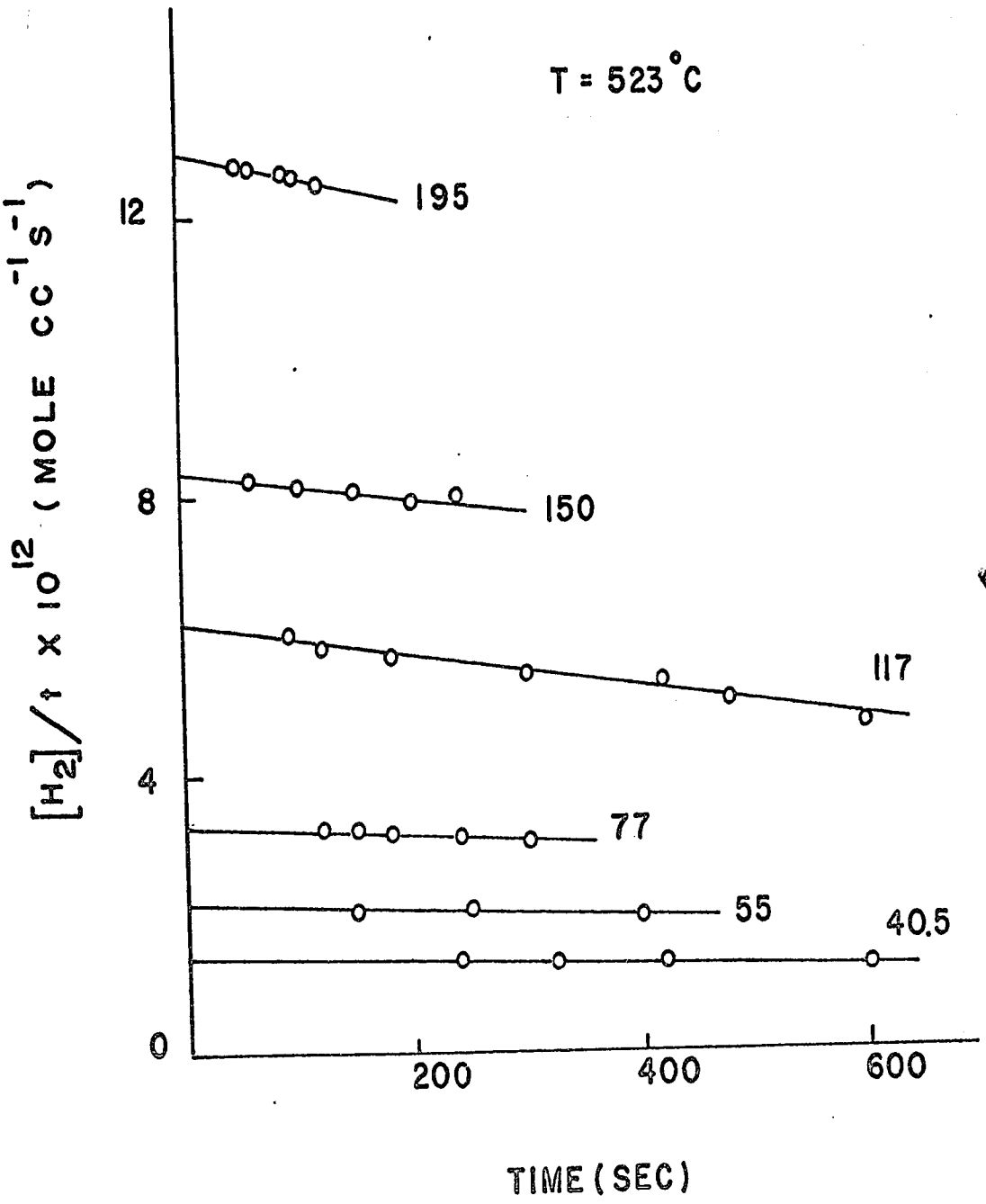
T = 523°C
195
150
117
77
55
40.5
12
8
4
0
200
400
600
TIME (SEC)
[H2]/t X 10^12 (MOLE CC^-1 S^-1)

Figure 23

Order plot for hydrogen production.

Data obtained from packed vessel (S/V = 9.4) are given by x and those from unpacked (S/V = 0.60) by o.

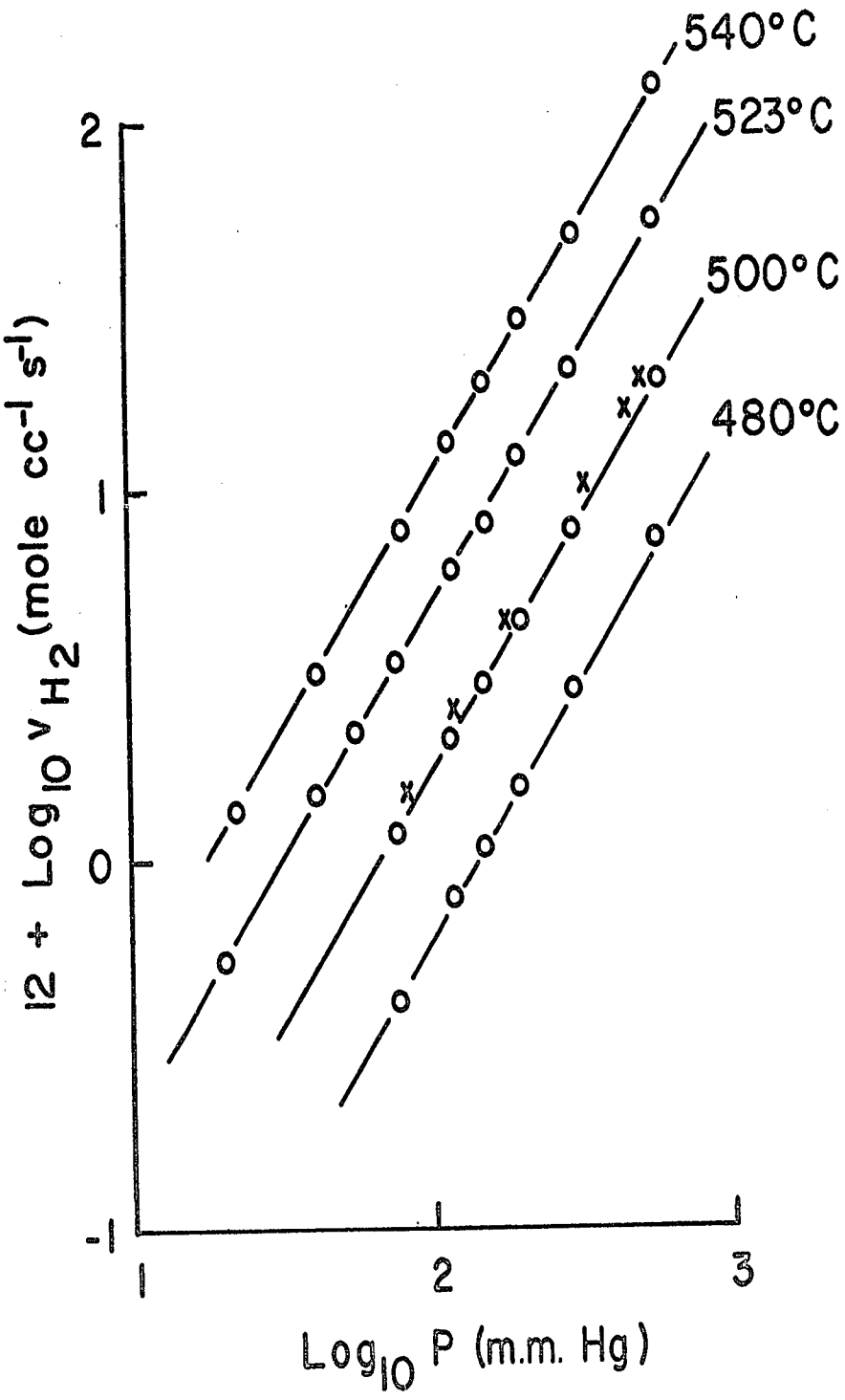
540°C
523°C
500°C
480°C
2
1
0
-1
1
2
3
12 + Log10 v H2 (mole cc-1 s-1)
Log10 P (m.m. Hg)

reactions [3], [7a] and [8], and the rate of its formation is not simply related to the rate of initiation. In Table 1 it is seen that the rate of hydrogen production is much greater than the rate of ethane formation so that the difference will have to be accounted for by other reactions which produce hydrogen. Application of the steady-state treatment leads to the following expression for the rate of hydrogen production:

$$v_{H_2} = k_1 \left[CH_3CHO\right] + \left(\frac{k_1}{k_9}\right)^{1/2} \left[\frac{k_{7a}\, k_6}{k_{7a} + k_{7b}\left[CH_3CHO\right] + k_{10}\left[CH_3\right]} + k_8\right] \left[CH_3CHO\right]^{3/2} \qquad (9)$$

$$= k_1 \left[CH_3CHO\right] + \left(\frac{k_1}{k_9}\right)^{1/2} (k_6' + k_8) \left[CH_3CHO\right]^{3/2}$$

$$\text{where } k_6' = \frac{k_{7a}\, k_6}{k_{7a} + k_{7b}\left[CH_3CHO\right] + k_{10}\left[CH_3\right]} \qquad (10)$$

According to this expression the order of hydrogen production should be between 1 and 3/2, in agreement with the experimental observation of 1.4. Fig. 24 shows a plot of $v_{H_2} / \left[CH_3CHO\right]$ against $\left[CH_3CHO\right]^{\frac{1}{2}}$; a straight line is obtained and from the intercept on the ordinate it is concluded that k_1 at 523°C is 5.2×10^{-7} sec^{-1}. It is interesting to note that the plot is still showing a linear relationship at a fairly low pressure and that no deviation from linearity is observed with the present data. This is attributed to the fact that k_1 and k_9

Figure 24

Plot of $v_{H_2} / [CH_3CHO]$ vs. $[CH_3CHO]^{\frac{1}{2}}$

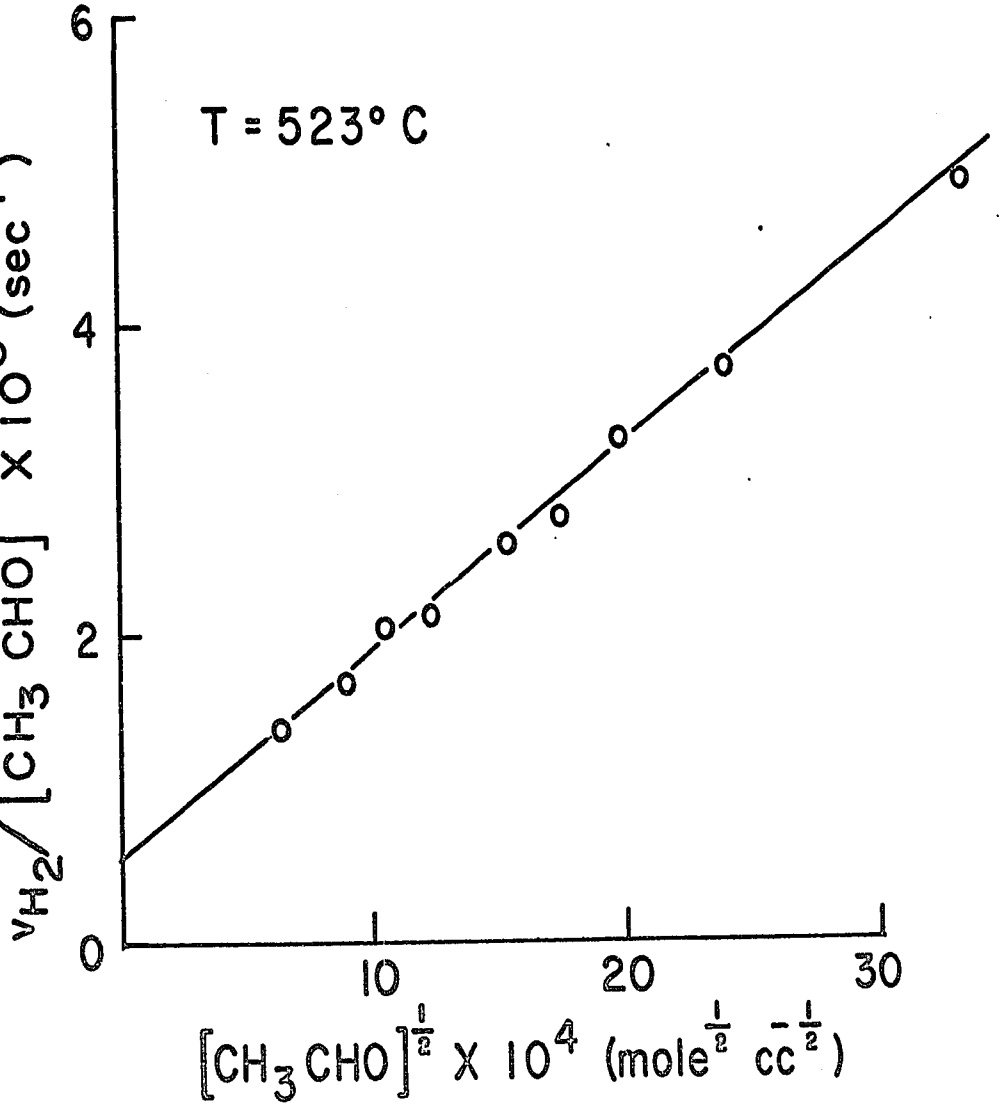
T = 523° C
$v_{H_2}/[CH_3CHO] \times 10^6 (sec^{-1})$
0
2
4
6
10
20
30
$[CH_3CHO]^{\frac{1}{2}} \times 10^4 (mole^{\frac{1}{2}} cc^{-\frac{1}{2}})$

compensate each other; the result is no net change in the ratio of k_1/k_9 although each rate constant is in its pressure-dependent region. In fact, the ratio k_1/k_9 falls off when the pressure is below 20 mm Hg (see section on inert gas effects, p. 86). Since the extrapolation of k_1 at different temperatures cannot be included in the above figure, the various values of k_1 are tabulated in Table 6. The standard deviation of k_1 from each extrapolation is included. The Arrhenius plot of k_1 is shown in Fig. 25, and its parameters are as follows:

$$\log k_1\ (\text{sec}^{-1}) = 16.12 - \frac{81{,}500 \pm 4{,}500}{2.303\ RT}$$

The value of $\Delta S_1^{\neq}$ is 11.3 e.u. at 783°K. The values of k_1'' obtained from ethane and propionaldehyde measurements are also included in this figure for comparison. The Arrhenius equation for k_1'' is

$$\log k_1''\ (\text{sec}^{-1}) = 15.3 - \frac{79{,}000 \pm 2{,}000}{2.303\ RT}$$

In view of certain difficulties involved in employing equation (9), the values of k_1'' are slightly lower than those of k_1 but they are essentially equal within the experimental errors. The values of k_1'' are considered to be more reliable than those obtained from extrapolation. The first and most important point is that k_1 itself is slightly pressure-dependent, so that there is some uncertainty in deriving k_1 from Fig. 24. Secondly, the term $k_{7b}\left[CH_3CHO\right]$ is not

Table 6 - Extrapolation of k_1 from hydrogen measurements

Pressure mm Hg	$[CH_3CHO]^{\frac{1}{2}} \times 10^4$ (mole per cc)$^{\frac{1}{2}}$	$\frac{v_{H_2}}{[CH_3CHO]} \times 10^6$ sec^{-1}
T = 540°C		
79	12.48	5.134
118	15.25	6.016
152	17.31	6.600
198	19.76	7.550
296	24.16	8.560
563	33.33	11.070
	$k_1 = 1.728 \pm 0.18 \times 10^{-6}$ sec^{-1}	
T = 523°C		
77	12.38	2.123
117	15.32	2.598
150	17.40	2.730
195	19.80	3.270
292	24.25	3.740
558	33.53	4.940
	$k_1 = 5.25 \pm 1.07 \times 10^{-7}$ sec^{-1}	
T = 500°C		
77	12.61	0.730
118	15.62	0.895
150	17.64	0.987
195	20.10	1.112
295	24.74	1.299
559	34.05	1.792
	$k_1 = 1.227 \pm 0.22 \times 10^{-7}$ sec^{-1}	
T = 480°C		
77	12.80	0.250
118	15.80	0.322
150	17.86	0.344
195	20.37	0.385
295	25.06	0.475

Table 6 (continued)

Pressure mm Hg	$[CH_3CHO]^{\frac{1}{2}} \times 10^4$ (mole per cc)	$\frac{v_{H_2}}{[CH_3CHO]} \times 10^6$ sec^{-1}
T = 480°C		
559	34.50	0.640

$k_1 = 0.300 \pm 0.097 \times 10^{-7}$ sec^{-1}

Figure 25

Arrhenius plots of k_1 and k_1''.

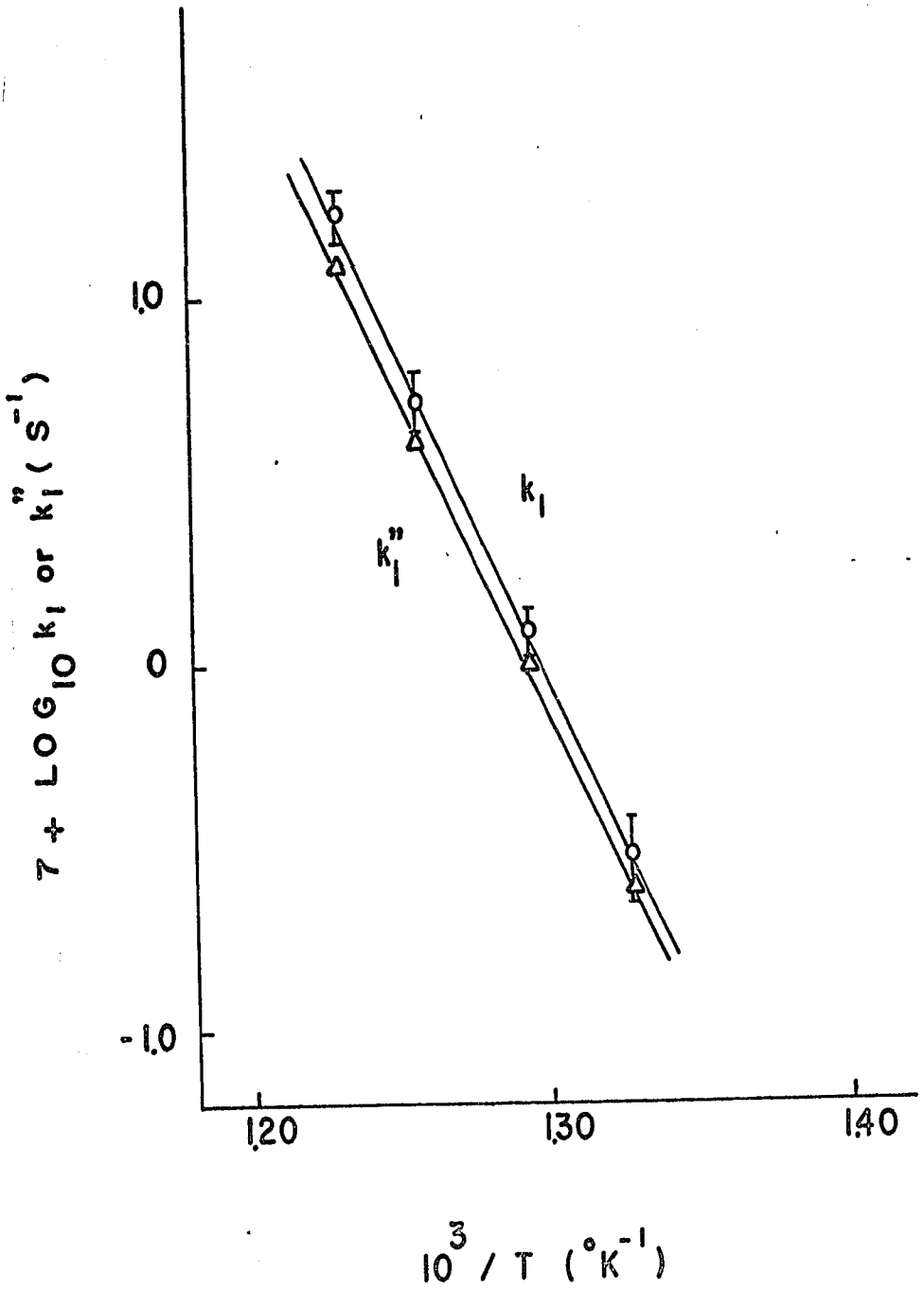
7 + LOG10 k1 or k1" (S-1)
1.0
0
-1.0
1.20
1.30
1.40
k1
k1"
10^3 / T (°K-1)

unimportant compared with k_{7a} and therefore cannot be neglected. The value for k_{7b} is not known but the rate constant for the hydrogen-atom abstraction by the ethyl radical from propionaldehyde

$$C_2H_5 + C_2H_5CHO \longrightarrow C_2H_6 + C_2H_5CO$$

has been found (76) to be given by

$$\log k \text{ (cc mole}^{-1}\text{sec}^{-1}) = 11.1 - \frac{5,900}{2.303\ RT}$$

Although the CH_2CHO will be considerably stabilized by resonance, reaction [7b] will still be quite efficient and the activation energy is not likely to exceed 10 kcal per mole. If this reaction is included in equation (9) the slope of the line will then be a function of acetaldehyde pressure and hence there will be a higher value of k_1. The slope of the plot in Fig. 24, together with the values of k_1 and k_9, allows $k_6' + k_8$ to be obtained: the value is 8.8×10^6 cc mole^{-1} sec^{-1}. From the rate of acetone production it was deduced that k_8 is 7.0×10^6 cc mole^{-1} sec^{-1}, so that it follows that k_6' is 1.8×10^6 cc mole^{-1} sec^{-1}. The controlling factor of the slope is thus mainly k_8 and the contribution due to k_6' is small. It is for this reason that the pressure term within k_6' does not affect the slope to a very great extent and the dependence on the square-root of the concentration of acetaldehyde still holds. Since k_6'

involves such a complicated function, it is not possible to gain meaningful information. The steady-state equation for the total radical concentration is

$$v_1 = v_9 + v_{10}$$

whence $$v_1 = v_{C_2H_6} + v_{C_2H_5CHO}$$

$$k_1 \left[CH_3CHO\right] = k_9 \left[CH_3\right]^2 + k_{10} \left[CH_3\right]\left[CH_2CHO\right]$$

$$= \left[CH_3\right]^2 \; k_9 + \left(\frac{k_{10}\, k_6 \left[CH_3CHO\right]}{k_{7a} + k_{7b} \left[CH_3CHO\right]}\right)$$

At the limit when P is large

$$k_1 \left[CH_3CHO\right] = \left[CH_3\right]^2 \; \left(k_9 + \frac{k_{10}\, k_6}{k_{7b}}\right)$$

Since the slopes of the two Arrhenius plots of k_1 and k_1' in Fig. 25 and 42 are essentially the same, this implies that $E_{10} + E_6 - E_{7b} \simeq 0$. If we assume that reaction [10] does not require any activation energy, E_6 is approximately equal to E_{7b}. It is interesting to note that in reaction [6] both of the reactants involve a stronger set of bonds than the corresponding bonds of the reactants in the isomerization reaction [7b], and it is likely that the activation energies for both reactions are similar.

Propionaldehyde Production

The fact that propionaldehyde is formed as an initial product suggests the presence of the radical CH_2CHO, which is presumably formed by reaction [6]. The participation of this radical was previously suggested by Wall and Moore (31) to account for the considerable amount of methane-d_2 formed in the pyrolysis of a mixture of CH_3CHO and CD_3CDO. Since the ordinary Rice-Herzfeld mechanism cannot account for the formation of the above product, a modified mechanism that includes the CH_2CHO radical is necessary:

$$CH_3CHO \longrightarrow CH_3 + CHO$$

$$CH_3 + CH_3CHO \longrightarrow CH_4 + CH_2CHO$$

$$CD_3CDO + CH_2CHO \longrightarrow CH_2D\,CHO + CD_2CDO$$

The CH_2CHO radicals in the acetaldehyde pyrolysis can undergo the following reactions:

(a) Recombination with methyl radicals to give propionaldehyde, as in reaction [10].

(b) Intermolecular isomerization to give acetyl radicals, as in reaction [7b].

(c) Unimolecular decomposition to give ketene and hydrogen atom, as in reaction [7a].

The steady-state concentration of this radical will thus be:

$$[CH_2CHO] = \frac{k_6 [CH_3] [CH_3CHO]}{k_{7a} + k_{7b} [CH_3CHO] + k_{10} [CH_3]}$$

On the assumption that the value of k_{10} is similar to that of k_9, the term $k_{10} [CH_3]$ will not be significant and can be omitted from this expression. Because propionaldehyde decomposes rapidly at the temperatures of these experiments (77), and because of the difficulty involved in determining small amounts of propionaldehyde in the presence of large amounts of acetaldehyde, it is difficult to make a reliable estimate of its initial rate of formation; the rate is smaller than the rate of ethane production. At a pressure of 117 mm Hg at 523°C, the rate of propionaldehyde formation is estimated to be 1.5×10^{-13} mole cc^{-1} sec^{-1}, as compared with a rate of 5.9×10^{-13} mole cc^{-1} sec^{-1} for the rate of ethane production. The rate of propionaldehyde production is

$$v_{C_2H_5CHO} = k_{10} [CH_3] [CH_2CHO]$$

$$= \frac{k_{10} k_6 [CH_3]^2 [CH_3CHO]}{k_{7a} + k_{7b} [CH_3CHO] + k_{10} [CH_3]} \qquad (11)$$

In Table 1 we have made a rough estimate of propionaldehyde formation at different pressures at 523°C, the order of which is closer to unity than 2. This suggests that the term $k_{7b} [CH_3CHO]$ is greater than k_{7a}. If the reverse were true, the order of propionaldehyde formation would have been

2. The CH_2CHO radical, by analogy with the allyl radical, will be considerably stabilized by resonance. It was pointed out in an earlier section, however, that the activation energy for the isomerization reaction is not likely to exceed 10 kcal per mole.

Ketene Production

Ketene decomposes rapidly under the conditions of the present experiments, so that it was not possible to make a direct measurement of its rate of formation. Beside its high reactivity, ketene also polymerizes with acetaldehyde at low temperatures (residual polymer is always observed in the -140°C trap after each run); as a result of this, ketene was not detected by gas chromatography. The rate of its formation can, however, be estimated on the basis of a material-balance equation,

$$v_{H_2} = v_{CH_3COCH_3} + v_{C_2H_6} + v_{C_2H_5CHO} + v_{CH_2CO} \qquad (12)$$

which is readily derived from the steady-state equations. At an initial acetaldehyde pressure of 117 mm Hg at 523°C the rate of ketene formation is found to be, from the rates in Table 1,

$$v_{CH_2CO} = 26.6 \times 10^{-13} \text{ mole cc}^{-1} \text{ sec}^{-1}$$

The steady-state equation for the radical CH_2CHO is

$$v_6 = v_{7a} + v_{7b} + v_{10} \qquad (13)$$

Both v_{7a} and v_{10} can be estimated. Unfortunately, the rate of the isomerization reaction [7b] cannot be measured because the product of this reaction decomposes into CH_3 and CO. It is therefore not possible to determine v_6 and k_6 in this system.

The relative concentrations of $[CH_2CHO]$ and $[CH_3]$ can be estimated from the following relations:

$$v_{C_2H_5CHO} = k_{10} [CH_3][CH_2CHO] \quad (11)$$

and

$$v_{C_2H_6} = k_9 [CH_3]^2 \quad (14)$$

It follows that

$$\frac{[CH_2CHO]}{[CH_3]} = \frac{k_9 \, v_{C_2H_5CHO}}{k_{10} \, v_{C_2H_6}} \quad (15)$$

If k_9 and k_{10} are equal, at 523°C,

$$\frac{[CH_2CHO]}{[CH_3]} = \frac{1.5 \times 10^{-13}}{5.9 \times 10^{-13}} = 0.25$$

It was noted that $[CH_3CO] / [CH_3]$ is 10^{-2} to 10^{-3}. Although formed much less rapidly CH_2CHO is present in much higher concentrations than CH_3CO, because of its lower reactivity.

The Decomposition of the CH_2CHO Radical

The decomposition of the CH_2CHO radical cannot be studied directly but its rate can be estimated according to the relationship

$$\frac{v_{7a}\, v_4}{v_{10}} = \frac{k_{7a}\, k_4}{k_{10}} \left[CH_3CHO\right] . \qquad (16)$$

v_4 is the rate of formation of methane from the overall reaction. v_{10} can be estimated by subtracting $v_{C_2H_6}$ from the rate of initiation, and v_{7a} can be obtained by subtracting $v_{acetone}$ and $k_1 \left[CH_3CHO\right]$ from the rate of hydrogen production. With the assumption that k_{10} is 4.2×10^{13} cc mole^{-1} sec^{-1}, k_{7a} can be calculated from assumed values for the rate of acetone formation at higher pressures. The values thus obtained are plotted in Fig. 26. The half darkened circles represent the values of k_{7a} calculated from assumed values for the rate of acetone formation at higher pressures. The slope of the line is one; the decomposition of the CH_2CHO radical is thus completely in its second-order region. The Arrhenius plot for the low-pressure limiting rate constant is shown in Fig. 27 and

$$\log k^0_{7a} \text{ (cc mole}^{-1} \text{ sec}^{-1}) = 14.44 - \frac{26,300}{4.576\ T}$$

On the basis of the Kassel-Rice-Ramsperger theories the theoretical activation-energy difference between the high and low pressure limits is

$$E_\infty - E_0 = (s - 3/2)\ RT \qquad (17)$$

Here s is the number of effective degrees of freedom, which is usually equal to about half of the total number of vibrational modes. If we assume that s = 6 for the CH_2CHO decomposition, then E_{7a} is equal to $\simeq$ 34 kcal per mole,

Figure 26

Plots of $\log_{10} k_{7a}$ vs. $\log_{10}$ P mm Hg.

Figure 26

Plots of $\log_{10} k_{7a}$ vs. $\log_{10}$ P mm Hg.

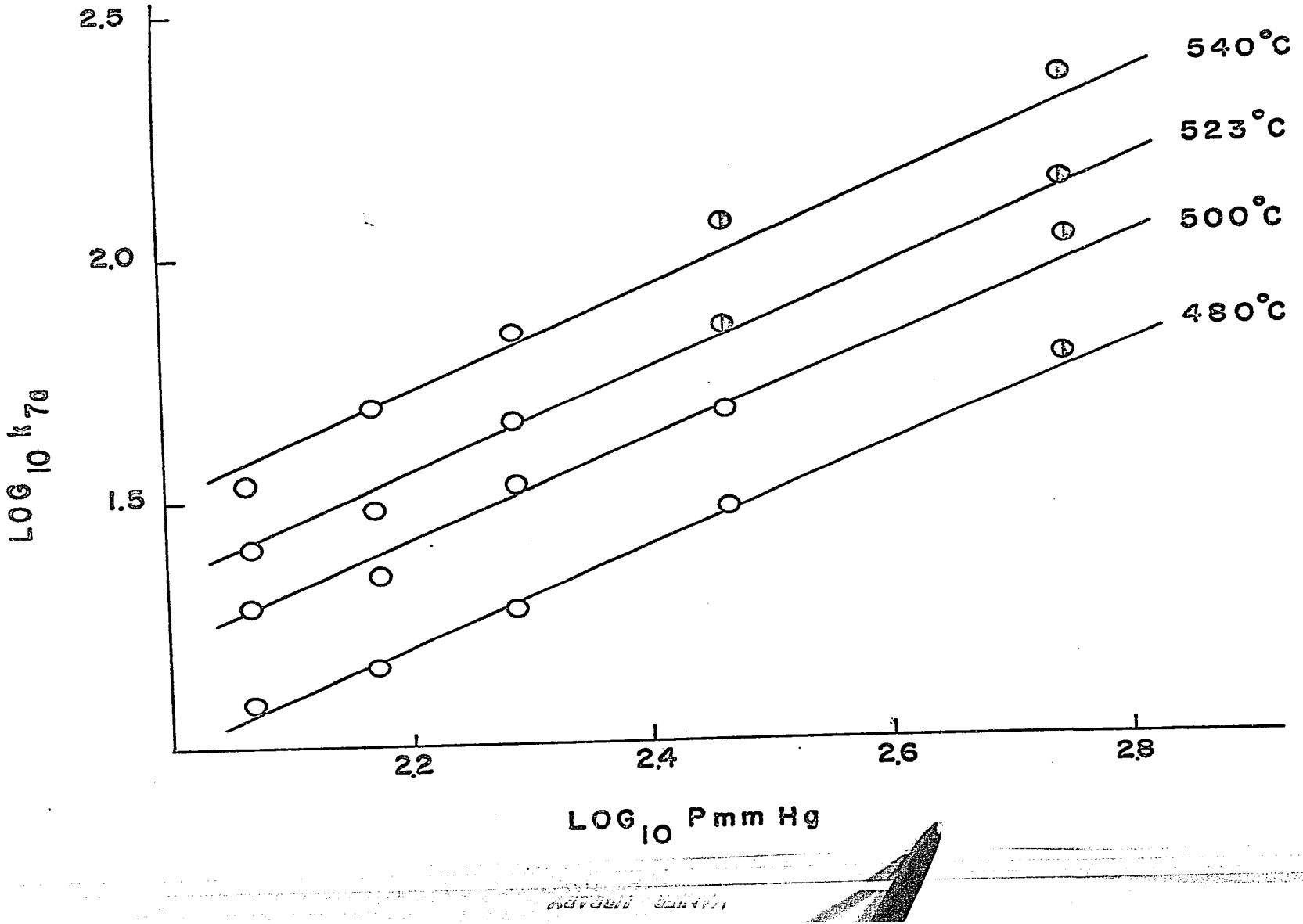
2.5
2.0
1.5
LOG10 k70
540°C
523°C
500°C
480°C
2.2
2.4
2.6
2.8
LOG10 P mm Hg

Figure 27

Arrhenius plot of k^{o}_{7a}.

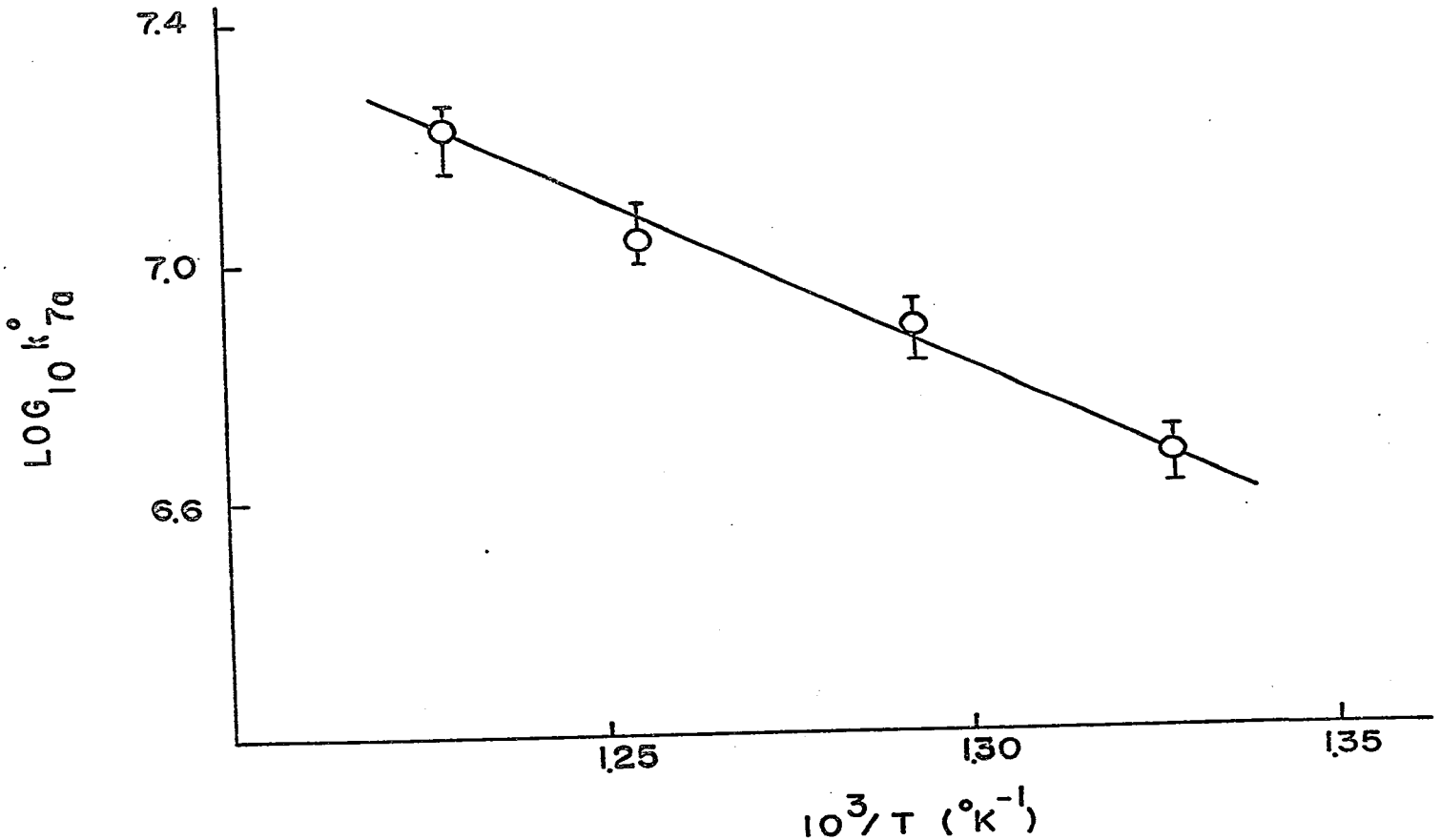
7.4
7.0
6.6
$LOG_{10} k^{\circ}_{7a}$
1.25
1.30
1.35
$10^3/T\ (^{\circ}K^{-1})$

which is in good agreement with the value of 35 kcal per mole estimated by Benson (78).

The CO_2 and C_2H_4 Production

The initial rates of formation of both CO_2 and C_2H_4 are non-zero, so that these substances are primary products. The double logarithmic plot for C_2H_4 formation is given in Fig. 28 and the order is 1.5 at 540°C, which suggests that the C_2H_4 production is resulting from the reaction between a methyl radical and a CH_3CHO molecule:

$$CH_3 + CH_3CHO \rightleftharpoons CH_3-O-\overset{H}{\underset{|}{C}}-CH_3$$

$$CH_3-O-\overset{H}{\underset{|}{C}}-CH_3 \longrightarrow CH_3O + C_2H_4$$

Other products such as CH_3OH or $CH_3OCH = CH_2$, which may be produced from the above reactions, were not detected. The time-course studies of CO_2 in Fig. 2 show a sharp increase in its production at high conversion, indicating that both primary and secondary reactions are occurring. The initial formation of CO_2 may be due to the reaction of the acetyl radical with acetaldehyde:

$$CH_3CO + CH_3CHO \longrightarrow CO_2 + C_3H_7$$

and the secondary contribution of CO_2 can be attributed to the following reactions:

Figure 28

Order plot for C_2H_4 formation at 540°C.

Figure 28

Order plot for C_2H_4 formation at 540°C.

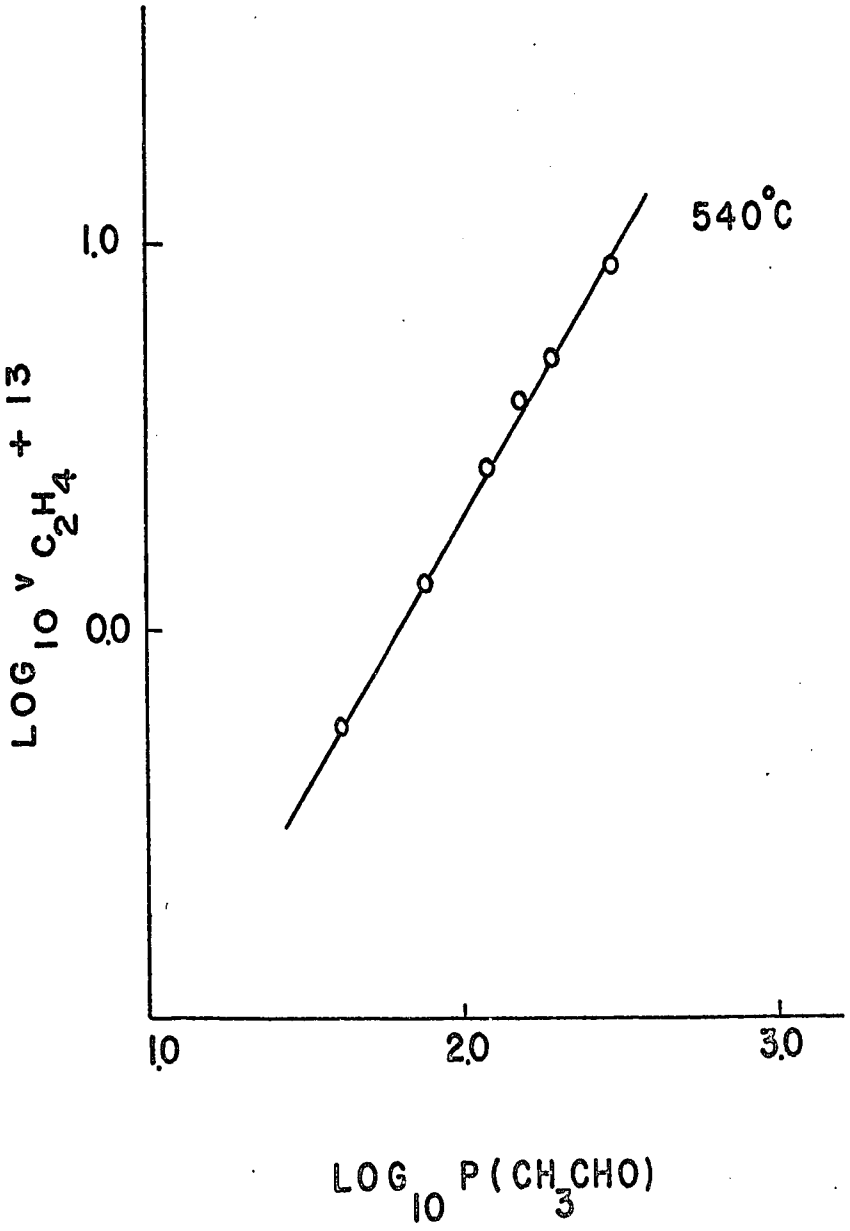
540°C
1.0
0.0
LOG10 v C2H4 + 13
1.0
2.0
3.0
LOG10 P(CH3CHO)

$$CH_2CO + CH_3CHO \longrightarrow CO_2 + C_3H_6$$

$$CH_3O + CO \longrightarrow CO_2 + CH_3$$

$$(CH_3)_2 CHO + CO \longrightarrow CO_2 + C_3H_7$$

The oxidation of carbon monoxide to carbon dioxide is quite probable in this system. On pyrolyzing a mixture of t-butyl peroxide and formaldehyde, Lin (79) has found a large amount of CO_2, which is probably due to

$$(CH_3)_3 CO + CO \longrightarrow CO_2 + (CH_3)_3 C$$

The reaction of carbon monoxide with itself,

$$CO + CO \longrightarrow CO_2 + C$$

was also studied but was found not to occur at 523°C.

Inert Gas Effect

The effect of inert gas on the rates of methane, ethane, acetone and hydrogen production was examined with different initial pressures of acetaldehyde at 540°C. Carbon dioxide was used in these experiments because it does not interfere with subsequent analysis of the above products. The main drawback in employing carbon dioxide in these experiments is its low efficiency in energy transfer processes; as a result, a much higher pressure of CO_2 has to be used in order to bring about the same effect as acetaldehyde.

In an earlier section (see Fig. 8) has been shown the pressure dependence of the overall rate constant, $k_{overall}$, which is a measure of the ratio k_1/k_9. The rate expression for methane formation is

$$v_{CH_4} = k_4 \left(\frac{k_1}{k_9}\right)^{1/2} \left[CH_3CHO\right]^{3/2} \qquad (1)$$

The ratio k_1/k_9 can be calculated from the rate of formation of methane; the values at different pressures are tabulated in Table 7 and represented by circles in Fig. 29. It is seen that the ratio k_1/k_9 falls off at low pressures.

The effect of CO_2 on methane production is examined and shown in Fig. 30. The first set of graphs corresponds to 42 mm CH_3CHO and 42 mm + 210 mm CO_2, the second set to 21 mm CH_3CHO and 21 mm CH_3CHO + 220 mm CO_2. The increase in rate of methane formation, i.e. $v^x_{CH_4} - v^0_{CH_4}/v^0_{CH_4}$ is only about 8-10% in both cases. In order to confirm our observations this work has been extended to a lower pressure range in which the rate of methane production is more sensitive to foreign gases, i.e. the ratio k_1/k_9 is well in its pressure-dependent region. The rate of methane production is increased by as much as 50% on the addition of CO_2. These results are summarized in Table 8. From Tables 7 and 8 it is seen that the addition of CO_2 increases the ratio k_1/k_9 at all pressures with the exception of 79 mm CH_3CHO. This is understandable as the ratio k_1/k_9 is not in its pressure-dependent region. It is also noted that, with the pressure of CH_3CHO kept constant, the ratio k_1/k_9 is

Table 7 - The values of k_1/k_9 at 540°C, calculated from methane production

P mm Hg	v_{CH_4} x 10^{12} mole cc^{-1} sec^{-1}	$\log_{10} v_{CH_4} + 12$	$\left(\frac{v_{CH_4}}{k_4 [CH_3CHO]^{3/2}}\right)^2$ x 10^{20} mole cc^{-1}
563	65,000	4.813	3.42
292	25,000	4.398	3.46
198	14,300	4.155	3.80
152	9,300	3.968	3.57
118	6,200	3.792	3.40
79	3,640	3.561	3.88
42	1,240	3.093	3.01
22	480	2.681	3.09
11.2	172	2.235	3.05
4.23	34.3	1.525	2.25
1.84	9.3	0.968	1.96
1.28	5.2	0.716	1.83
0.767	2.3	0.362	1.58

Figure 29

Plot of $\log_{10} k_1/k_9$ vs. $\log_{10} P$ (mm Hg).

o Pure CH_3CHO

x $P(CH_3CHO) + \lambda P(CO_2)$; $\lambda = 0.5$

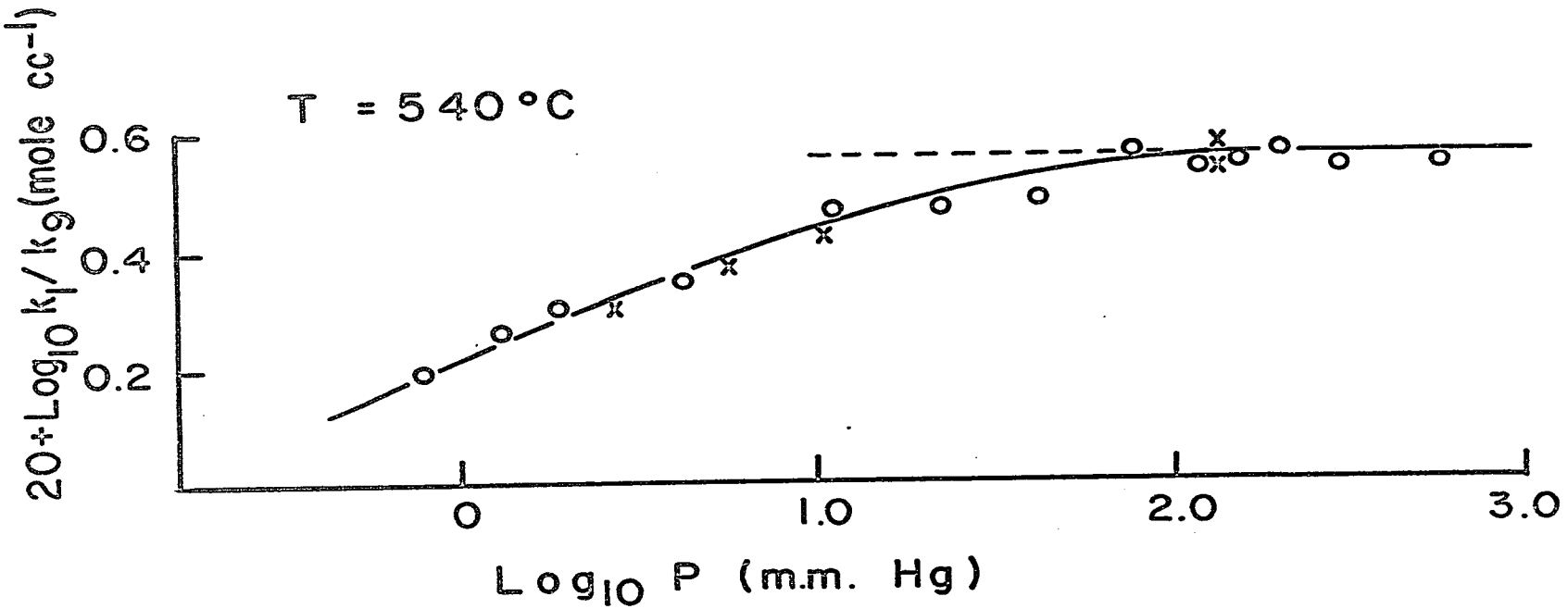
T = 540°C
0.6
0.4
0.2
0
1.0
2.0
3.0
$20+\mathrm{Log}_{10} k_1/k_9 (\mathrm{mole\ cc}^{-1})$
Log_{10} P (m.m. Hg)

Figure 30

Typical yield-time plots for methane formation in the presence of CO_2.

▲ 42 mm CH_3CHO

▲ 42 mm CH_3CHO + 210 mm CO_2

o 22 mm CH_3CHO

o 22 mm CH_3CHO + 220 mm CO_2

Figure 30

Typical yield-time plots for methane formation in the presence of CO_2.

Δ 42 mm CH_3CHO

▲ 42 mm CH_3CHO + 210 mm CO_2

o 22 mm CH_3CHO

o 22 mm CH_3CHO + 220 mm CO_2

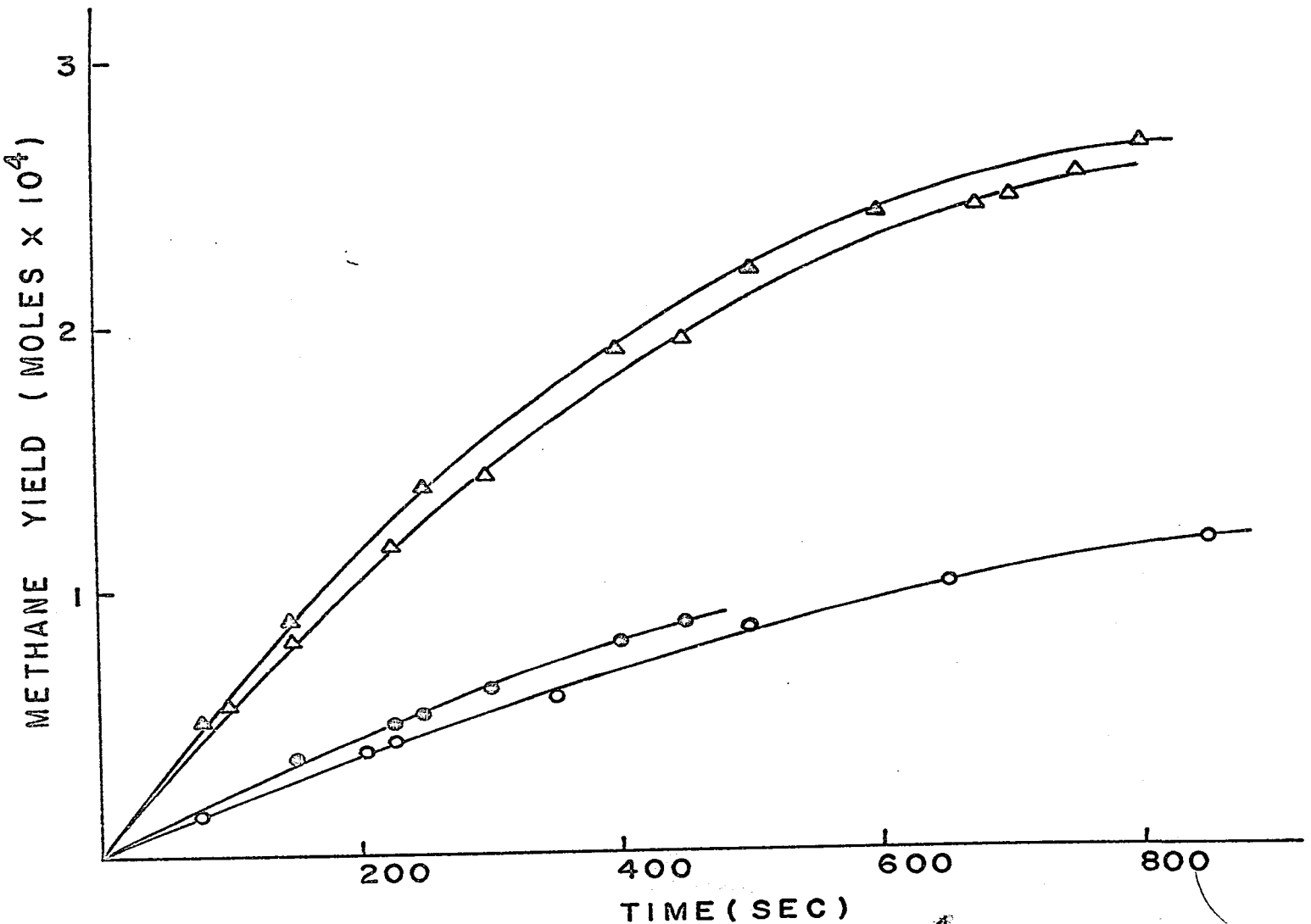
METHANE YIELD (MOLES X 10^4)
3
2
1
200
400
600
800
TIME (SEC)

Table 8 - Effect of CO_2 on methane production

P CH_3CHO mm Hg	P CO_2 mm Hg	P Total mm Hg	$\left(\frac{v_{CH_4}}{k_4 \left[CH_3CHO \right]^{3/2}} \right)^2 \times 10^{20}$ mole cc^{-1}	Effective Pressure, mm Hg	Efficiency of CO_2
79	79	158	3.80	-	-
42	210	252	3.52	-	-
22	220	242	3.80	-	-
1.28	18.70	19.98	2.77	11.0	0.52
1.28	8.76	10.04	2.33	6.6	0.6
1.28	3.0	4.28	2.03	2.4	0.37

increased towards its high-pressure value by adding different amounts of CO_2 each time. This ratio will be brought back to its pressure-independent region if enough CO_2 is added. The results indicate that in the intermolecular transfer of energy, carbon dioxide is only about half as efficient as acetaldehyde, according to the relationship

$$P_{effective} = P(CH_3CHO) + \lambda P_{CO_2} \qquad (18)$$

The efficiency of acetaldehyde is assumed to be unity. The results with added CO_2 are indicated by X in Fig. 29.

The effect of carbon dioxide on ethane formation is shown in Fig. 31 and the rates are given in Table 9. $v^{5x}_{C_2H_6}$ and $v^{10x}_{C_2H_6}$ represent the rates of formation of ethane in the presence of five and ten-fold amounts of CO_2. The rates of 5×10^{-13} and 2.54×10^{-13} mole cc^{-1} sec^{-1} for the two different pressures of CH_3CHO correspond to the rates of ethane formation in the first-order region. The rate expression for ethane formation is

$$v_{C_2H_6} = k_9 \left[CH_3\right]^2 \simeq k_9 \left(\frac{k_1}{k_9}\right) \left[CH_3CHO\right] \qquad (14)$$

It is to be noted that the percentage increase in the rate of ethane formation is higher than for methane formation mainly because there are more pressure-dependent terms involved in this rate expression.

The effect of CO_2 on the rate of acetone formation is small and the percentage increase in rate is similar to that of methane formation. The yield-time plot for acetone

Figure 31

Typical yield-time plots for ethane formation in the presence of CO_2.

Δ 42 mm CH_3CHO

▲ 42 mm CH_3CHO + 210 mm CO_2

o 22 mm CH_3CHO

o 22 mm CH_3CHO + 110 mm CO_2

o 22 mm CH_3CHO + 220 mm CO_2

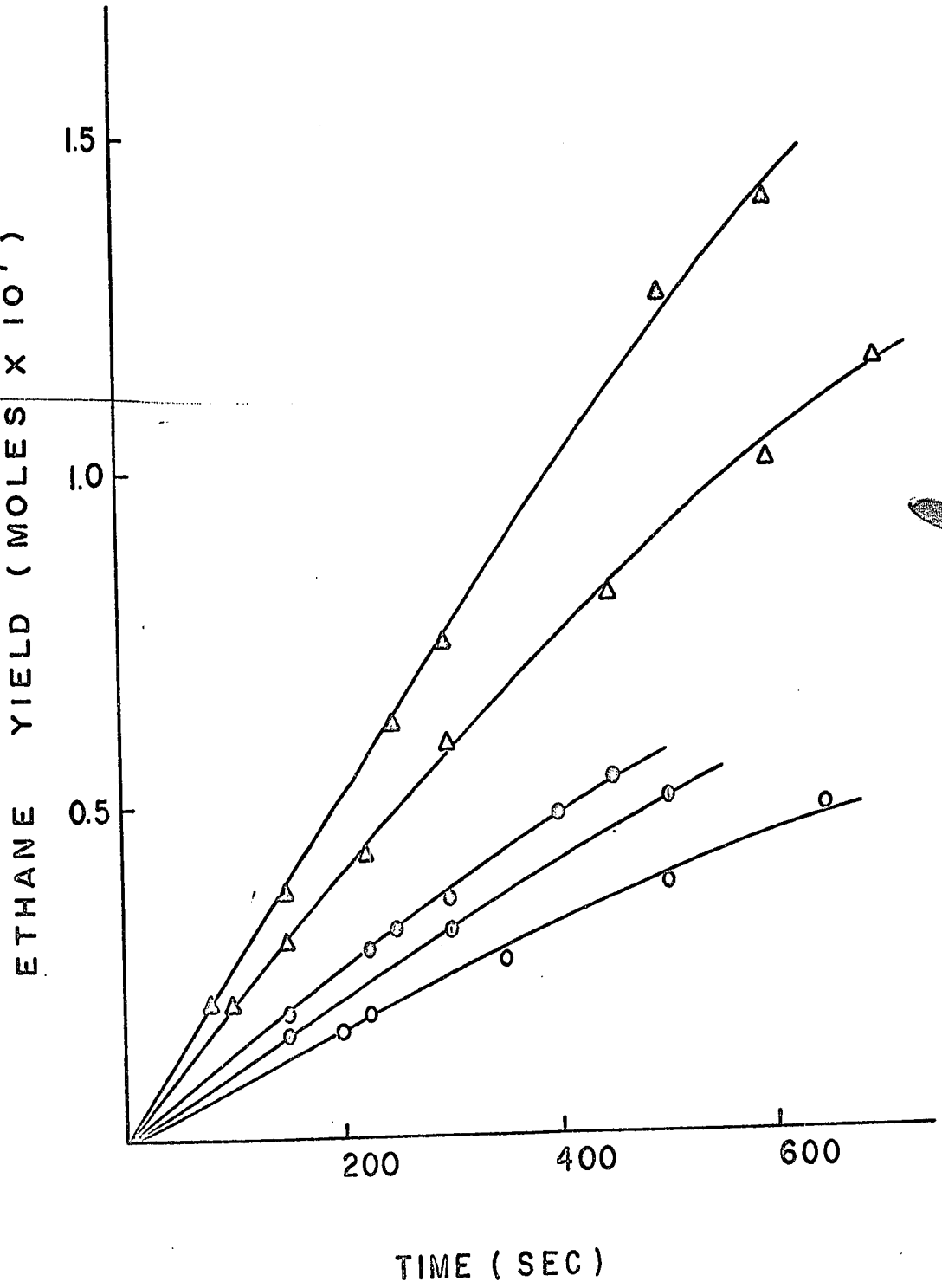
ETHANE YIELD (MOLES X 10^7)
1.5
1.0
0.5
200
400
600
TIME (SEC)

Table 9 - Effect of CO_2 on ethane formation at 540°C. All rates are in mole cc^{-1} sec^{-1}

P CH_3CHO mm Hg	$v^{0}_{C_2H_6} \times 10^{13}$	$v^{5x}_{C_2H_6} \times 10^{13}$	$v^{10x}_{C_2H_6} \times 10^{13}$
42	4.0	5.0	-
22	1.6	2.1	2.54

formation is shown in Fig. 32 and the rates of formation of acetone are given in Table 10. Table 11 shows the ratio k_1/k_9 calculated from the rates of acetone formation at 540°C. These values can be superimposed with those calculated from methane formation shown in Fig. 29. The rate expression for acetone formation is

$$v_{acetone} = k_8 \left(\frac{k_1}{k_9}\right)^{1/2} \left[CH_3CHO\right]^{3/2} \qquad (6)$$

Both equations (1) and (6) contain the square root of the ratio k_1/k_9 and both show 3/2-order dependence on acetaldehyde. If it is assumed that the decomposition of acetaldehyde is completely in its second-order region, the relevant equations are

$$[i] \quad CH_3CHO + CH_3CHO \longrightarrow CH_3CHO + CH_3 + CHO$$

$$[i'] \quad CH_3CHO + X \longrightarrow CH_3 + CHO + X$$

$$[t] \quad CH_3 + CH_3 + CH_3CHO \longrightarrow C_2H_6 + CH_3CHO$$

$$[t'] \quad CH_3 + CH_3 + X \longrightarrow C_2H_6 + X$$

The steady-state treatment leads to

$$\frac{v^X_{CH_4}}{v^o_{CH_4}} = \frac{v^X_{CH_3COCH_3}}{v^o_{CH_3COCH_3}} = \left\{ \frac{\left[CH_3CHO\right] + \frac{k_i'}{k_i}\left[X\right]}{\left[CH_3CHO\right] + \frac{k_t'}{kt}\left[X\right]} \right\}^{1/2} \qquad (19)$$

where X represents any third body.

Theoretically, the rates of methane and acetone production should be influenced to the same extent by

Figure 32

Typical yield-time plots for acetone formation in the presence of CO_2.

Δ 42 mm CH_3CHO

▲ 42 mm CH_3CHO + 210 CO_2

o 22 mm CH_3CHO

● 22 mm CH_3CHO + 220 mm CO_2

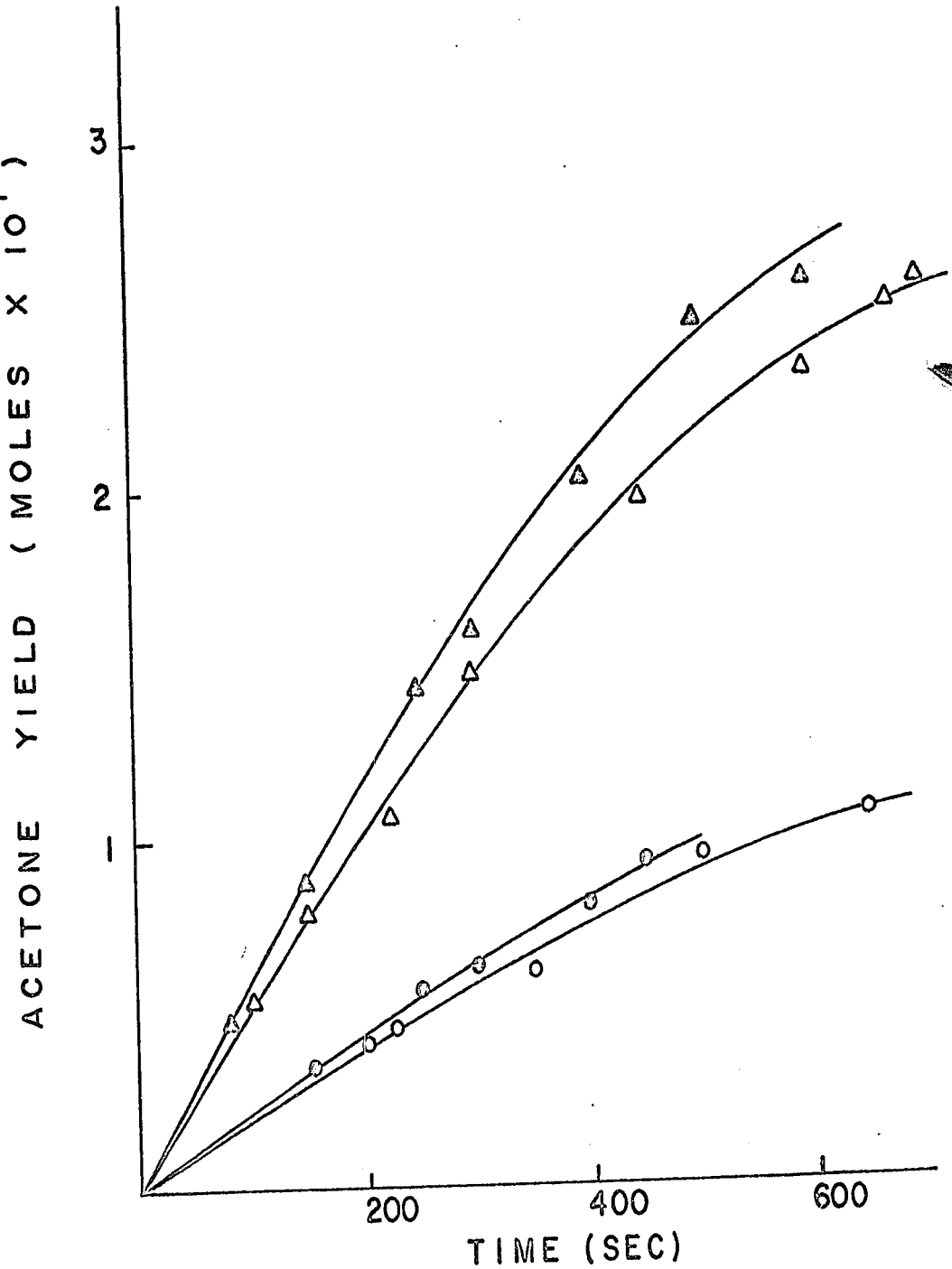
ACETONE YIELD (MOLES X 10^7)
3
2
1
200
400
600
TIME (SEC)

Table 10 - Effect of CO_2 on rate of formation of acetone at 540°C. All rates are in mole cc^{-1} sec^{-1}

P CH_3CHO mm Hg	$v^{0}_{acetone} \times 10^{13}$	$v^{5x}_{acetone} \times 10^{13}$	$v^{10x}_{acetone} \times 10^{13}$
42	11.5	12.4	-
22	4.3	-	4.7

Table 11 - The values of k_1/k_9 at 540°C
calculated from values of acetone production

P CH_3CHO mm Hg	P CO_2 mm Hg	$\left(\frac{v_{acetone}}{k_8 \left[CH_3CHO\right]^{3/2}}\right)^2 \times 10^{20}$ mole cc^{-1}
198	-	3.88
152	-	3.50
118	-	3.40
79	-	4.16
42	-	3.65
22	-	3.53
42	210	4.2
22	220	4.2

addition of inert-gas, and this is actually observed.

The rate of hydrogen production is influenced by the addition of inert gas to a greater extent than that of the other products. This is shown in Fig. 33. The rates of formation are given in Table 12. The rate expression for hydrogen production is given by

$$v_{H_2} = k_1 \left[CH_3CHO\right] + \left(\frac{k_1}{k_9}\right)^{1/2} (k_6' + k_8) \left[CH_3CHO\right]^{3/2} \qquad (9)$$

The rates of hydrogen production are increased to a greater percentage than those of ethane. This is to be expected since the rate expression contains at least three terms which are in their pressure-dependent regions.

On the whole, the results of the inert-gas studies are consistent with the mechanism proposed. However, the main factor behind all these operations is the understanding of the ratio. The results of Dexter and Trenwith (17) can be explained on the same basis. When 250 mm of acetaldehyde was pyrolyzed in the presence of 200 mm CO_2, they found that the yields of acetone and methane remained unchanged and the rates of formation of hydrogen and of ethane increased. These observations are consistent with our mechanism; the individual rate constants k_1 and k_9 are pressure-dependent while the ratio of the rate constants shows very little dependence.

Figure 33

Typical yield-time plots for hydrogen formation in the presence of CO_2.

Δ 42 mm CH_3CHO

▲ 42 mm CH_3CHO + 210 mm CO_2

o 22 mm CH_3CHO

● 22 mm CH_3CHO + 110 mm CO_2

o 22 mm CH_3CHO + 220 mm CO_2

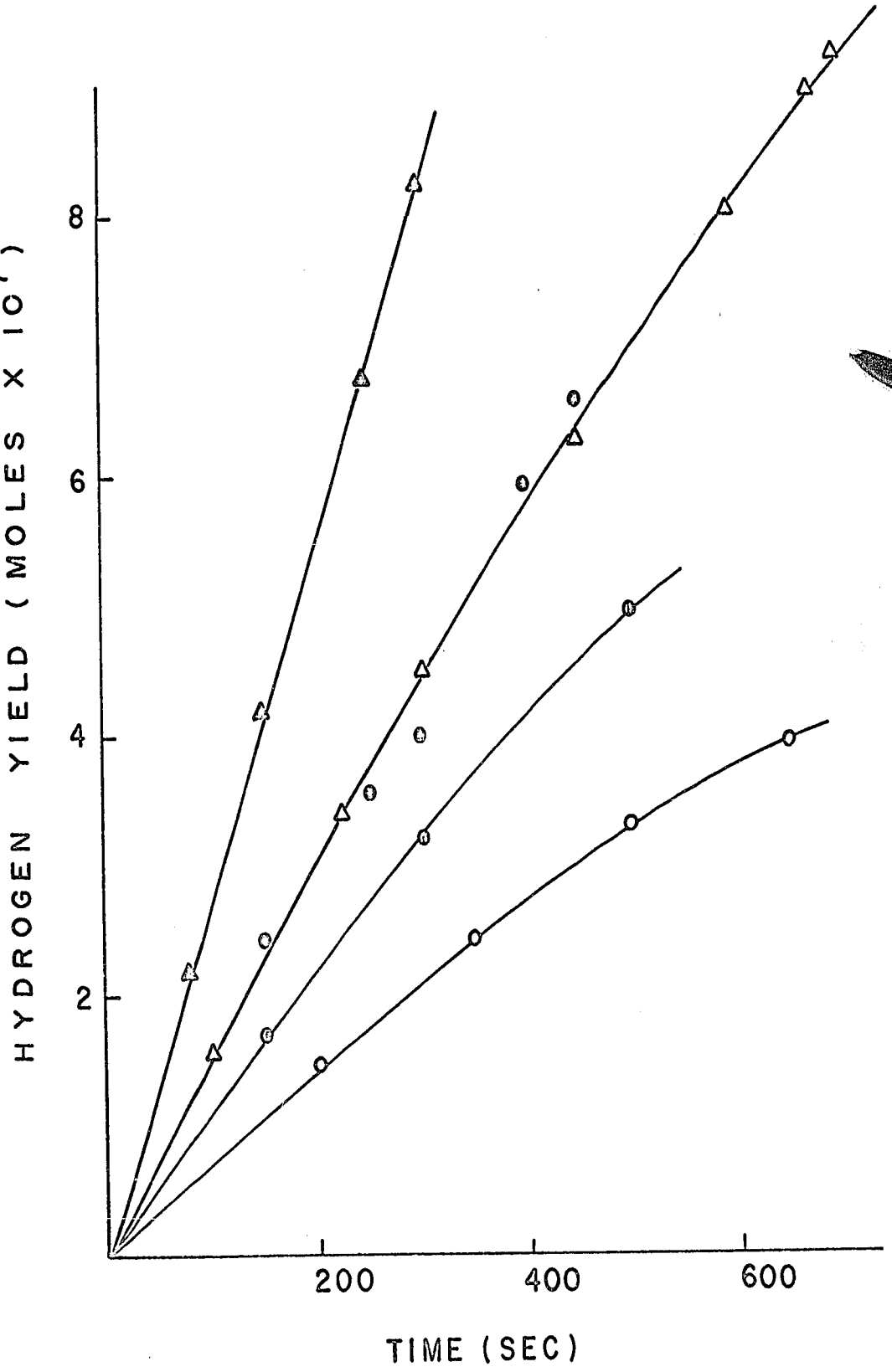
HYDROGEN YIELD (MOLES X 10^7)
8
6
4
2
200
400
600
TIME (SEC)

Table 12 - Effect of CO_2 on rates of hydrogen production at 540°C. All rates are in mole cc^{-1} sec^{-1}

P CH_3CHO mm Hg	$v^{o}_{H_2} \times 10^{13}$	$v^{5x}_{H_2} \times 10^{13}$	$v^{10x}_{H_2} \times 10^{13}$
42	32	56	-
22	14	23	32.6

Surface Effects

(a) Packing

In experiments with the packed vessel at 500°C the S/V ratio has increased 16-fold from 0.6 to 9.38 cm^{-1}. All the products show a small increase in rate, the results being shown in Figures 5, 12, 18, and 23. The initial rates of formation of various products are given in Table 13. The increases in the rates of formation of CH_4, CH_3COCH_3, H_2 and C_2H_6 are about 10, 10-15, 20 and 15-20 percent respectively. The ratios $v_{C_2H_6}^{\frac{1}{2}}/v_{CH_4}$ at 118 mm pressure of CH_3CHO at 500°C are equal to 8.4×10^{-5} and 8.3×10^{-5} for the packed and unpacked vessels. Although the individual rates have increased, the ratios of the rates remain essentially constant. These results suggest that the small increase in rate can be attributed to a surface initiation reaction. As soon as the chain is initiated, the rest of the products will increase proportionally according to the relationships

$$\frac{k_9^{\frac{1}{2}}}{k_4} = \frac{v_{C_2H_6}^{\frac{1}{2}}}{v_{CH_4}} \left[CH_3CHO\right] \qquad (3)$$

and

$$\frac{k_8}{k_4} = \frac{v_{acetone}}{v_{CH_4}} \qquad (8)$$

The ratio $v_{acetone}/v_{CH_4}$ can be explained on similar grounds.

Table 13 - Initial rate of formation for various products at 500°C in packed and unpacked vessels. The data for unpacked vessel were obtained by interpolation of the results given in Table. 1. All rates are in mole cc^{-1} sec^{-1}

P CH_3CHO mm Hg	$v_{CH_4} \times 10^{10}$		$v_{H_2} \times 10^{13}$		$v_{acetone} \times 10^{13}$		$v_{C_2H_6} \times 10^{13}$	
	Packed	Unp.	Packed	Unp.	Packed	Unp.	Packed	Unp.
81	9.35	8.52	15.8	13.8	7.05	6.50	1.25	1.05
118	16.2	14.80	25.0	21.8	12.3	11.0	1.86	1.49
181	31.2	29.1	45.2	40.8	22.34	21.0	2.82	2.34
325	76.6	71.0	105.0	91.3	-	-	5.13	4.27
452	129.0	116.0	166.0	145.0	-	-	-	-
520	155.0	142.0	200.0	174.0	-	-	-	-

It has been shown by Lin and Back (55) that the process $C_2H_6 \longrightarrow 2CH_3$ is not effected by changing the surface:volume ratio, and from the principle of microscopic reversibility, $CH_3 + CH_3 \longrightarrow C_2H_6$ should not be influenced by the nature of the surface. Taking the rates of formation of various products at S/V values of 9.38 cm^{-1} and 0.6 cm^{-1} the rate at zero S/V ratio can be obtained by extrapolation. This has essentially the same value as the one obtained for the unpacked vessel. Therefore, the rates of formation in the unpacked vessel for various products are homogeneous. The initiation on the surface may be of the type proposed by Wojciechowski and Laidler (80), in which initiation may occur as

$$CH_3CHO + S \longrightarrow CH_3CO + S\text{-}H$$

probably followed by

$$S\text{-}H \longrightarrow S + H$$

or partially by

$$CH_3 + HS \longrightarrow CH_4 + S$$

If the latter reaction dominates, i.e. surface is equally involved in both initiation and termination, there will be no net effect of surface on the overall kinetics. There is no direct evidence as to whether the termination occurs on the surface or not, but it is clear that the initiation is more sensitive to surface than the termination reaction.

In the thermal decomposition of CF_3CHO (65), an

increase in rate was also observed when the reaction vessel was packed with silica tubing. The overall activation energy is similar in both cases. Since the minor products were not analyzed, the detailed role of surface is unknown.

(b) Carbon Coating

In kinetic studies of the gas-phase pyrolysis of alkyl halides, it has proved necessary to "season" the reaction vessel in order that reproducible kinetics may be obtained (81). "Seasoning" may be achieved by prolonged treatment of the vessel with the compound under investigation until a carbonaceous deposit is observed. It was believed that this coating covers active sites in the polar glass surface so that heterogeneous reactions were eliminated. Holbrook (82) found in 1964, however, that the carbon deposit from the gas-phase pyrolysis of allyl bromide showed a strong e.s.r. signal and that it had an odd electron content of 10^{18} per gm. He proposed that such carbons might therefore be reactive rather than inactive as previously believed. Holmes (83) found that allyl-bromide carbon catalyzes the HI decomposition and olefin isomerizations. The activation energies for these heterogeneous reactions are lower than those of the corresponding homogeneous reactions. In the present work, it was found that the rate of the acetaldehyde decomposition was almost doubled when the reaction vessel was coated with allyl bromide carbon. These results are shown in Tables 14 and 15. The double logarithmic plot for methane formation is shown in Fig. 34. The order of

Table 14 - Effect of carbon coating on the overall rate of acetaldehyde pyrolysis at 480°C. All rates are in mole cc^{-1} sec^{-1}

Uncoated Vessel		Coated Vessel	
P CH_3CHO mm Hg	$v_{CH_4} \times 10^{10}$	PCH_3CHO mm Hg	$v_{CH_4} \times 10^{10}$
77	3.3	86	7.2
118	6.24	93	9.2
150	9.13	120	12.3
195	13.2	157	19.4
295	25.2	204	24.5
559	65.3	241	36.4

Table 15 - Rate constants for the homogeneous and heterogeneous decomposition of CH_3CHO, HI and the cis ⟷ trans isomerization of but-2-ene

Compound	T°C	k (hom)	E_a	k (het)	E_a	v_{het}/v_{hom} for 100 mm Reactant
CH_3CHO	480	0.16 $cc^{\frac{1}{2}}$ $mole^{-\frac{1}{2}}$ sec^{-1}	49.1	0.30 $cc^{\frac{1}{2}}$ $mole^{-\frac{1}{2}}$ sec^{-1}	-	1.9
HI	454	4.6×10^{-3} 1 $mole^{-1}$ sec^{-1}	42.5	2.4×10^{-5} sec^{-1}	9.5	10.0
Cis C_4H_8	369	5×10^{-8} sec^{-1}	65.0	1.2×10^{-5} sec^{-1}	15.2	240.0

Figure 34

Order plots for methane production at 480°C in coated and uncoated vessels.

o uncoated vessel

o vessel coated with allyl bromide carbon

Note: no change in overall rate.

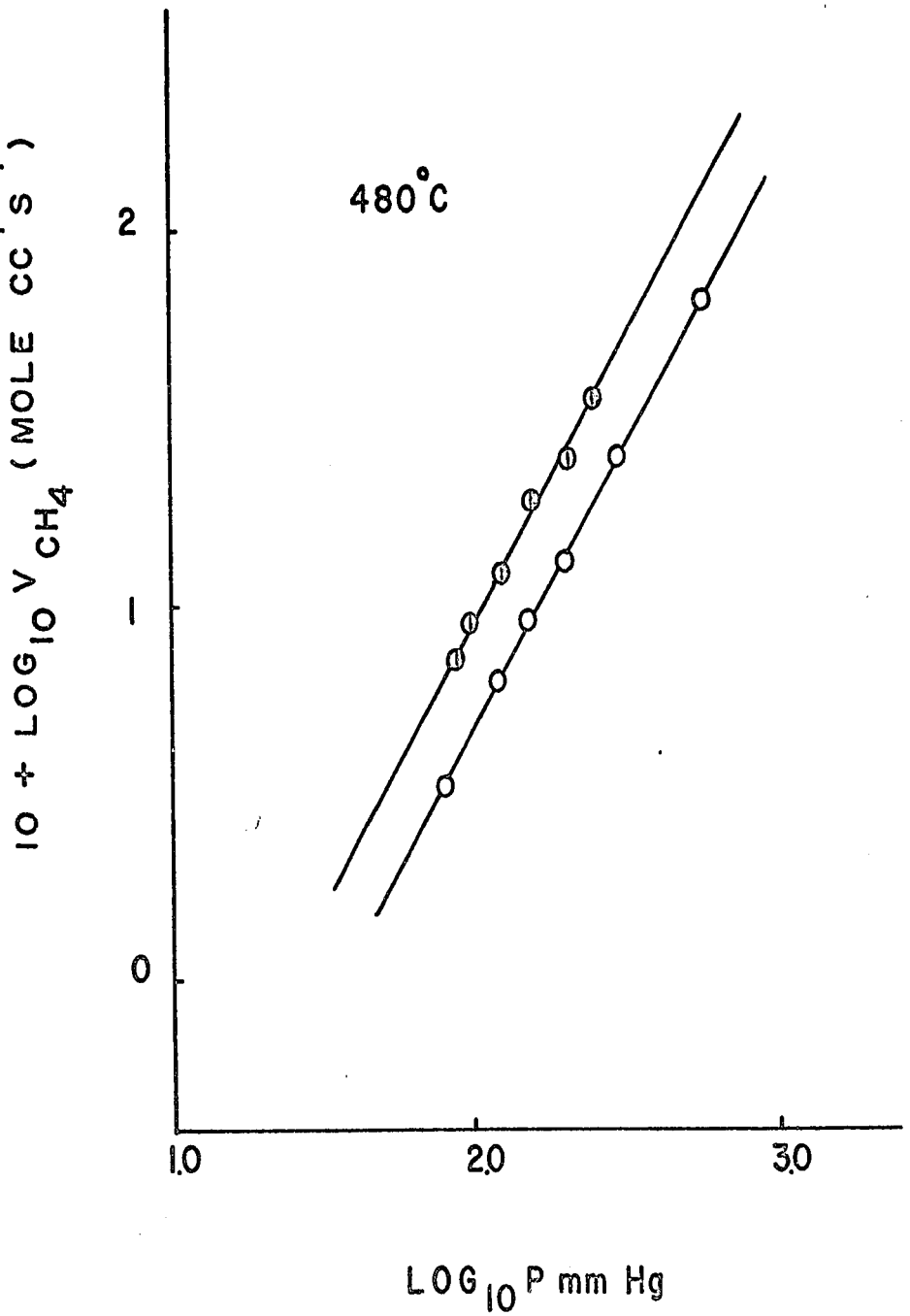
480°C
2
1
0
1.0
2.0
3.0
10 + LOG10 V CH4 (MOLE CC-1 S-1)
LOG10 P mm Hg

methane production is 3/2 in both the uncoated and coated vessels. The processes responsible for the surface-initiation reactions are suggested to be either

(i) $CH_3CHO + S \longrightarrow SH + CH_3CO$

or

(ii) $CH_3CHO + S \longrightarrow CH_3CHO^*$

$CH_3CHO^* + CH_3CHO \longrightarrow CH_3CHOH + CH_3CO$

where CH_3CHO^* represents an excited species. If reaction (ii) is significant in the initiation process the steady-state treatment leads to an overall order which is higher than 3/2; this is not observed. Reaction (i), the abstraction of the hydrogen atom of the aldehyde group by the surface, therefore, seems more probable. These observations show that a pyrolytic carbon with a high odd electron content is capable of initiating free-radical reactions, as postulated by Wojciechowski and Laidler (80).

Time-Course Studies

Attempts have been made to derive some mathematical functions to fit the experimental time-course data. Since the rate of dissappearence of acetaldehyde is

$$-\frac{d[M]}{dt} = k[M]^{3/2}$$

it follows that

$$[M] = \left[\frac{2 [M]_o^{\frac{1}{2}}}{kt [M]_o^{\frac{1}{2}} + 2} \right]^2 \qquad (20)$$

where $[M]_o$ is the initial concentration of acetaldehyde. The concentration of methane as a function of $[M]_o$, t and k can be expressed using

$$[CH_4] = [M]_o - [M] \qquad (21)$$

Comparison of calculated yield-time curves with experimental results for methane production is shown in Fig. 35. The calculated curve agrees well with the experimental results even to very high conversion (70%), indicating that the bending of the curve is due to the disappearence of acetaldehyde only. It is of interest here to mention a few points regarding the analysis of the kinetic results. In Fig. 36, curve A is calculated from equation (21) divided by t and curve B is calculated from the equation

$$\frac{d [CH_4]}{dt} = k \left[\frac{2 [M]_o^{\frac{1}{2}}}{kt [M]_o^{\frac{1}{2}} + 2} \right]^3 \qquad (22)$$

which is obtained by differentiating equation (20). The circles represent $[CH_4]/t$ obtained from experiment. It is noted that both methods give the same initial rate and that the differential method deviates from linearity at a much earlier stage. The extrapolation to obtain the initial rate by the differential method is therefore less reliable than the corresponding integration method.

Figure 35

Comparison of calculated yield-time curves with experimental results for methane production.

Solid curve calculated from equation (21).

Experimental points indicated by circles.

A = 523°C 117 mm Hg
B = 500°C 118 mm Hg

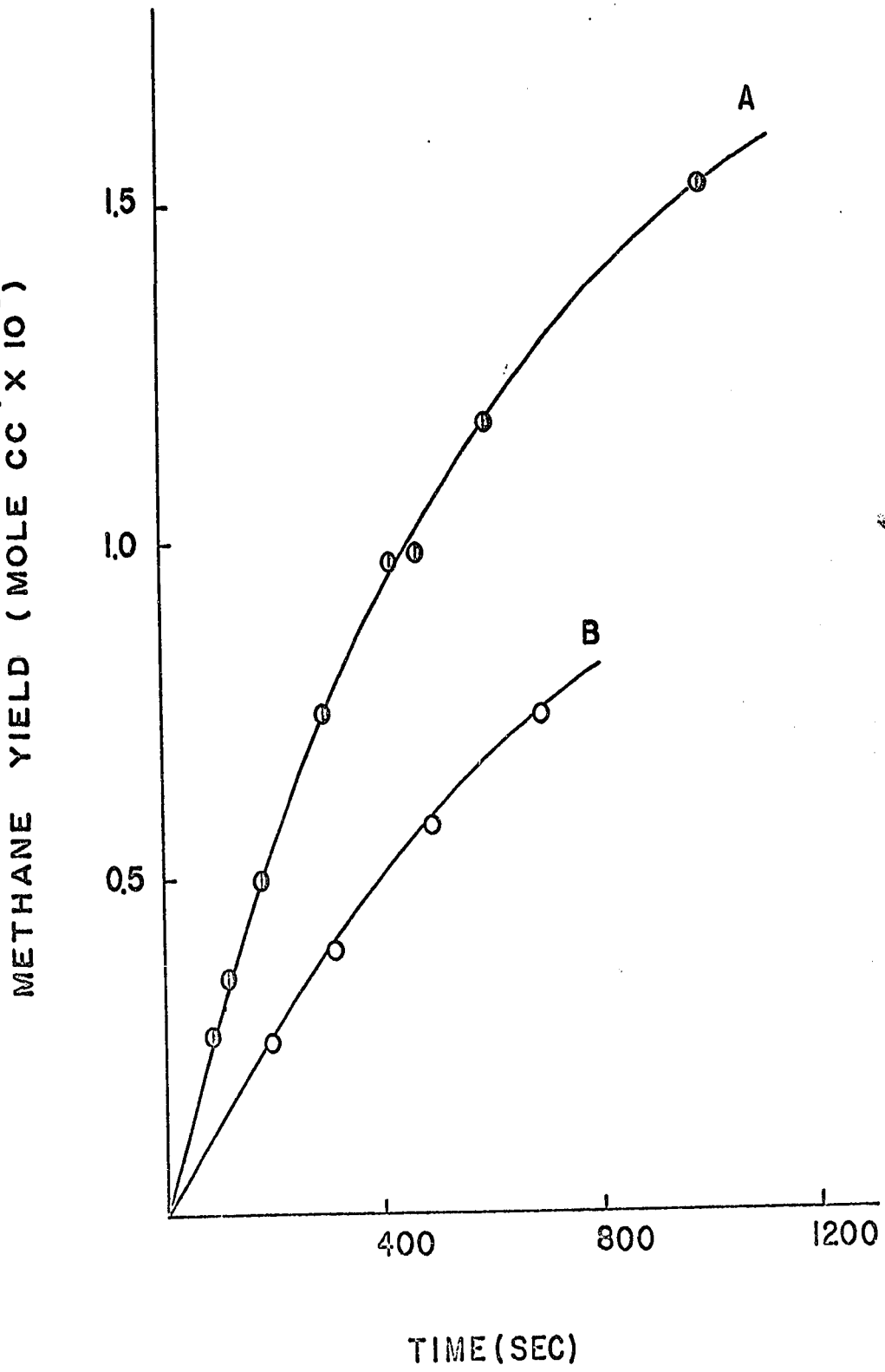
METHANE YIELD (MOLE CC^{-1} X 10^{6})
1.5
1.0
0.5
A
B
400
800
1200
TIME (SEC)

Figure 36

Comparison of integrated and differential rate. Experimental points indicated by circles.

$$(A)\quad \frac{\left[CH_4\right]}{t} = \left[M\right]_o - \left[\frac{2\left[M\right]_o^{\frac{1}{2}}}{kt\left[M\right]_o^{\frac{1}{2}} + 2}\right]^3 \Big/ t$$

$$(B)\quad \frac{d\left[CH_4\right]}{dt} = k\left[\frac{2\left[M\right]_o^{\frac{1}{2}}}{kt\left[M\right]_o^{\frac{1}{2}} + 2}\right]^3$$

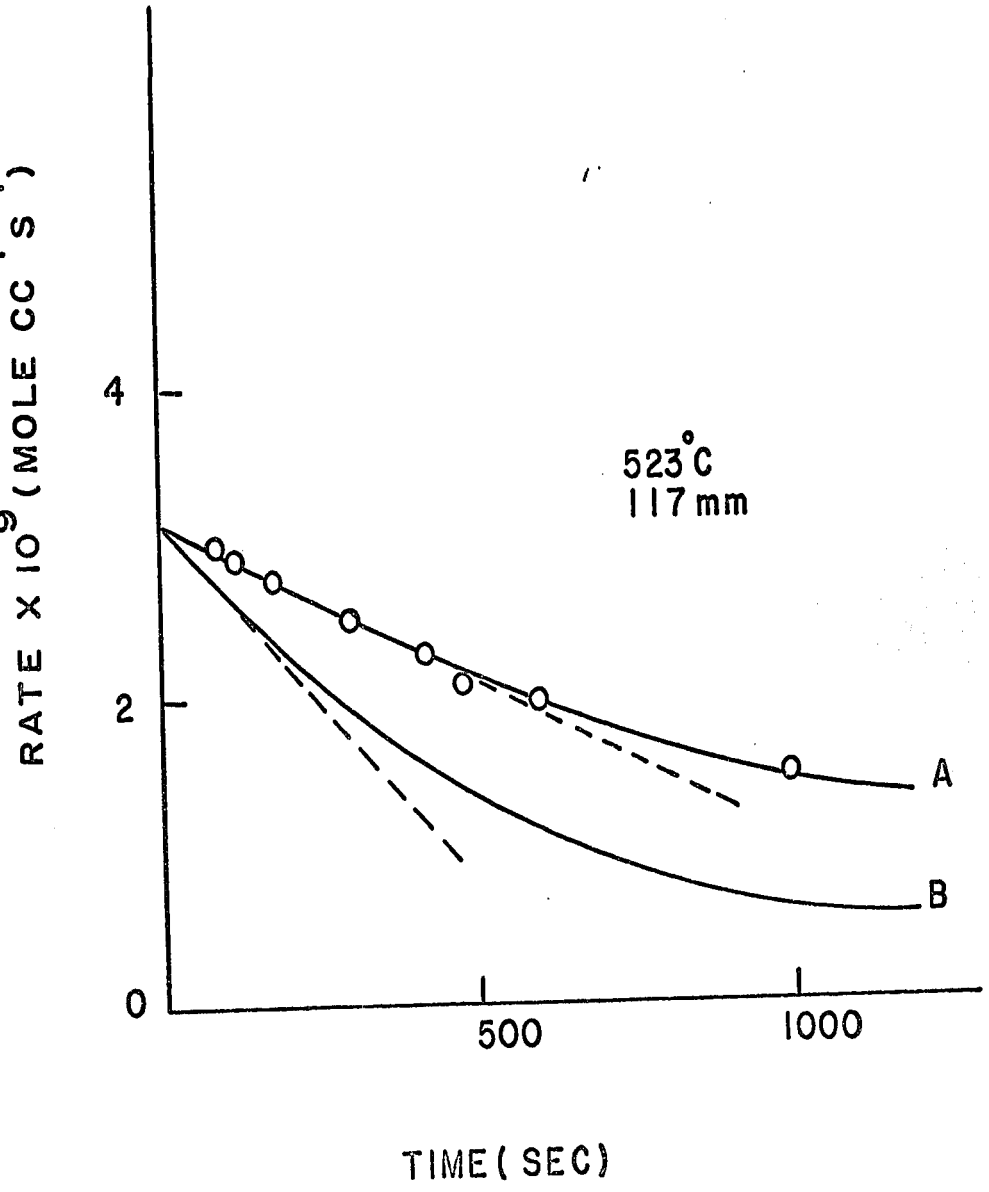
RATE X 10^9 (MOLE CC^-1 S^-1)
4
2
0
523°C
117 mm
A
B
500
1000
TIME (SEC)

According to the proposed mechanism, the rate of formation of acetone is

$$\frac{d\left[\text{Acetone}\right]}{dt} = k_8 \left(\frac{k_1}{k_9}\right)^{1/2} \left[M\right]^{3/2}$$

and hence

$$\left[\text{Acetone}\right] = k_8 \left(\frac{k_1}{k_9}\right)^{\frac{1}{2}} \int_0^t \left(\frac{a}{bt + c}\right)^3 dt$$

where $a = 2\left[M\right]_o^{\frac{1}{2}}$

$b = k\left[M\right]_o^{\frac{1}{2}}$

$c = 2$

$$\left[\text{Acetone}\right] = k_8 \left(\frac{k_1}{k_9}\right)^{1/2} \left[M\right]_o^{3/2} \frac{4}{k\left[M\right]_o^{1/2}} \left[\frac{1}{4} - \frac{1}{\left(kt\left[M\right]_o^{1/2} + 2\right)^2}\right] \qquad (23)$$

and

$$\lim_{t \longrightarrow 0} \frac{\left[\text{Acetone}\right]}{t} = k_8 \left(\frac{k_1}{k_9}\right)^{1/2} \left[M\right]_o^{3/2} \qquad (24)$$

since

$$\lim_{t \longrightarrow 0} \frac{1}{t}\left[\frac{1}{4} - \frac{1}{\left(kt\left[M\right]_o^{\frac{1}{2}} + 2\right)^2}\right] = \frac{k\left[M\right]_o^{\frac{1}{2}}}{4}$$

The calculated yields of acetone calculated from equation (23), agree with the experimental yields up to 50% conversion, as shown in Fig. 37. Again, the curvature in the plot is due to the disappearence of acetaldehyde alone.

Similarly, the yield of ethane production can be derived using the equation

Figure 37

Comparison of calculated yield-time curves
with experimental results for acetone production.
Solid curve calculated from equation (23).
Experimental points indicated by circles.

A = 523°C 117 mm Hg
B = 500°C 118 mm Hg

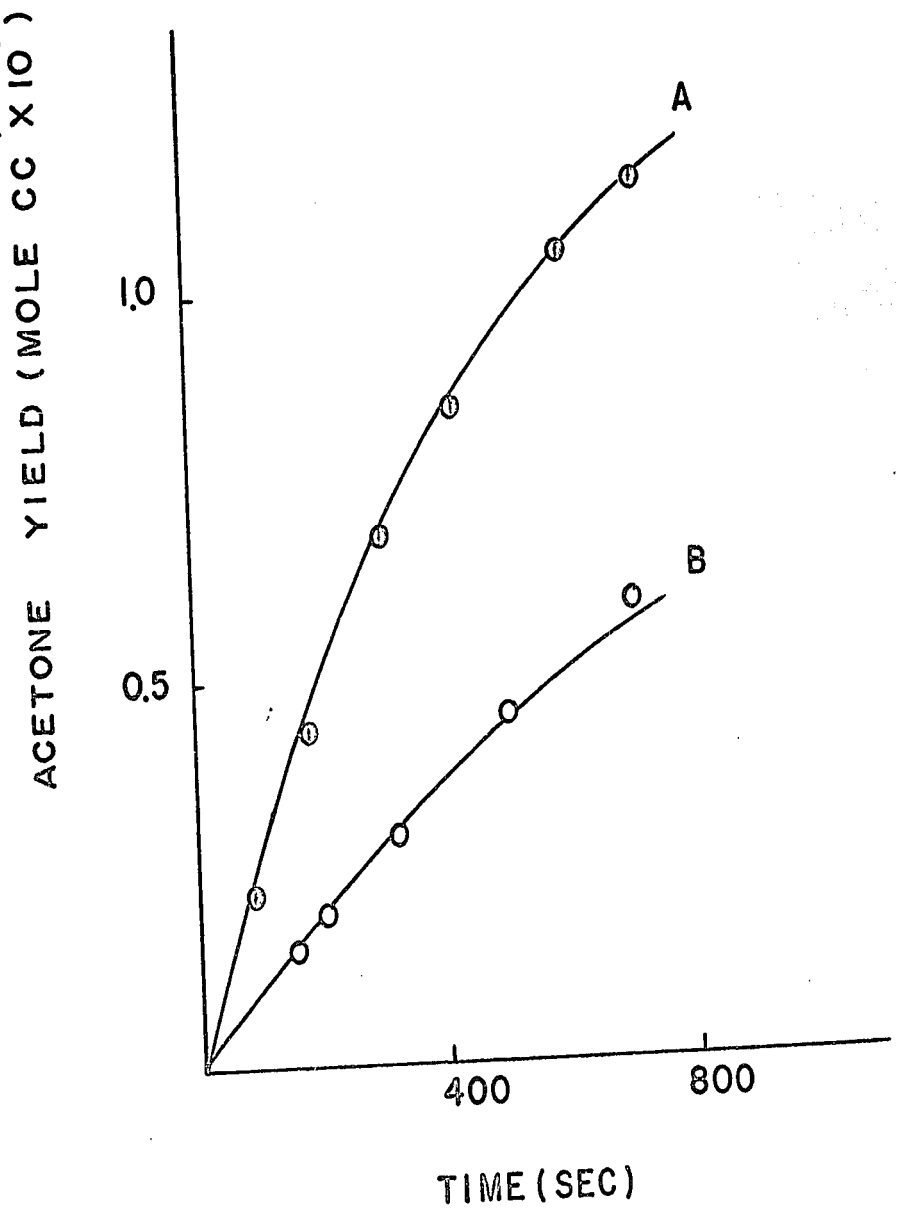
ACETONE YIELD (MOLE CC^{-1} X 10^{9})
1.0
0.5
A
B
400
800
TIME (SEC)

$$\left[C_2H_6\right] = k_9 \left(\frac{k_1}{k_9}\right) \frac{4}{k} \left[M\right]_o^{\frac{1}{2}} \left[\frac{1}{2} - \frac{1}{\left(kt \left[M\right]_o^{\frac{1}{2}} + 2\right)} \right] \qquad (25)$$

Fig. 38 shows the calculated curves and the experimental points.

The rate of hydrogen production is given by the equation

$$\frac{d\left[H_2\right]}{dt} = k_1 \left[M\right] + \left(k_6' + k_8\right) \left(\frac{k_1}{k_9}\right)^{1/2} \left[M\right]^{3/2} \qquad (9)$$

and hence,

$$\frac{\left[H_2\right]}{t} = \frac{4\ k_1}{k} \left[M\right]_o^{\frac{1}{2}} \left[\frac{1}{2t} - \frac{1}{\left(kt \left[M\right]_o^{\frac{1}{2}} + 2\right) t} \right] + 4 \left(k_6' + k_8\right) \left(\frac{k_1}{k_9}\right)^{\frac{1}{2}} \frac{\left[M\right]_o}{k} \left[\frac{1}{4t} - \frac{1}{\left(kt \left[M\right]_o^{\frac{1}{2}} + 2\right)^2 t} \right] \qquad (26)$$

or

$$\frac{\left[H_2\right]}{t} - f(t) = y.g.(t) \qquad (27)$$

where

$$f(t) = \frac{4\ k_1}{k} \left[M\right]_o^{\frac{1}{2}} \left[\frac{1}{2t} - \frac{1}{\left(kt \left[M\right]_o^{\frac{1}{2}} + 2\right) t} \right]$$

$$y = 4 \left(k_6' + k_8\right) \left(\frac{k_1}{k_9}\right)^{\frac{1}{2}} \frac{\left[M\right]_o}{k}$$

$$g(t) = \left[\frac{1}{4t} - \frac{1}{\left(kt \left[M\right]_o^{\frac{1}{2}} + 2\right)^2 t} \right]$$

Figure 38

Comparison of calculated yield-time curves with experimental results for ethane production. Solid curve calculated from equation (25). Experimental points indicated by circles.

A = 523°C 117 mm Hg
B = 500°C 118 mm Hg

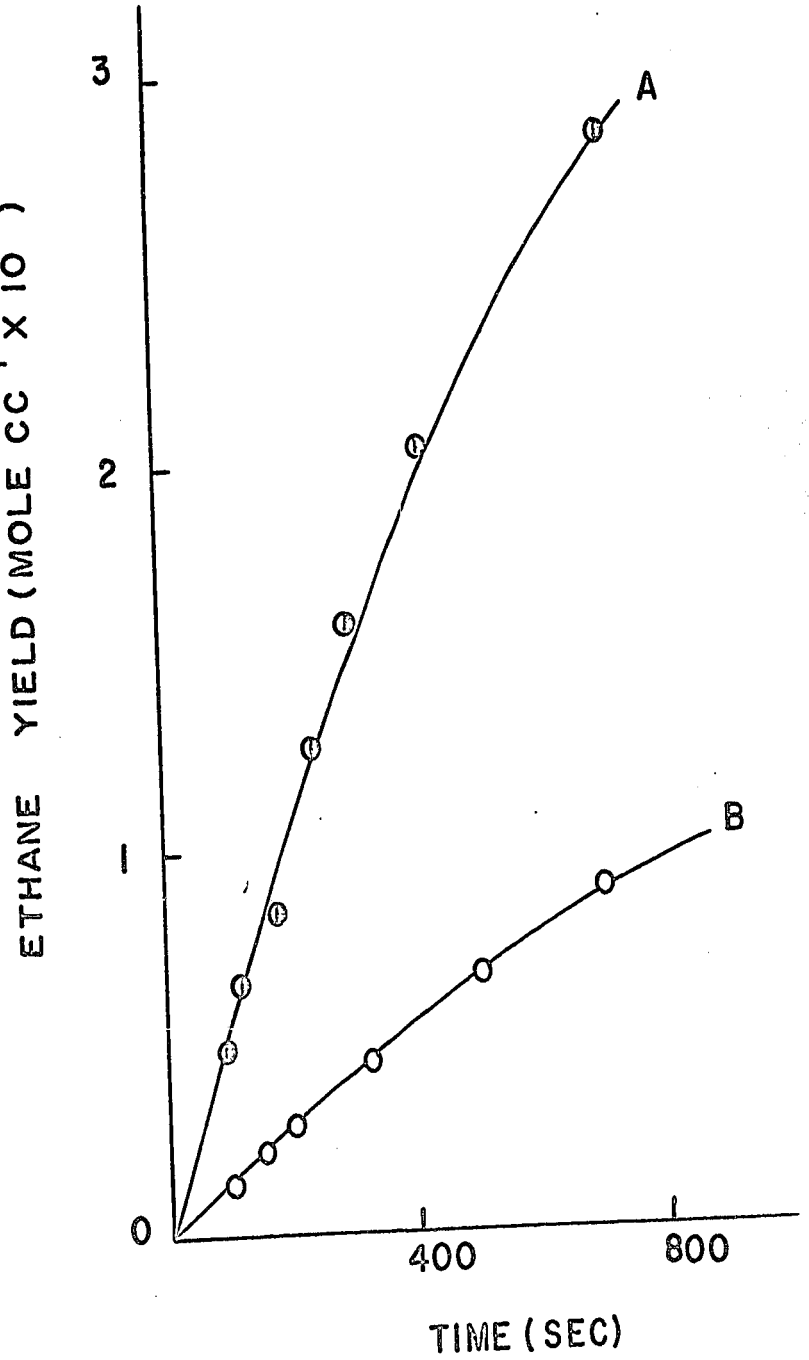
ETHANE YIELD (MOLE CC^{-1} X 10^{10})
3
2
1
0
400
800
TIME (SEC)
A
B

The plot of $\left[H_2\right] / t - f(t)$ vs. $g(t)$ is given in Fig. 39; a linear relationship is obtained.

It is concluded that the production of CH_4, CH_3COCH_3, C_2H_6 and H_2 is consistent with the proposed mechanism, and that there is no loss or gain of these products resulting from other secondary processes.

Figure 39

Plot of $\left[H_2\right]/t - f(t)$ vs. $g(t)$ at 523°C.

523°C
117 mm
7
6
5
4
3.0
2.5
2.0
g(t) x 10^4
{[H2]/t - f(t)} x 10^12

CHAPTER IV

GENERAL DISCUSSION

In this chapter, additional discussion is made on a few special topics which previously have not been described in detail.

Unimolecular Decomposition of Acetaldehyde

It is seen from Fig. 29 that the ratio k_1/k_9 at 540°C becomes pressure-dependent below 20 mm Hg. On the other hand, the rate constant k_9 shows a drastic pressure dependence below 80 mm Hg and a small pressure dependence at higher pressures (see Fig. 13). From these observations, it is obvious that k_1 must experience a pressure dependence similar to that of k_9 at higher pressures. However, at lower pressures, k_1 must be falling-off faster than k_9 so that an overall decrease in the ratio k_1/k_9 is noted. Since the rate of initiation must be equal to the rate of termination,

$$v_1 = v_{C_2H_6} + v_{C_2H_5CHO} \tag{28}$$

$$k_1'' \left[CH_3CHO\right] = k_1' \left[CH_3CHO\right] + v_{C_2H_5CHO}$$

$$k_1'' = k_1' + \frac{v_{C_2H_5CHO}}{\left[CH_3CHO\right]} \tag{29}$$

The values of k_1' at different pressures can be calculated from the rate of formation of ethane. These results are listed in Table 16. Fig. 40 depicts the falling-off of this rate constant k_1' as a function of pressure. The effect is very pronounced at lower pressures and still noticeable in the high-pressure region. Since k_1' is a function of pressure, an average value of k_1' would be meaningless. It is necessary to obtain the extrapolated value of k_1' by plotting $\left[CH_3CHO\right] / v_{C_2H_6}$ against the reciprocal of the square root of the acetaldehyde pressure. This is shown in Fig. 41. The Arrhenius plot of k_1' is given in Fig. 42 where darkened circles indicate the extrapolated values; squares represent a pressure of 77 mm, open circles 150 mm, darkened triangles 295 mm and crosses 559 mm. The rate equation, obtained by the method of least squares, is

$$\log k_1' \ (sec^{-1}) = 16.25 \pm 0.45 - \frac{82,700 \pm 1500}{2.303 \ RT}$$

In order to obtain k_1, the term $v_{C_2H_5CHO} / \left[CH_3CHO\right]$ must be added to k_1' according to equation (29). Accurate determination of propionaldehyde is difficult due to the presence of large amount of acetaldehyde and also because propionaldehyde decomposes rapidly at the temperatures of these experiments. The results for the rates of propionaldehyde production quoted in Tables 1 and 17 are therefore subject to a large margin of error. The values

Table 16 - The values of k_1' obtained from rates of ethane production

Pressure mm Hg	$\frac{v_{C_2H_6}}{[CH_3CHO]} \times 10^7$ sec^{-1}	$\frac{1}{k_1'} \times 10^{-7}$ sec	extrapolated $\frac{1}{k_1'} \times 10^{-7}$ sec
T = 480°C			
77	0.1335	-	
118	0.1321	7.57	
150	0.1368	7.31	6.10
195	0.1387	7.21	
295	0.1416	7.06	
559	0.1470	6.80	
T = 500°C			
20	0.3048	3.28	
30	0.4226	2.37	
77	0.5948	1.68	
118	0.6089	1.64	
150	0.5786	1.73	1.30
195	0.6477	1.54	
295	0.6537	1.53	
559	0.6855	1.46	
T = 523°C			
20	1.365	0.7326	
30.5	1.546	0.6468	
40	2.022	0.4945	
55	2.085	0.4796	
77	2.4820	0.4029	0.30
117	2.50	0.4000	
150	2.42	0.4132	
195	2.42	0.413	
292	2.66	0.376	
558	2.73	0.366	

Table 16 (continued)

Pressure mm Hg	$\frac{v_{C_2H_6}}{[CH_3CHO]}$ x 10^7 sec^{-1}	$\frac{1}{k_1'}$ x 10^{-7} sec	extrapolated $\frac{1}{k_1'}$ x 10^{-7} sec
T = 540°C			
22	3.687	0.271	
42	4.828	0.207	
79	6.418	0.155	
118	6.102	0.164	
152	6.804	0.147	0.10
198	7.324	0.137	
296	7.14	0.140	
563	7.20	0.139	

Figure 40

Plots of $\log_{10} k_1'$ vs. $\log_{10} P$ (mm Hg).

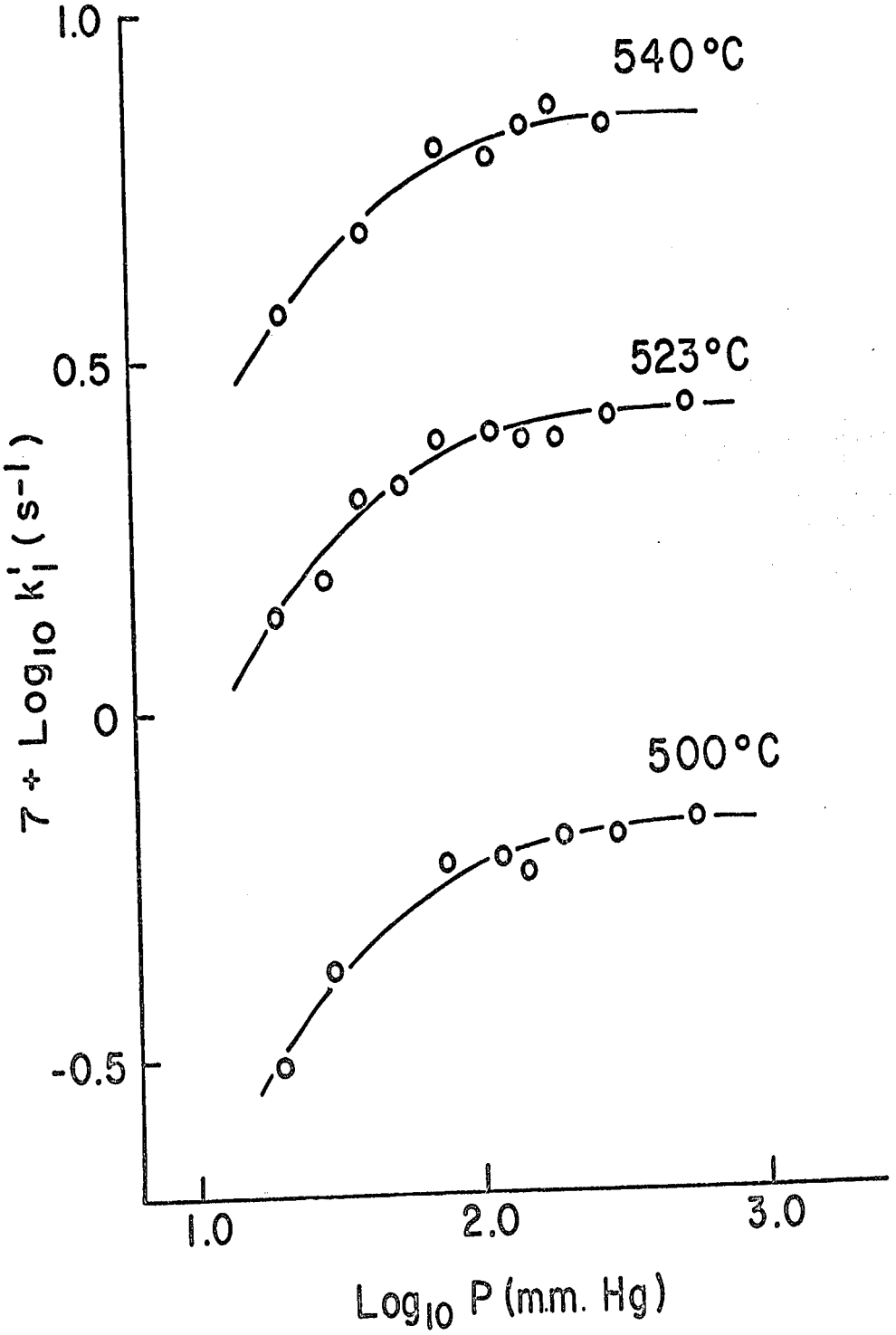
1.0
0.5
0
-0.5
540°C
523°C
500°C
7 + Log10 k'1 (s-1)
1.0
2.0
3.0
Log10 P (m.m. Hg)

Figure 41

Plots of $\left[CH_3CHO\right] / \nu_{C_2H_6}$ vs. $1/P^{\frac{1}{2}}$.

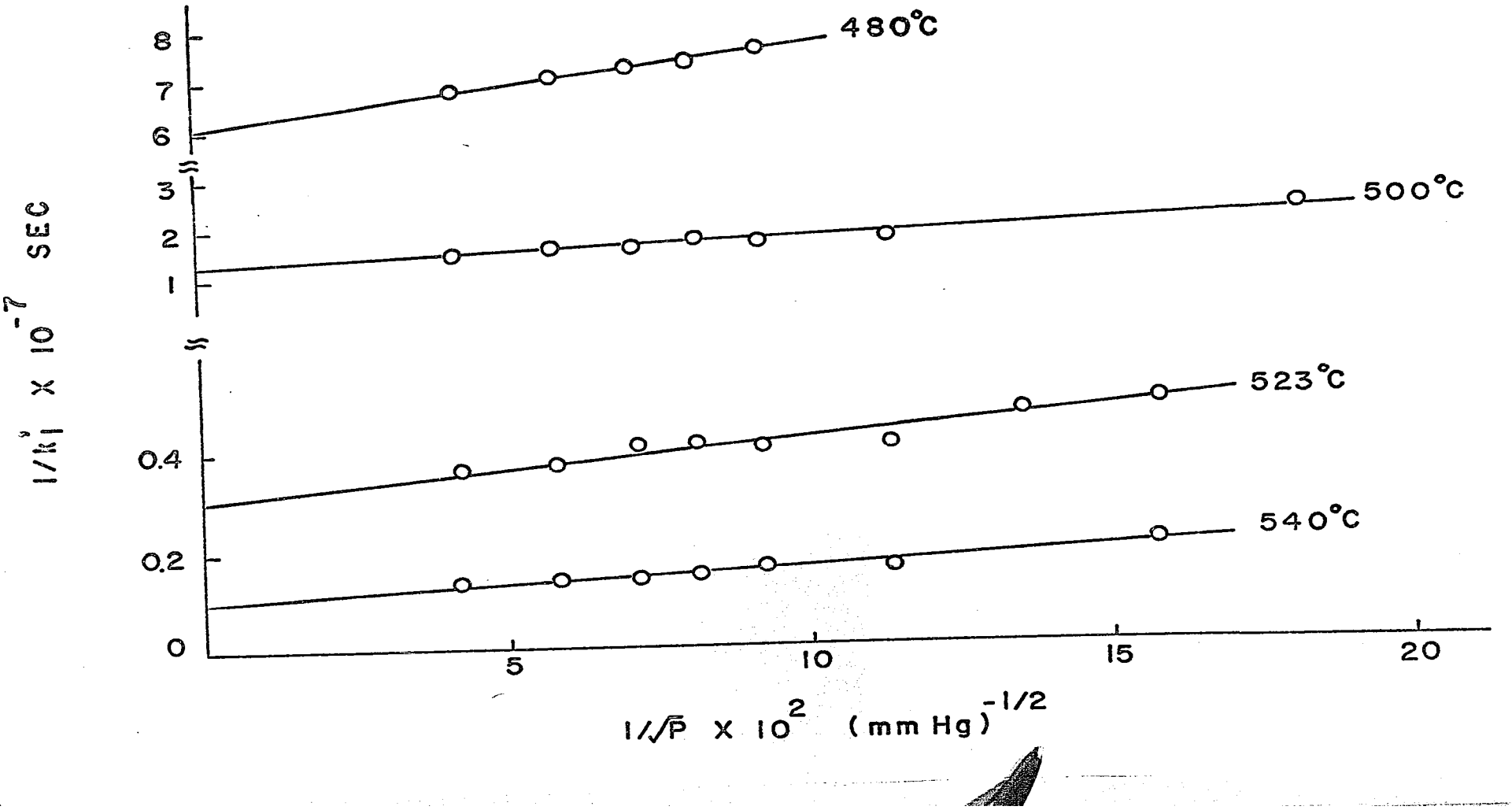
480°C
500°C
523°C
540°C
8
7
6
3
2
1
0.4
0.2
0
5
10
15
20
$1/k_1' \times 10^{-7}$ SEC
$1/\sqrt{P} \times 10^2$ (mm Hg)$^{-1/2}$

Figure 42

Arrhenius plot of k_1' and k_1''

□ k_1' at 77 mm

o k_1' at 150 mm

Δ k_1' at 295 mm

x k_1' at 559 mm

o k_1' extrapolated

o k_1''

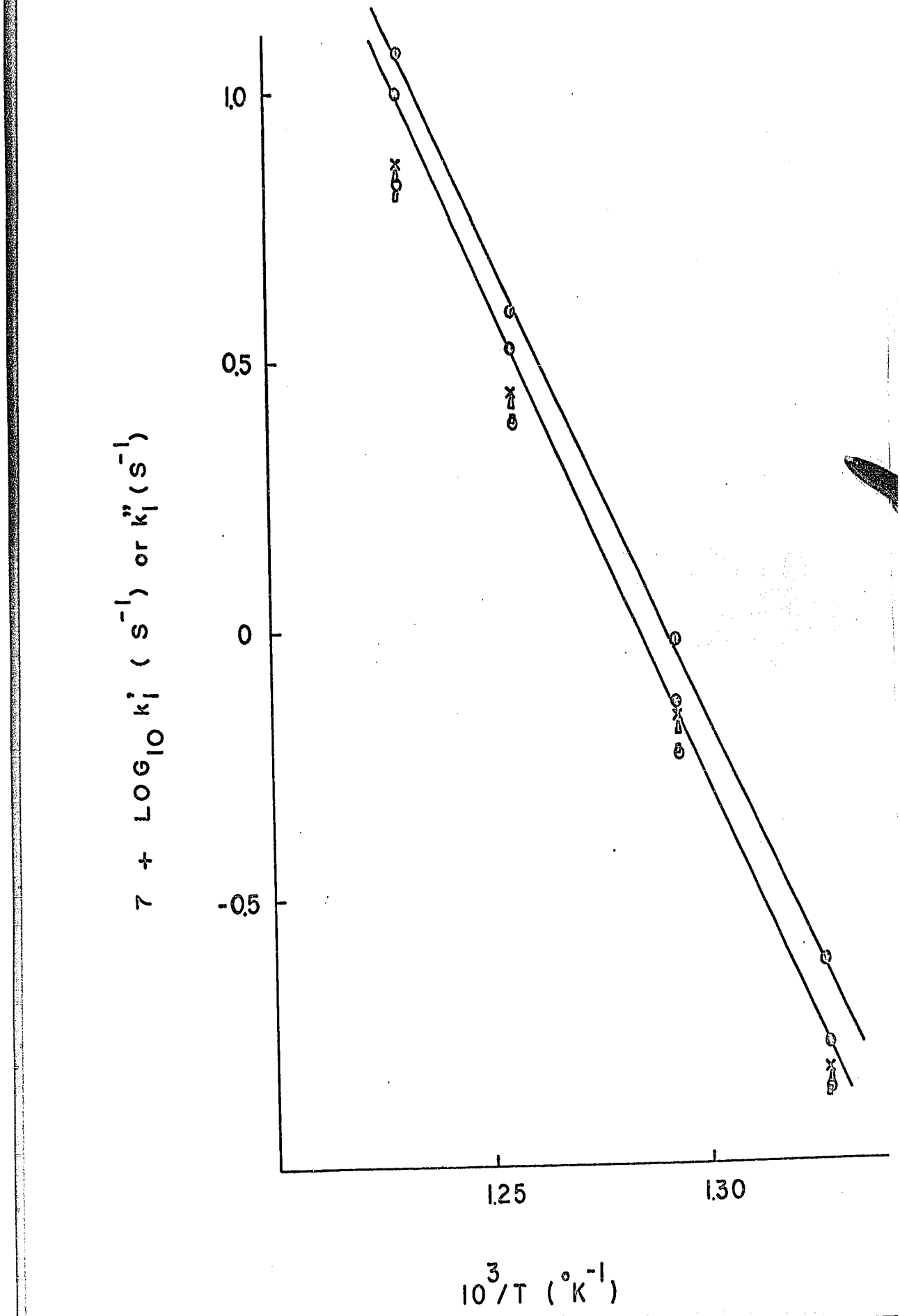
1.0
0.5
0
-0.5
7 + LOG10 k1' (S-1) or k1'' (S-1)
1.25
1.30
10^3/T (°K-1)

Table 17 - Values of $v_{C_2H_5CHO}/[CH_3CHO]$ at 118 mm and k_1' as a function of temperature

Temperature °C	$\frac{v_{C_2H_5CHO}}{[CH_3CHO]} \times 10^7$	$k_1' \times 10^7$
540	2.15	10.0
523	0.64	3.33
500	0.21	0.77
480	0.08	0.16

of k_1'' obtained from the rates of ethane and propionaldehyde production are shown by half-darkened circles in Fig. 42; the rate equation is

$$\log k_1'' \,(\mathrm{sec}^{-1}) = 15.30 - \frac{79{,}000 \pm 2{,}000}{2.303\ RT}$$

The frequency factor of a unimolecular reaction in the high-pressure region can be related to the entropy of activation by the expression

$$A = \kappa\, e\, \left(\frac{kT}{h}\right) e^{\Delta S^{\neq}/R}$$

where $\Delta S^{\neq}$ is the entropy of activation and κ the transmission coefficient, assumed to be unity. The ratio kT/h is approximately equal to 10^{13} sec^{-1} at ordinary temperatures. A frequency factor of this order of magnitude is referred to as a "normal frequency factor" and will have a value of $\Delta S^{\neq}$ close to zero. Most unimolecular reactions possess A factors in the range $10^{12.5}$ to $10^{14.5}$ sec^{-1}. However, there are some reactions whose frequency factors are higher than 10^{13} sec^{-1} by several powers of ten; for example, the value for the decomposition of acetaldehyde is of the order of 10^{15} sec^{-1}. These high frequency factors are related to positive entropies of the dissociation reaction; in other words, the entropies of the activated complexes are abnormally high. This type of activated complex is generally known as a "loose complex", because certain vibrations in the activated state are softened. The theory of high frequency

factors has been considered in some detail by Steel and Laidler (84). In view of the similarity between the acetaldehyde and ethane molecules, the entropy changes and frequency factors for both decompositions are very close to each other. The A factor for the ethane decomposition (55) is 1.00×10^{16} sec^{-1}. The entropy change (85) for reaction [1] is 36.5 e.u. (standard state 1 atm.) or 16.4 e.u. (standard state 1 mole per cc). The frequency factor for the combination of the methyl and formyl (CHO) radicals is estimated to be 1.4×10^{12} cc $mole^{-1}$ sec^{-1}. The combination of CH_3 and CHO radicals has not been observed; this may be because disproportionation dominates combination (86,87) but it may also be due to the fact that most work has been done only at very low pressures (87).

It is interesting to compare the pyrolysis of acetaldehyde and ethane at this stage since these two systems are quite similar in many respects. They both have $2CH_3 \longrightarrow C_2H_6$ as a chain-ending step and they are in the pressure-dependent region in both cases. Both initiation processes involve a homolytic cleavage of C-C bond and become pressure dependent at lower pressures. Although it is not possible to measure the values of k_1 in acetaldehyde as a function of pressure, the partial measurement of k_1 (i.e. k_1') is possible from the ethane measurements. This behaviour has already been shown in Fig. 40. Setser (88) calculated the unimolecular reaction rate for the unimolecular dissociation of the acetaldehyde molecule on

the basis of different models and found that the initiation is in its pressure-dependent region at 800°K and 100 mm pressure. It was pointed out that the results suggest that k_1 falls off at somewhat higher pressures than the k_1 for the C_2H_6 dissociation, as revealed by the fall-off in the overall rate constant. However, the fall-off in k_1 in acetaldehyde is compensated by the fall-off in k_9, so that the fall-off in the overall rate constant is not noted until at very low pressures. The overall rate for the CH_3CHO pyrolysis is expressed as

$$v_{overall} = k_4 \left(\frac{k_1}{k_9}\right)^{1/2} \left[CH_3CHO\right]^{3/2} \qquad (1)$$

In the pyrolysis of ethane, the fall-off in the overall rate constant is noted at a much higher pressure than in the CH_3CHO decomposition. The mechanism of ethane pyrolysis used by Lin and Back (55) is

[1] $C_2H_6 \longrightarrow 2\ CH_3$

[2] $CH_3 + C_2H_6 \longrightarrow CH_4 + C_2H_5$

[3] $C_2H_5 \longrightarrow C_2H_4 + H$

[4] $H + C_2H_6 \longrightarrow C_2H_5 + H_2$

[5a] $C_2H_5 + C_2H_5 \longrightarrow C_4H_{10}$

[5b] $C_2H_5 + C_2H_5 \longrightarrow C_2H_6 + C_2H_4$

The overall rate of the decomposition is the rate of formation of hydrogen or ethylene; hence,

$$v_{overall} = k_3 \left(\frac{k_1}{k_5}\right)^{1/2} \left[C_2H_6\right]^{1/2} \qquad (30)$$

The value of k_5 is not a function of pressure. The rate constant for reaction [1], k_1, is pressure-dependent below 200 mm and the rate constant for the ethyl radical decomposition, k_3, is pressure-dependent from pressures of 1 to 600 mm. Since both of the pressure-dependent terms appear in the numerator of equation (30), it is obvious that no compensation effect was observed, unlike the situation in the acetaldehyde pyrolysis.

The relationships between bond dissociation energy and the experimental activation energy can be established in the following manner for the reaction

[1] $\quad CH_3CHO \longrightarrow CH_3 + CHO$

The enthalpy change for this reaction is related to the activation energies (E_1 and E_{-1}) of the forward and reverse reactions by

$$\Delta H_1^o = \Delta E + RT = (E_1 - E_{-1}) + RT$$

and ΔH_1^o can also be represented as

$$\Delta H_1^o = \Delta H_{1,o}^o + \int_o^T \Delta C_p^o \, dT$$

Here $\Delta H_{1,o}^o$ is the standard enthalpy change at 0^oK. By definition

$$\Delta H_{1,o}^o = D\,(CH_3 - CHO)$$

$$v_{overall} = k_3 \left(\frac{k_1}{k_5}\right)^{1/2} \left[C_2H_6\right]^{1/2} \qquad (30)$$

The value of k_5 is not a function of pressure. The rate constant for reaction [1], k_1, is pressure-dependent below 200 mm and the rate constant for the ethyl radical decomposition, k_3, is pressure-dependent from pressures of 1 to 600 mm. Since both of the pressure-dependent terms appear in the numerator of equation (30), it is obvious that no compensation effect was observed, unlike the situation in the acetaldehyde pyrolysis.

The relationships between bond dissociation energy and the experimental activation energy can be established in the following manner for the reaction

[1] $\quad CH_3CHO \longrightarrow CH_3 + CHO$

The enthalpy change for this reaction is related to the activation energies (E_1 and E_{-1}) of the forward and reverse reactions by

$$\Delta H_1^o = \Delta E + RT = (E_1 - E_{-1}) + RT$$

and ΔH_1^o can also be represented as

$$\Delta H_1^o = \Delta H_{1,o}^o + \int_o^T \Delta C_p^o \, dT$$

Here $\Delta H_{1,o}^o$ is the standard enthalpy change at 0^oK. By definition

$$\Delta H_{1,o}^o = D\,(CH_3 - CHO)$$

where D represents the dissociation energy at $0^{o}K$; hence

$$D\ (CH_3 - CHO) = (E_1 - E_{-1}) + RT - \int_0^T \Delta C_p^o \quad dT$$

and ΔC_p^o, the difference in heat capacity of products and reactant, can be found by integrating from zero to the temperature under study. Unfortunately, the values of C_p^o for acetaldehyde as a function of temperature are not known. Lin and Back (70), however, have shown that in the case of ethane the value of $D(CH_3 - CH_3)$ is approximately equal to $E_1 - \frac{1}{2} RT$.

There are two types of unimolecular decompositions:

(a) Decomposition leading to the formation of two products, the recombination of which requires activation energy.

(b) Decomposition leading to the formation of two radicals the recombination of which requires no activation energy.

Szwarc (89) has shown that for a reaction of the latter class, the activation energy may be related to the bond dissociation energy in the following way:

$$D + RT \ > E_{exp} \ > D$$

In the case of the acetaldehyde decomposition,

$$D\ (CH_3 - CHO) = E_1 - \tfrac{1}{2} RT$$

$$= 78.2 \pm 2 \text{ kcal per mole}$$

This value leads to

$$\Delta H_f^o\ (CHO) \simeq 7 \text{ kcal per mole}$$

and $D\ (H - CHO) \simeq 87$ kcal per mole

in good agreement with the recent determination of Walsh and Benson (90). The recent value of D (CH_3CO-H) in CH_3CHO is 88 kcal per mole (72) and the present estimates appear to support the view that D (H - CHO) $\simeq$ D (CH_3CO - H) as suggested by several other authors (71,91,92). Using the above value, we get

$$D\ (H - CO) = \Delta H_f^o\ (CO) + \Delta H_f^o\ (H) - \Delta H_f^o\ (HCO)$$

$$\simeq 19 \text{ kcal}$$

There has been some controversy regarding the value for D (H - CO). Klein and Schoen (93,94) favor the high value of D (H - CO) $\sim$ 27 kcal as opposed to the low value of $\sim$ 15 kcal chosen by Calvert (92,95). Klein and Schoen have argued that D (H - CHO) $\leq$ 78 kcal per mole since photodecomposition of CH_2O by a free-radical mechanism initiated by 3650 Å radiation would not have occurred. Early electron-impact studies (96) and a recent reinterpretation of the electronic spectrum of CH_2O (97) have suggested that D (H - CHO) = 75 $\pm$ 2.3 kcal per mole. Further electron-impact data give the value of 79.5 kcal per mole (98). However, Walsh and Benson (90) have pointed out that the wave length of 3650 Å which corresponds to 78.3 kcal per mole is not sufficient to break the C-H bond. In order to explain the experimental facts, they have postulated a mechanism in which the initiation is via an excited state of CH_2O, possibly a triplet, as follows:

$$^1CH_2O \xrightarrow{h\nu} {}^1CH_2O^* \longrightarrow {}^3CH_2O^*$$

$$^3CH_2O^* + CH_2O \longrightarrow CH_2OH + CHO$$

$$M + CHO \longrightarrow M + H + CO$$

In addition, consideration of the role of the formyl radical in the dimethyl ether pyrolysis (99) supports a value for D (H - CHO) of 87 kcal per mole. Our estimated value is consistent with the "low" value of D (H - CO). It is interesting to point out that the information obtained from radical reactions are quite consistent and that values from electron-impact studies are always low.

The π -bond energy in formaldehyde can be obtained by the expression

$$D_{\pi} \text{ (HCHO)} = D \text{ (H - CHO)} - D \text{ (H - CO)}$$

$$\simeq 68 \text{ kcal per mole}$$

Thus, the π -bond energy in formaldehyde is about 7 kcal per mole lower than that of acetone obtained in our estimation (see below).

The Decomposition of the Isopropoxy Radical

The rate constant k_8 is not a simple rate constant but an apparent rate coefficient involving two elementary steps, as follows:

[11] $CH_3 + CH_3CHO \rightleftharpoons (CH_3)_2 \overset{O}{\overset{|}{C}}H$ (i-PrO)

[12] $(CH_3)_2\overset{O}{\overset{|}{C}}H \longrightarrow CH_3COCH_3 + H$

Application of the steady-state treatment to these reactions leads to

$$v_{(CH_3)_2\,CO} = k_{12}\left[\text{i-PrO}\right] = \frac{k_{11}k_{12}\left[CH_3\right]\left[CH_3CHO\right]}{k_{-11} + k_{12}}$$

$$= k_8\left[CH_3\right]\left[CH_3CHO\right]$$

whence

$$k_8 = \frac{k_{11}k_{12}}{k_{-11} + k_{12}} \qquad (31)$$

In normal molecules, the carbon-hydrogen bond is stronger than the carbon-carbon bond, and this relation is also true for radicals (100). If on this basis one assumes that $k_{-11} >> k_{12}$, then equation (31) reduces to (32)

$$k_8 = \frac{k_{11}k_{12}}{k_{-11}} \text{ or } K_{11}\,k_{12} \qquad (32)$$

It is possible to estimate k_{12} since $K_{11} = k_{11}/k_{-11}$ can be calculated from the enthalpy and entropy changes, ΔH_{11} and ΔS_{11}:

$$K_{11} = \exp\left(-\frac{\Delta H_{11}}{RT}\right)\exp\left(\frac{\Delta S_{11}}{R}\right) \qquad (33)$$

In Table 18 (85) are tabulated values of S^o and ΔH_f^o to be used in estimating K_{11}. The above entropy changes are in pressure units; if one chooses to have unit concentration (1 mole per cc) as the standard state, the

Table 18 - Approximate enthalpies of formation and entropies of gaseous compounds and free radicals (Ideal gas 298.2°K, 1 atm.)

	CH_3	CH_3CHO	i-PrO
S^o cal/deg mole	46.0	63.2	75.3
ΔH_f^o kcal per mole	32.0	-39.7	-15.0

ΔH_{11} = -7.3 kcal per mole

ΔS_{11} = -33.9 eu. (standard state 1 atm.)

Table 18 - Approximate enthalpies of formation and entropies of gaseous compounds and free radicals (Ideal gas 298.2°K, 1 atm.)

	CH_3	CH_3CHO	i-PrO
S^0 cal/deg mole	46.0	63.2	75.3
ΔH_f^0 kcal per mole	32.0	-39.7	-15.0

ΔH_{11} = -7.3 kcal per mole

ΔS_{11} = -33.9 eu. (standard state 1 atm.)

following equation will apply (101):

$$\Delta S_c = \Delta S_p - \Delta n \, R \ln RT \qquad (34)$$

Hence

$$\Delta S_{11} = -13.8 \text{ eu.} \quad (1 \text{ mole per cc})$$

whence

$$K_{11} = \exp - (-7300/RT) \exp (-13.8/R)$$

$$= 10^{\frac{-13.8}{4.576}} \; 10^{\frac{7300}{4.576\,T}} \text{ cc mole}^{-1}$$

at 298.2°K

$$K_{11} = 10^{-3.02} \; 10^{5.35} \text{ cc mole}^{-1}$$

$$= 10^{2.33} \text{ cc mole}^{-1}$$

From equation (32)

$$k_{12} = \frac{k_8}{K_{11}}$$

If we extrapolate our value of k_8 to 298.2°K

$$k_{12} \; (298.2^{\circ}K) = 6.82 \times 10^{-2} \text{ sec}^{-1}$$

Taking E_{12} = 19.1 kcal per mole (see below), the Arrhenius equation for k_{12} is

$$\log k_{12} \; (\text{sec}^{-1}) = 12.83 - \frac{19{,}100}{2.303 \; RT}$$

This compares well with the activation energy obtained for the decomposition of the ethoxy radical by carbon-hydrogen

bond fission (75):

$$C_2H_5O \longrightarrow H + CH_3CHO$$

The activation energy for decomposition was estimated to be 21 kcal per mole. Therefore, the value we derived for the decomposition of the isopropoxy radical by carbon-hydrogen bond fission is reasonable. The only value available in the literature for the decomposition of the isopropoxy radical by carbon-carbon fission is by Cox, Livermore and Phillips (102); their result is

$$k_{-11} = 10^{11.8}\ 10^{-17,300/4.576T}\ sec^{-1}$$

At 298.2°K

$$k_{-11} = 1.3 \times 10^{-1}\ sec^{-1}$$

$$k_{12} = 0.68 \times 10^{-1}\ sec^{-1}\ \text{(present work)}$$

The value of k_{-11} is slightly greater than k_{12} at 298.2°K. Since both rate constants are of the same order of magnitude, and both reactions will compete strongly with each other, it may be necessary to include reaction [12] in their mechanism. According to their scheme the only process which gives rise to acetone is hydrogen abstraction by nitric oxide

$$(CH_3)_2\ CHO + NO \longrightarrow (CH_3)_2CO + HNO$$

and if the total acetone formation is attributed to this reaction, k_{-11} would have been underestimated. It therefore

seems likely that k_{-11} has a larger value than given above, and that k_{-11} may be much greater than k_{12} over the temperature range of the present investigation.

Reaction [11] is exothermic by 7.3 kcal. The heat of activation can be related to the experimental activation energy by the relationship (101)

$$\Delta H^{\neq} = E_{exp} + (\Delta n^{\neq} - 1)\, RT \qquad (35)$$

where $\Delta n^{\neq}$ is the increase in the number of molecules from reactants to activated complex. This gives the value of -6.7 kcal for ΔE_{11} at 298.2°K. If E_{-11} is taken to be 17.3 kcal per mole (102) at 298.2°K, E_{11} and E_{12} will be 10.6 and 19.1 kcal per mole. The heats of formation of acetone (103) and H (104) are -51.7 and 52.1 kcal per mole respectively. With the use of the ΔH_f^0 values of the species involved in reaction [12], the heat of reaction turns out to be 15.4 kcal per mole which leads to ΔE_{12}= 14.8 at 298.2°K, hence E_{-12} = 4.3 kcal per mole.

Although the activation energy is low for reaction [-12], it is not important in the present system as the concentration of the hydrogen atom is small. The activation energy diagram at 298.2°K for these processes is given in Fig. 43 in which the first activated state shows the simultaneous formation of a C-C bond and the rupture of the C = O π bond. The second activated state shows the hydrogen atom elimination and the formation of the C = O π bond. The difference between these two states is 1.8 kcal

Figure 43

Activation energy diagram for addition and decomposition reactions at 298.2°K.

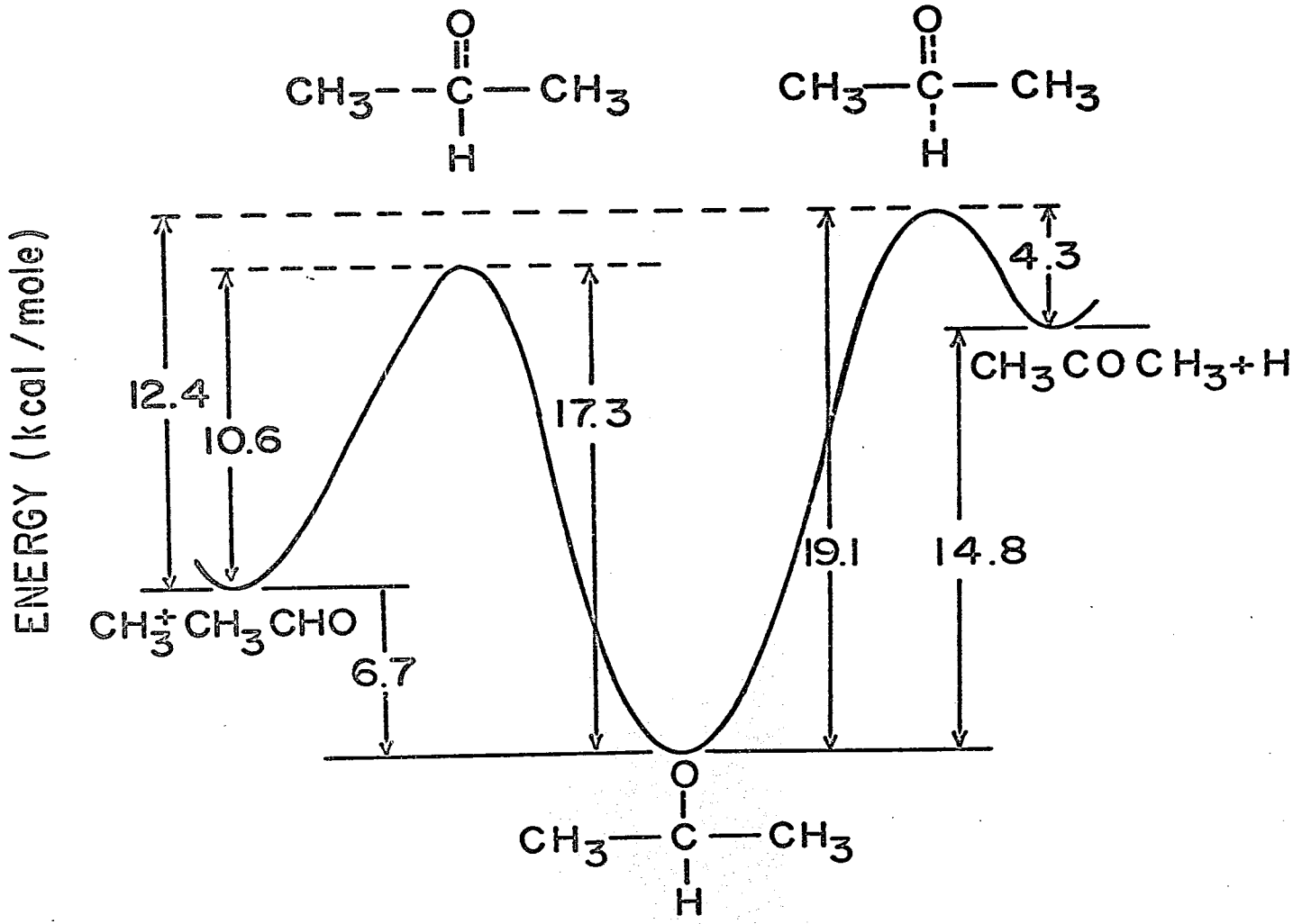
ENERGY (kcal / mole)
12.4
10.6
17.3
19.1
14.8
4.3
6.7
CH3 + CH3CHO
CH3COCH3 + H

per mole and is equal to a fraction of D (C-H) - D (C-C).

It is seen from the diagram that not only is E_{12} greater than E_{-11}, but also the endothermicity is twice as great. This would favor an alkyl elimination and seems to support our earlier assumption that $k_{-11} >> k_{12}$.

It is interesting to compare the above system with its homolog in which the methyl radical is added to formaldehyde to give an ethoxy radical which can then decompose by either a carbon-carbon bond fission or a carbon-hydrogen bond fission:

$$[17] \quad CH_3 + CH_2O \longrightarrow CH_3CH_2O$$

$$[18] \quad CH_3CH_2O \longrightarrow CH_3CHO + H$$

The thermochemical data are briefly summarized in the review of Gray and Williams (75).

It is noted that the endothermicities of reactions [18] and [-17] are both about 13 kcal per mole. The activation energy for reaction [-17] is almost as high as E_{18}, which is 21 kcal per mole. From the knowledge of the thermochemistry one would expect to find that in the C_2H_5O radical decomposition the carbon-hydrogen bond fission may be as important as the carbon-carbon bond fission. There appears to be a parallel between the thermochemistry and reactivity of the alkoxy radicals. The least thermochemically-stable radical will decompose at the fastest rate. If we include a few other radicals in our series, the general

order of stability will be CH_3O > C_2H_5O > iso-C_3H_7O > tert-C_4H_9O.

Multiple Bond Formation

Good discussions of radical decompositions and the energies of π bonds have been given by Benson (105) and Semenoff (106).

If we consider the C-H bond in ethane, D (CH_3CH_2 -H)= 98 kcal per mole, but if the methyl group contains a free valence in the α position, then D is lowered by approximately 60 kcal; thus D (CH_2CH_2-H) = 39 kcal per mole. The explaination for this is that on removing an H atom from C_2H_5 radical, we also formed a double bond. Therefore, we can define a π-bond energy, D_π , as the difference in strengths of the first and second bond-dissociation energies:

$$D_\pi \quad (C\text{-}C) = D\ (CH_3CH_2 - H) - D\ (CH_2CH_2 - H)$$

$$= (98 - 39)\ \text{kcal} = 59\ \text{kcal}$$

Similarly, D_π in propylene is found to be 58.5 kcal (105, 106). Using a similar approach, one is able to obtain the π-bond energy of acetone on the basis of the relationships

[19] $(CH_3)_2\text{-}\overset{H}{\underset{|}{C}}\text{-}OH \longrightarrow (CH_3)_2\text{-}C\text{-}OH + H$

[12] $(CH_3)_2\text{-}\overset{H}{\underset{|}{C}}\text{-}O \longrightarrow (CH_3)_2\,CO + H$

The tertiary carbon-hydrogen bond strength in isopropyl alcohol has been estimated by Barnard (107) and

recently measured by Walsh and Benson (108). The value is D $((CH_3)_2C$ (OH)-H) = 90.3 ± 1.1 kcal per mole. The enthalpy change for reaction [12] is 15.4 kcal per mole; hence

$$D_{\pi} \ (CH_3COCH_3) = D \ ((CH_3)_2C \ (OH)\text{-}H) - D((CH_3)_2 \ CO - H)$$

$$= 74.9 \text{ kcal per mole}$$

This is in excellent agreement with the π-bond energy in acetone estimated by Walsh and Benson (108) from the reactions

[20] $(CH_3)_2$ CHOH ⟶ $(CH_3)_2$ CHO + H

[21] $(CH_3)_2$ COH ⟶ $(CH_3)_2$ CO + H

By using Gray and Williams's estimate (109) of 102 kcal per mole for reaction [20] and Walsh and Benson's measurements of 27.4 kcal per mole for reaction [21], they obtain D'_{π} (CH_3COCH_3) = 74.6 ± 1.5 kcal per mole.

Reaction [-12] involves a hydrogen-atom addition to the carbon end of the carbonyl group and has an activation energy of 4.3 kcal per mole; reaction [-21] has the same reactants but a different intermediate because the addition takes place at a different site. The addition of an H atom to the oxygen end of the carbonyl bond would probably require more energy than the one reacting on the carbon end. For this reason, one would expect that E_{21} must be greater than 31.5 kcal per mole. It is not

surprising that hydrogen-atom addition to the carbonyl bond has a higher activation energy than the addition to olefins (110-112) since the π-bond energy in an olefin is about 10 - 15 kcal lower than for those compounds containing a carbonyl group.

Possible Tunnelling in the Reaction $CH_3 + CH_3CHO \longrightarrow CH_4 + CH_3CO$

The abstraction by the methyl radical of a hydrogen atom from acetaldehyde has been studied by many workers and by various methods; the results are tabulated in Table 19. The Arrhenius plot for different values of $k_4/k_9^{\frac{1}{2}}$ is shown in Fig. 44. Our results agree very well with Dodd's results and, in fact, a straight line can be drawn to link up his and our set of points in the Arrhenius plot. It is noted that his temperature range is the next highest to ours. Taken all together the results seem to suggest a slight increase in activation energy over the range of temperatures investigated. One question is whether our methane production could arise from another source. The only other plausible route of methane formation is by reaction [6],

$$CH_3 + CH_3CHO \longrightarrow CH_4 + CH_2CHO$$

The rate constant for this process is not known but the rate constant for the hydrogen atom abstraction by a methyl radical from acetone is well established. If we assume the

surprising that hydrogen-atom addition to the carbonyl bond has a higher activation energy than the addition to olefins (110-112) since the π-bond energy in an olefin is about 10 - 15 kcal lower than for those compounds containing a carbonyl group.

Possible Tunnelling in the Reaction $CH_3 + CH_3CHO \longrightarrow CH_4 + CH_3CO$

The abstraction by the methyl radical of a hydrogen atom from acetaldehyde has been studied by many workers and by various methods; the results are tabulated in Table 19. The Arrhenius plot for different values of $k_4/k_9^{\frac{1}{2}}$ is shown in Fig. 44. Our results agree very well with Dodd's results and, in fact, a straight line can be drawn to link up his and our set of points in the Arrhenius plot. It is noted that his temperature range is the next highest to ours. Taken all together the results seem to suggest a slight increase in activation energy over the range of temperatures investigated. One question is whether our methane production could arise from another source. The only other plausible route of methane formation is by reaction [6],

$$CH_3 + CH_3CHO \longrightarrow CH_4 + CH_2CHO$$

The rate constant for this process is not known but the rate constant for the hydrogen atom abstraction by a methyl radical from acetone is well established. If we assume the

Table 19 - Hydrogen atom abstraction reaction by a methyl radical from acetaldehyde

Reference	Method	Temperature °C	Rate Constant cc mole^{-1} sec^{-1}
This Work	Pyrolysis of Acetaldehyde	480-540	$10^{12.2}$ $10^{-8,400/4.576T}$
Dodd, R.E. (113)	Photolysis of Acetaldehyde	117.8-266.8	$10^{12.3}$ $10^{-8,000/4.576T}$
Birrell, R.N. and Trotman-Dickenson (114)	Thermal Decomposition of di-t-butyl peroxide in Presence of Acetaldehyde	121.4-174.1	$10^{11.9}$ $10^{-7,500/4.576T}$
Ausloos, P. and Steacie, E.W.R. (116)	Photolysis of Azomethane in Presence of Acetaldehyde	27-165	$10^{11.2}$ $10^{-6,800/4.576T}$
Volman, D.H. and Brinton, R.K. (73,74)	Thermal Decomposition of di-t-butyl peroxide in presence of acetaldehyde	124.4-155.8	$10^{11.9}$ $10^{-7,500/4.576T}$
Kerr, J.A. and Calvert, J.S. (115)	Photolysis of Azomethane in Presence of Acetaldehyde	32-121.4	$10^{11.5}$ $10^{-6,800/4.576T}$

Figure 44

Arrhenius plot of $k_4/k_9^{\frac{1}{2}}$.

+ Present work
x Dodd
o Kerr and Calvert
◊ Birrell and Trotman-Dickenson
o Ausloos and Steacie
□ Volman and Brinton
◊ Côme et al.

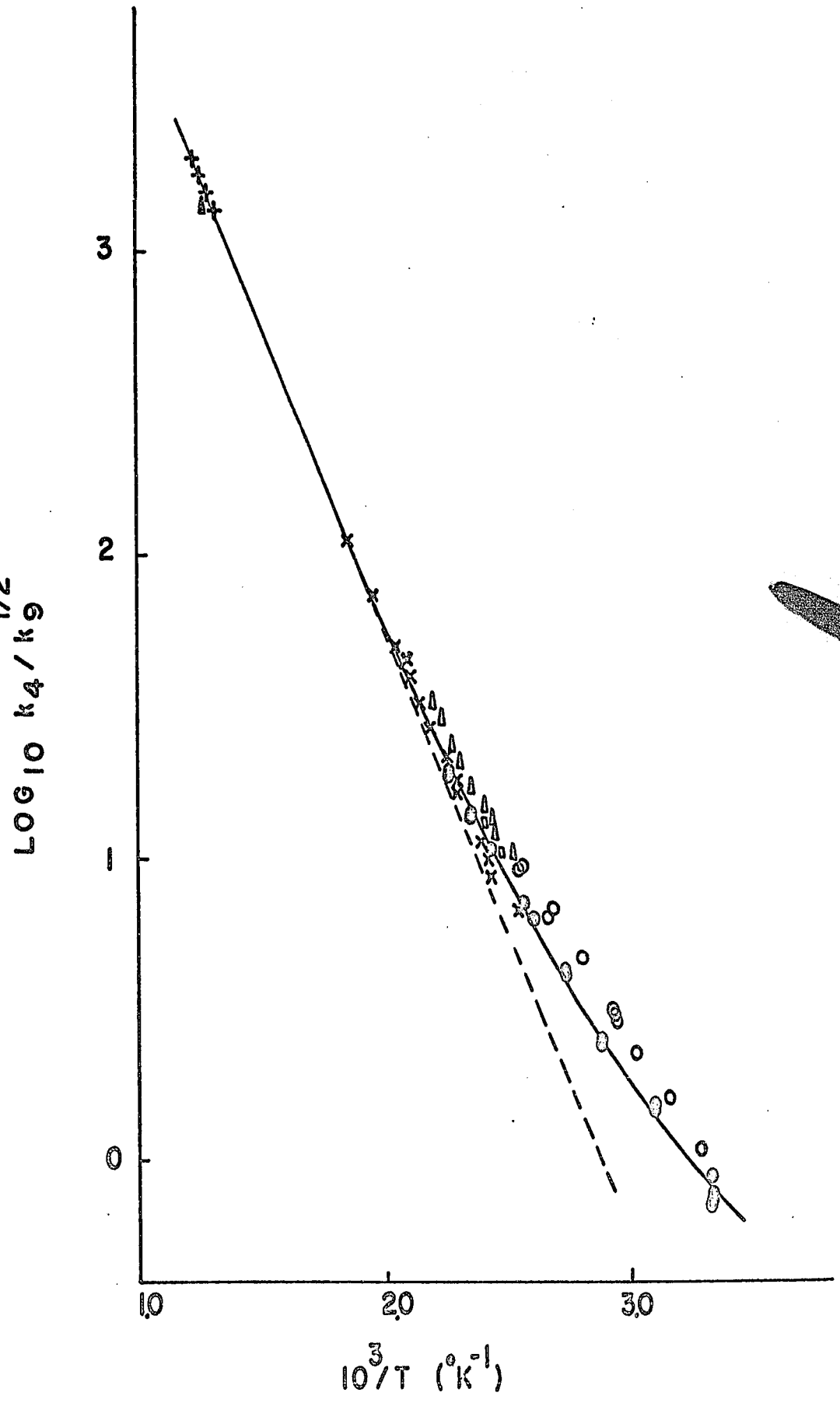
3
2
1
0
1.0
2.0
3.0
LOG10 k4 / k9 1/2
10^3/T (°K^-1)

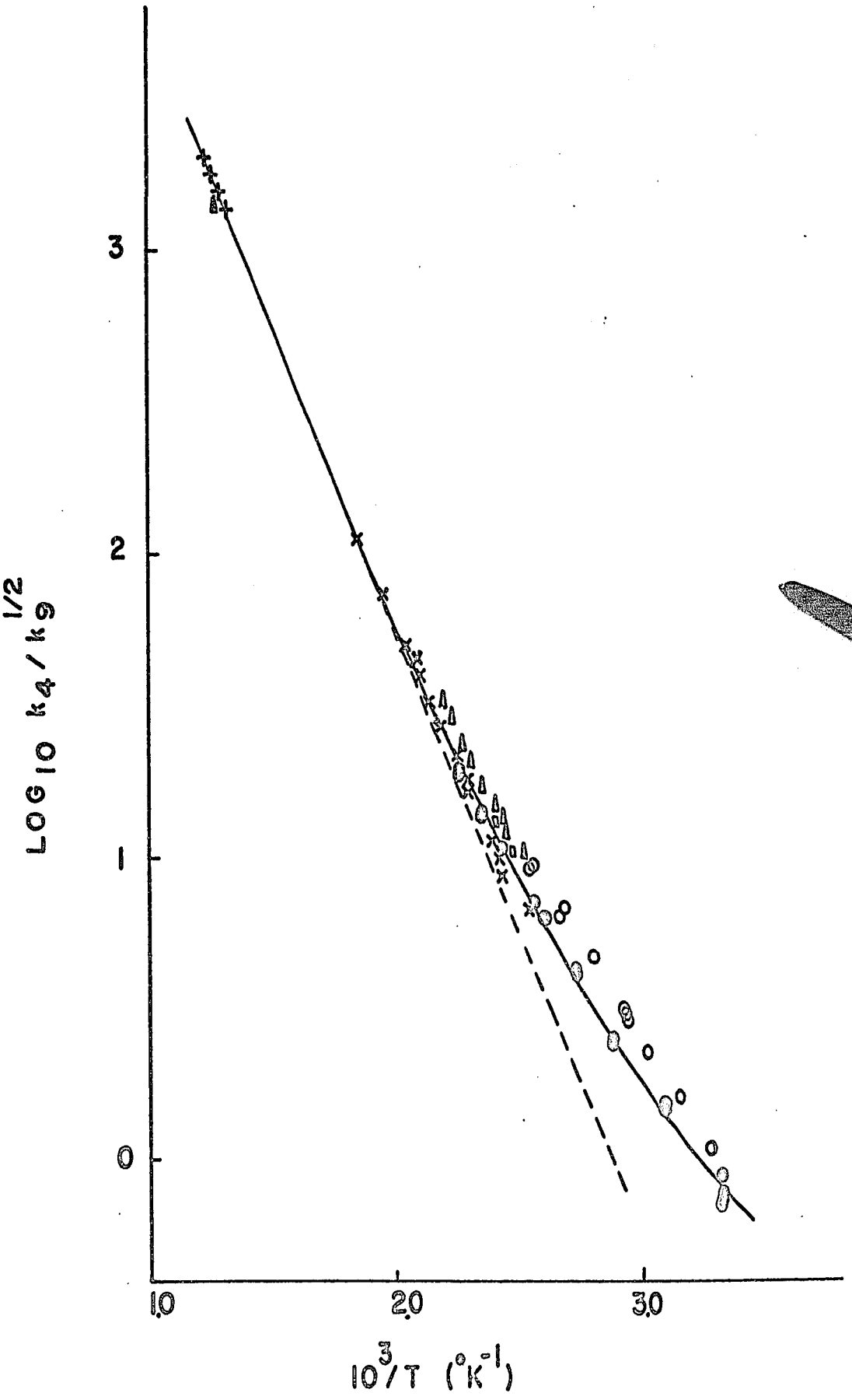
3
2
1
0
1.0
2.0
3.0
LOG10 k4 / k9 1/2
10^3/T (°K^-1)

rates of abstraction of a methyl hydrogen atom from acetaldehyde and acetone to be the same (except for a statistical factor of 2 in the pre-exponential factor) the ratio k_6/k_4 at 523°C turns out to be 0.045; i.e., 5% of the total methane may arise from reaction [6]. If a correction is made for reaction [6], the ratio $k_4/k_9^{\frac{1}{2}}$ will be lowered by 0.02 of a logarithmic unit in Fig. 44. In order that the ratio $k_4/k_9^{\frac{1}{2}}$ is in line with the values at lower temperatures, the value of k_6/k_4 = 0.5 must be used. This is highly improbable. The contribution to methane formation by reaction [6] is therefore a minor one.

Côme, Dzierzynski, Martin and Niclause (19,20) have shown graphically the rate of ethane production vs. time at 500°C and 200 mm Hg of acetaldehyde pressure. The rate of ethane formation at 300 sec is about 5×10^{-3} mm Hg, which is 1.037×10^{-10} mole per cc or 3.47×10^{-13} mole cc^{-1} sec^{-1}. The rate of methane formation is not given in their paper, but they reported that the overall order is 3/2 at 500°C and 50 to 400 mm Hg of initial pressure. Taking their rate of ethane formation together with our rate of methane production or that of Ausuf and Laidler (18) gives rise to 1.39×10^3 $cc^{\frac{1}{2}}$ $mole^{-\frac{1}{2}}$ $sec^{-\frac{1}{2}}$ for the value of $k_4/k_9^{\frac{1}{2}}$. This point is indicated by a darkened triangle in Fig. 44; it supports the present results and suggests that the curvation is real.

This anomaly has been ascribed to hot-radical

reactions, but this suggestion can be rejected on the grounds that some of the work involved photosensitized production of radicals and still showed similar results to those obtained from photolysis experiments. The occurrence of this curvature at a lower temperature indicates extensive tunnelling. Johnston (117) has applied a tunnelling correction for the reaction

$$CH_3 + CH_3COCH_3 \longrightarrow CH_4 + CH_2COCH_3,$$

which has been extensively studied by several workers (118-124). The calculated curve shows a sharp bending of the Arrhenius plot around 400°K but the experimental data do not show this bending until the temperature is a hundred degrees lower. There has been controversy whether this effect is due to hot-radical reactions; Johnston believed it to indicate extensive tunnelling. McNesby and Gordon (125,126) have studied mixtures of CH_3COCH_3 and CD_3COCD_3 and obtained directly the ratio of rates for $H_3D + H - CH_2COCH_3$ and $H_3C + D - CD_2COCD_3$. Using these data, together with studies of low-temperature photolysis and high-temperature pyrolysis, Johnston confirmed that a small tunnelling correction is necessary to fit the calculated curve to the experimental data. Excellent agreement between calculated functions and observed data for the reaction $CD_3 + C_2H_6 \longrightarrow CD_3H + C_2H_5$ has been shown by Johnston (127) using a tunnelling correction.

It is hoped that detailed work will be carried out using deuterated acetaldehyde so that this effect may be better understood.

The Overall Chain Reaction

Originally there was controversy regarding the importance of a chain mechanism as compared with a molecular mechanism for the acetaldehyde decomposition. There is now much evidence that this reaction is almost entirely a chain reaction. There is no doubt that reactions [4] and [5] are the propagation steps and that the methyl radical is the main chain carrier in the system. There are at least five radicals in this system and three of these will attack acetaldehyde. Reactions [2] and [3] constitute a secondary chain. It is noted that each CHO radical will give a molecule of H_2 and, in doing so, will put back a CH_3CO radical into the chain. The activation energy for the chain initiation, which is much higher than that of the chain propagation, suggests a very long chain. Examination of Table 1 shows that the rates of methane formation are always 10^2 - 10^3 greater than those of hydrogen and ethane. The fact that these products are extremely minor indicates that the rate of chain propagation is very rapid compared to the rate of termination, and that each radical must perform many cycles before being destroyed. The chain length (ϕ) is defined as the rate of the overall reaction divided by the rate of initiation, and in this system

$$\phi = k_4 \left(\frac{1}{k_1 k_9}\right)^{\frac{1}{2}} \left[CH_3CHO\right]^{\frac{1}{2}} \qquad (36)$$

Table 20 tabulates the chain length as a function of

Table 20 - Chain lengths $\bar{\nu}$ as functions of pressure and temperature

T°C/P (mm Hg)	77	118	559
480	9,850	12,160	26,540
500	5,570	6,890	15,030
523	3,110	3,850	8,430
540	1,920	2,340	5,080

temperature and pressure. It is seen that $\underline{\phi}$ increases with increase in pressure and decrease in temperature. Since the decrease of $\underline{\phi}$ with temperature is exponential, $\underline{\phi}$ will approach unity when $T \longrightarrow \infty$, under which conditions the rate of initiation would be equal to that of propagation. Allen and Sickman (34) have studied the azomethane-sensitized decomposition of acetaldehyde and found the chain length to be as high as 500.

CLAIMS TO ORIGINAL RESEARCH

(1) The pyrolysis of acetaldehyde has been reinvestigated at temperatures from 480 to 540°C at pressures between 1 and 560 mm. The rates, as well as the order of formation of methane, ethane, acetone and hydrogen have been studied in detail. A modified Rice-Herzfeld is proposed to account for all experimental results.

(2) The pressure dependence of the second-order rate coefficient for the combination of methyl radicals has been examined in the light of the inert-gas effect.

(3) The initial split of acetaldehyde is concluded to be first-order at the higher pressures. The bond dissociation energy, D (CH_3 - CHO), has been determined.

(4) The apparent rate constant for methyl radical addition to acetaldehyde has been measured. From this, the rate constant for the decomposition of i-PrO $\longrightarrow$ CH_3COCH_3 + H has been estimated. The π-bond energy in the acetone thus formed has been calculated.

(5) The falling-off of the overall rate constant at low pressures has been studied. The pressure dependence of the ratio k_1/k_9 has been confirmed by the addition of inert gas.

(6) Studies have been made of various types of surface effects on the decomposition of acetaldehyde.

(7) Different time-course equations have been derived and demonstrate the consistency of the proposed mechanism.

REFERENCES

1. W.H. Heckert and E. Mack, J. Am. Chem. Soc., 51 2706 (1929).
2. F.O. Rice and K.F. Herzfeld, ibid., 56 284 (1934).
3. M. Letort, Comptes rendus, 197 1042 (1933).
4. M. Letort, ibid., 200 312 (1935).
5. M. Letort, J. Chim. Phys., 34 428 (1937).
6. A. Boyer, M. Niclause and M. Letort, J. Chim. Phys., 49 337, 345 (1945).
7. M.W. Travers, Proc. Roy. Soc., A 146 248 (1934).
8. M.W. Travers, Nature, 134 569 (1934).
9. M.W. Travers and R.V. Seddon, Nature, 137 906 (1936).
10. M.W. Travers and R.V. Seddon, Proc. Roy. Soc., A 156 234 (1936).
11. C.A. Winkler and C.N. Hinshelwood, Proc. Roy. Soc., A 149 355 (1935).
12. C.N. Hinshelwood, C.J.M. Fletcher, F.H. Verhoek and C.A. Winkler, ibid., A 146 327 (1934).
13. C.J.M. Fletcher and C.N. Hinshelwood, ibid, A 141 41 (1933).
14. G.R. Freeman, C.J. Danby and C.N. Hinshelwood, ibid, A 245 456 (1958).
15. N. Imai, Y. Yoshida and O. Toyama, Bull. Chem. Soc. Japan, 35 752 (1962).
16. A.B. Trenwith, J. Chem. Soc., 4426 (1963).

REFERENCES

1. W.H. Heckert and E. Mack, J. Am. Chem. Soc., 51 2706 (1929).
2. F.O. Rice and K.F. Herzfeld, ibid., 56 284 (1934).
3. M. Letort, Comptes rendus, 197 1042 (1933).
4. M. Letort, ibid., 200 312 (1935).
5. M. Letort, J. Chim. Phys., 34 428 (1937).
6. A. Boyer, M. Niclause and M. Letort, J. Chim. Phys., 49 337, 345 (1945).
7. M.W. Travers, Proc. Roy. Soc., A 146 248 (1934).
8. M.W. Travers, Nature, 134 569 (1934).
9. M.W. Travers and R.V. Seddon, Nature, 137 906 (1936).
10. M.W. Travers and R.V. Seddon, Proc. Roy. Soc., A 156 234 (1936).
11. C.A. Winkler and C.N. Hinshelwood, Proc. Roy. Soc., A 149 355 (1935).
12. C.N. Hinshelwood, C.J.M. Fletcher, F.H. Verhoek and C.A. Winkler, ibid., A 146 327 (1934).
13. C.J.M. Fletcher and C.N. Hinshelwood, ibid, A 141 41 (1933).
14. G.R. Freeman, C.J. Danby and C.N. Hinshelwood, ibid., A 245 456 (1958).
15. N. Imai, Y. Yoshida and O. Toyama, Bull. Chem. Soc. Japan, 35 752 (1962).
16. A.B. Trenwith, J. Chem. Soc., 4426 (1963).

17. R.W. Dexter and A.B. Trenwith, J. Chem. Soc., 5459 (1964).

18. M. Eusuf and K.J. Laidler, Can. J. Chem., 42 1851 (1964).

19. G.M. Côme, M. Dzierzynski, R. Martin et M. Niclause, Comptes rendus, 264 serie C 548 (1967).

20. G.M. Côme, M. Dzierzynski, R. Martin et M. Niclause, ibid, 264 serie C 836 (1967).

21. F.O. Rice, W.R. Johnston and B.L. Evering, J. Am. Chem. Soc., 54 3529 (1932).

22. M. Letort, Thesis, Paris (1937).

23. M. Burton, J.E. Ricci and T.W. Davis, J. Am. Chem. Soc., 62 265 (1940).

24. F. Patat, Z. Physik Chem., B 32 294 (1936).

25. F. Patat and H. Sachsse, Naturwiss, 23 247 (1935).

26. F. Patat and H. Sachsse, Z. Physik Chem., B 31 105 (1935).

27. H. Sachsse and F. Patat, Electrochem., 41 493 (1935).

28. J.C. Morris, J. Am. Chem. Soc., 63 2535 (1941).

29. J.C. Morris, ibid, 66 584 (1944).

30. P.O. Zemany and M. Burton, J. Phys. & Colloid Chem., 55 949 (1951).

31. L.A. Wall and W.J. Moore, ibid, 55 965 (1951).

32. F.O. Rice and R.E. Varnerin, J. Am. Chem. Soc., 76 2629 (1954).

33. A.O. Allen and D.V. Sickman, ibid, 56 1251 (1934).

34. A.O. Allen and D.V. Sickman, ibid, 56 2031 (1934).

35. J.G. Calvert and J.T. Gruver, J. Am. Chem. Soc., 80 1313 (1958).

36. A. Boyer, M. Niclause and M. Letort, J. Chim. Phys., 49 345 (1952).

37. F.O. Rice and W.D. Walters, J. Am. Chem. Soc., 63 1701 (1941).

38. C.J.M. Fletcher, ibid, 58 534 (1936).

39. C.J.M. Fletcher and G.K. Rollefson, ibid, 58 2135 (1936).

40. C.J.M. Fletcher and G.K. Rollefson, ibid, 58 2129 (1936).

41. M.W. Travers and C.G. Silcocks, Nature, 139 1018 (1937).

42. J.G. Roof, J. Am. Chem. Soc., 66 358 (1944).

43. J.G. Roof and F. Daniel, J. Am. Chem. Soc., 62 2912 (1940).

44. M. Letort and M. Niclause, Rev. Inst. Franc. Petrole et Ann. Combustibles Liquides, 4 319 (1949).

45. M. Niclause, P. Goldfinger and M. Letort, Comptes rendus, 299 437 (1949).

46. R.F. Faull and G.K. Rollefson, J. Am. Chem. Soc., 58 1755 (1936).

47. R.F. Faull and G.K. Rollefson, ibid, 59 625 (1937).

48. E. O'Neal and S.W. Benson, J. Chem. Phys., 40 302 (1964).

49. C.J.M. Fletcher and C.N. Hinshelwood, Trans. Faraday Soc., 30 614 (1934).

50. C.N. Hinshelwood and P.J. Askey, Proc. Roy. Soc., A 116 163 (1927).

51. C.J.M. Fletcher, J. Am. Chem. Soc., 58 2646 (1936).

52. K. Bril, P. Goldfinger, M. Letort, H. Matthys and M. Niclause, Bull. Soc. Chim. Belg., 59 263 (1950).

53. K. Bril, P. Goldfinger, M. Letort, H. Matthys and M. Niclause, Nature, 166 405 (1950).

54. C.P. Quinn, Proc. Roy. Soc., A 275 190 (1963).

55. M.C. Lin and M.H. Back, Can. J. Chem., 505 (1966)

56. M. Niclause, Rev. Inst. Franc. Petrole, 9 327, 419 (1954).

57. A.C. Panson and L.M. Adams, J. Gas Chromatog., 2, 164 (1964).

58. H. Paushmann, Z. Anal. Chem., 203 16 (1964).

59. G. Castello, E. Biagini and S. Munari, J. Chromatog., 20 447 (1965).

60. C. N. Hinshelwood and W.K. Hutchson, Proc. Roy. Soc., A 111 380 (1926).

61. N. Imai and O. Toyama, Bull. Chem. Soc. Japan, 33 1408 (1960).

62. P. Goldfinger, M. Letort and M. Niclause, Volume Commemoratif Victor Henri: Contribution à l'étude de la structure moléculaire, p. 283. Liège: Desoer (1948)

63. A. Boyer, M. Niclause and M. Letort, J. Chim. Phys., 49 337 (1952).

64. K. J. Laidler and M.T.H. Liu, Proc. Roy. Soc., A 297 365 (1967).

65. N.L. Arthur and T.N. Bell, Aust. J. Chem., 18 1561 (1965).

66. A. J. Shepp, J. Chem. Phys., 24 939 (1956).

67. R.E. Dodd and E.W.R. Steacie, Proc. Roy. Soc., Ser. A 223 283 (1954).

68. L.F. Loucks and K. J. Laidler, Can. J. Chem., To be published.

69. S. Toby and B.H. Weiss, J. Phys. Chem., 68 2492 (1964).

70. M.C. Lin and M.H. Back, Can. J. Chem., 44 2357 (1966).

71. E. O'Neal and S.W. Benson, J. Chem. Phys., 36 2196 (1962).

72. J.A. Kerr and J.G. Calvert, J. Phys. Chem., 69 1022 (1965).

73. D.H. Volman and R.K. Brinton, J. Chem. Phys., 20 1764 (1952).

74. D.H. Volman and R.K. Brinton, ibid, 20 1053 (1952).

75. P. Gray and A. Williams, Chemical Reviews, 59 239 (1959).

76. J.A. Kerr and A.F. Trotman-Dickenson, J. Chem. Soc., 1161 (1960).

77. M. Eusuf and K.J. Laidler, Can. J. Chem., 43 268 (1965).

78. S.W. Benson, J. Chem. Phys., 105 40 (1964).

79. M.C. Lin, Private communication.

80. B.W. Wojciechowski and K.J. Laidler, Trans. Faraday Soc., 59 369 (1963).

81. A. Maccoll and P.J. Thomas, J. Chem. Soc., 979 (1955).

82. K.A. Holbrook, Proc. Chem. Soc., 418 (1964).

83. J.L. Holmes, Private communication.

84. C. Steel and K.J. Laidler, J. Chem. Phys., 34 1827 (1961).

85. J.G. Calvert and J.N. Pitts Jr., "Photochemistry" Wiley, New York, pp. 815-820 (1966).

86. R.J. Cvetanovic, Prog. Reaction Kinetics, 2 112 (1964).

87. F.P. Lossing, Can. J. Chem., 35 305 (1957).

88. D.W. Setser, J. Phys. Chem., 70 826 (1966).

89. M. Szwarc, Chem. Rev., 67 75 (1950).

90. R. Walsh and S.W. Benson, J. Am. Chem. Soc., 88 4570 (1966).

91. A.F. Trotman-Dickenson, "Gas Kinetics," Butterworths Scientific Publications London (1955).

92. J.G. Calvert, J. Chem. Phys., 29 954 (1958).

93. R. Klein and L.J. Schoen, J. Chem. Phys., 29 953 (1958).

94. R. Klein and L.J. Schoen, ibid, 24 1094 (1956).

95. J.G. Calvert, J. Phys. Chem., 61 1206 (1957).

96. R.I. Reed, Trans Far. Soc., 62 1195 (1956).

97. J.C.D. Brand and R.I. Reed, J. Chem. Soc., 2386 (1957).

98. T.W. Shannon and A.G. Harrison, Can. J. Chem., 39 1392 (1961).

99. K.H. Anderson and S.W. Benson, J. Chem. Phys., 39 1677 (1963).

100. M.C. Lin and K.J. Laidler, Can. J. Chem., 44 2927 (1966).

101. S. Glasstone, K.J. Laidler and H. Eyring, The Theory of Rate Processes. McGraw Hill Book Company (1941).

102. D.L. Cox, R.A. Livermore and L. Phillips, J. Chem. Soc., 245 (1966).

103. S.W. Benson and J.H. Buss, J. Chem. Phys. 29 546 (1958).

104. JANAF Interim Thermochemical Tables, Thermal Laboratory, The Dow Chemical Company, Midland, Mich. (1960).

105. S.W. Benson, J. Chem. Ed., 42 502 (1965).

106. N. Semenoff, Some Problems in Chemical Kinetics and Reactivity Vol. 1 Pergamon Press(1958).

107. J.A. Barnard, Trans. Far. Soc., 56 72 (1960).

108. R. Walsh and S.W. Benson, J. Am. Chem. Soc., 88 3480 (1966).

109. P. Gray and A. Williams, Trans. Far. Soc., 55 760 (1959).

110. H.W. Melville and J.C. Robb, Proc. Roy. Soc., A 202 181 (1950).

111. K. Yang, J. Am. Chem. Soc., 84 719 (1962).

112. R.R. Baldwin, R.F. Simmons and R.W. Walker, Trans. Far. Soc., 63 2486 (1966).

113. R.E. Dodd, Can. J. Chem., 33 699 (1955).

114. R.N. Birrell and A.F. Trotman-Dickenson, J. Chem. Soc., 2059 (1960).

115. J.A. Kerr and J [illegible]. Calvert, J. Phy. Chem., 69 1022 (1965).

116. P. Ausloos and E.W.R. Steacie, Can. J. Chem., 33 31 (1955).

117. H.S. Johnston, Adv. In Chem. Phys., P 131 Vol. III 1961 Interscience Publishers Inc., New York.

118. L. Mandelcorn and E.W.R. Steacie, Can. J. Chem., 32 331 (1954).

119. T.C. Marjury and E.W.R. Steacie, Can. J. Chem., 30 800 (1952).

120. R.G. Oswin, R. Rebbert and E.W.R. Steacie, ibid., 33 472 (1955).

121. A. F. Trotman-Dickenson and E.W.R. Steacie, J. Chem. Phys., 18 1097 (1950).

122. A.F. Trotman-Dickenson, J.R. Birchard and E.W.R. Steacie, ibid., 19 163 (1951).

123. L.M. Dorfman and W.A. Noyes, Jr., ibid., 16 557 (1948).

124. A.J.C. Nicholson, J. Am. Chem. Soc., 73 3981 (1951).

125. J.R. McNesby and A.S. Gordon, J. Am. Chem. Soc., 76 1416 (1954).

126. J.R. McNesby,, T.W. Davis and A.S. Gordon, ibid, 76 823 (1954).

127. H.S. Johnston, Gas Phase Reaction Rate Theory, Ronald Press Co., New York (1966)

END OF REEL